

## Hayder Naser Mnati Al-Lami

## Oncampus Assignment Coversheet

Student ID: 0061061532  
Course: ENG8414  
Class: 19471



**Name:** Hayder Naser Mnati Al-Lami  
**Postal Address:** 248 Cortless Street  
Harristown  
Toowoomba QLD 4350  
Australia

**Assessment:** DISSERTATION & DEMONSTRATIONS

**Due Date:** 19-Oct-2017

**Submitted To:** Fac of Hlth, Eng & Sciences

**Examiner:** Karu Karunasena



**Marker Signature:** \_\_\_\_\_

**Mark Given (Office Use Only):** \_\_\_\_\_

**Tutorial Group Number:**

**Room:**

**Day:**

**Time:**

**Campus:** Toowoomba

### STUDENT DECLARATION:

I hold a copy of this assignment which I can produce if the original is lost or damaged.

I hereby certify that no part of this assignment has been copied from any other student's work or from any other source except where due acknowledgement is made in the assignment. No part of this assignment has been written for me by any other person except where such collaboration has been authorised by the Course Team Leader or the examiner concerned.

**Signature:** \_\_\_\_\_

A handwritten signature in black ink, appearing to be "Hayder Naser Mnati Al-Lami".

**Date:** \_\_\_\_\_

- Notes:**
1. An Examiner or a Course Team Leader has, and may exercise, the right not to mark this assignment if the above declaration has not been signed.
  2. If the above declaration is found to be false, further appropriate action will be taken.

Make sure that you have used the **CORRECT** Assignment Cover for your assignment.  
Incorrect assignment cover sheets will cause delays.

**DISSERTATION SUBMISSION FORM**

STUDENT USE ONLY:

Student Name:	<b>Hayder Al-Lami</b>
Student Number:	<b>0061061532</b>
Program:	<b>MENS</b>
Mode:	<b>On-campus</b>
Project Title:	<b>Detailed simulations of sub-surface boundary layer in wind-generated waves</b>
Supervisor/s:	<b>Andrew Wandel , Khalid Saleh</b>

2 printed and soft bound assessment copy	<b>Attached</b>
Inclusion of a Title page	<b>Attached</b>
Inclusion of a Disclaimer page (it should be titled Limitations of Use)	<b>Attached</b>
Inclusion of a signed Certification page	<b>Attached</b>
Inclusion of Appendix A – Project Specification	<b>Attached</b>
single PDF file identical to the printed copy submitted to the ENG8002 Study Desk	<b>Attached</b>
2 CDs( or DVDs) containing a single PDF file identical to the printed copy (refer Project Reference Book section 11.11)	<b>Attached</b>

I declare that I have submitted (Student to sign):  
Date: 03/11/2017



Assignment Label	Date Stamp	Library Copy
		Does the Supervisor give permission for a copy to be forwarded to the Library?*

\* If a formal undertaking of Confidentiality has been given, then both CD copies will remain with the Supervisor (refer 6.4 of the Project Reference Book).

**Students should submit this form, the assignment cover sheet and the materials requested above before the submission deadline. On-campus students must submit to the engineering office (Z Building level 4 reception). External students should post their material before the deadline.**

*USQ collects personal information to assist the University in providing tertiary education and related ancillary services and to be able to contact you regarding enrolment, assessment and associated USQ services. Personal information will not be disclosed to third parties without your consent unless required by law.*

*USQ collects personal information to assist the University in providing tertiary education and related ancillary services and to be able to contact you regarding enrolment, assessment and associated USQ services. Personal information will not be disclosed to third parties without your consent unless required by law.*

University of Southern Queensland

Faculty of Health, Engineering and Sciences

**Detailed simulations of sub-surface boundary  
layer in wind-generated waves**

A dissertation submitted by

**Hayder Naser Al-Lami**

In fulfillment of the requirements of

**Courses ENG8414 Research Project**

Towards the degree of

**Master of Engineering Sciences in Mechanical engineering**

Submitted: November, 2017

**This page intentionally left blank**

**University of Southern Queensland**

**Faculty of Health, Engineering and Sciences**

**ENG8414**

(This is 6 unit research project in a 16 unit Master of Engineering Science program)

## **Limitations of Use**

The Council of the University of Southern Queensland, its Faculty of Health, Engineering and Science, and the staff of the University of Southern Queensland, do not accept any responsibility for the truth, accuracy or completeness of material contained within or associated with this dissertation.

Persons using all or any part of this material do so at their own risk, and not at the risk of the Council of the University of Southern Queensland, its Faculty of Health, Engineering and Science or the staff of the University of Southern Queensland.

This dissertation reports an educational exercise and has no purpose or validity beyond this exercise. The sole purpose of this dissertation project is to contribute to the overall education within the student's chosen degree program. This document, the associated hardware, software, drawings, and other material set out in the associated appendices should not be used for any other purpose: if they are so used, it is entirely at the risk of the user.

## CERTIFICATION

I certify that the ideas, designs and experimental work, results, analyses and conclusions set out in this dissertation are entirely my own effort, except where otherwise indicated and acknowledged.

I further certify that the work is original and has not been previously submitted for assessment in any other course or institution, except where specifically stated.

**Student Name: Hayder Al-Lami**

**Student Number: 0061061532**



Signature

29/10/2017

Date

## ABSTRACT

Evaporation from water resources is considered as a significant issue that impacts the economic growth especially in areas where the climate tends to have a big change. It plays a significant role in reducing the amount of quality water. Therefore, reducing evaporation is a very important factor to reduce the influence of the drought. Monolayer is the best technique to reduce the evaporation especially in large reservoirs because of the benefits of using it, such as the ease of spread it, its lower cost, and the required time for install and maintain it (Schouten et al., 2011); (Jennison, 2003). However, Monolayers is likely to be ineffective under the effects of harsh winds and waves generated by wind. Due to the lack with studying the winds generated wave's processes. This project has been carried out to study wind generated waves. The aim of this study is to develop a Computational Fluid Dynamics (CFD) model to study the sub-surface layer of water under the effects of wind. The model will be a three-dimensional model, comparison a tank ( $15 \times 0.85 \times 0.092$  m/s) with two phases' water (bottom prism) and air (top prism). Detached eddy simulation (DES) has been used to solve the equation of the simulation. The simulation has been run at four wind speeds (0.9, 1.3, 2 and 3.2 m/s) for two residence time. Mesh independency has not been reached because of some limitations. The results show a direct proportional between winds speeds and the properties of waves. With increasing wind speeds, waves with high frequency and longer wavelength will be generated. The expected results can be used to help in evaporation mitigation strategies.



## **ACKNOWLEDGEMENTS**

I would like to thank both my supervisors Dr Andrew Wandel and my co-supervisor Dr Khalid Salah for all their support, patience, motivation, and knowledge during my research and writing of this dissertation. I would not reach such a stage of research without their support.

Also, I would like to thank my colleagues in and out the University for their encouragement and making the life easier for me.

My sincere thanks to my parents who bear all the difficulties and stand with me to complete my study. Also, I cannot forget the support from my wife Milad during my life and especially during my study.

Hayder Al-Lami

University of Southern Queensland

November 2017

# TABLE OF CONTENTS

CHAPTER	PAGE
ABSTRACT.....	viii
ACKNOWLEDGEMENTS.....	ix
TABLE OF CONTENTS.....	x
LIST OF TABLES.....	xv
LIST OF FIGURES.....	xvi
GLOSSARY.....	xxiv
CHAPTER 1: INTRODUCTION.....	1
1.1 Background.....	1
1.2 Objectives.....	3
1.3 Research questions.....	4
1.4 Project Contributions.....	4
1.5 Project Rationale.....	5
1.6 Consequential Effects.....	5
1.7 Outline.....	6
1.7.1 Chapter 1. Introduction.....	6

1.7.2	Chapter 2. Background and Literature Review .....	7
1.7.3	Chapter 3. Preliminary model.....	7
1.7.4	Chapter 4. Final model .....	7
1.7.5	Chapter 5. Conclusions and Recommendations .....	8
CHAPTER 2: BACKGROUND AND LITERATURE REVIEW .....		9
2.1	Evaporation .....	9
2.2	Monolayers .....	18
2.3	Wind generated waves .....	28
2.3.1	General.....	28
2.3.2	Modelling.....	30
2.4	Computational fluid dynamics (CFD) .....	40
2.4.1	Governing equation .....	41
2.4.2	Detached eddy simulation .....	47
2.5	Summary .....	52
CHAPTER 3: PRELIMNERY MODEL .....		53
3.1	Introduction:.....	53
3.2	Software ANSYS Fluent.....	54

3.2.1	Journey of learning .....	54
3.3	Preliminary Computational Domain .....	62
3.4	Mesh generation.....	65
3.5	Setup .....	66
3.6	Analysing data .....	70
3.6.1	Simulation for different mesh sizes .....	70
3.6.2	Simulation for different residence time .....	72
3.7	Summary .....	74
CHAPTER 4: FINAL MODEL .....		75
4.1	Introduction:.....	75
4.2	Final Computational Domain.....	75
4.3	Mesh generation.....	76
4.4	Setup .....	78
4.5	Flow Field Data Analysis.....	79
4.6	Results and discussion .....	85
4.6.1	Volume fraction Plots.....	85
4.6.2	Waves' frequency and amplitude plots .....	90

4.6.3	Shear Stress plots.....	93
4.7	Limitations of this study .....	96
4.8	Summary .....	98
CHAPTER 5: CONCLUSIONS .....		99
REFERENCES .....		102
APPENDIX A: Project Specification .....		111
APPENDIX B: Further results and plots .....		114
B.1	At wind speed 0.9 m/s .....	114
B.2	At wind speed 1.3 m/s .....	121
B.3	At wind speed 2 m/s .....	127
B.4	At wind speed 3.2 m/s .....	134
APPENDIX C: Matlab codes.....		141
C.1:	Code for plotting the temperature for different mesh sizes.....	141
C.2:	Code for plotting the velocity magnitude for different mesh sizes. ....	145
C.3:	Code for plotting the velocity magnitude for different residence time. ....	149
C.4:	Code for plotting the total temperature for different residence time. ....	155
C.5:	Code for plotting the temperature for different mesh sizes (final model).....	161

C.6: Code for plotting the velocity magnitude for different mesh sizes/final model .....	165
C.7: Code for plotting the volume fraction (final model).....	169
C.8: Code for determining and plotting the amplitude of waves (final model).....	172
C.9: Code for determining the shear stress on water surface/final model .....	175

## LIST OF TABLES

Table 1: Comparing between three evaporation mitigations (Craig et al., 2005).....	21
Table 2: The properties of air and water.....	67
Table 3: Initialization values.....	68
Table 4: calculations for time residence, time steps and the appropriate time step.....	69
Table 5: Comparison for different mesh sizes .....	77
Table 6: Dimensions for the plane .....	81
Table 7: Exported data .....	82
Table 8: wave's amplitude .....	90
Table 9: max shear stress at different wind speeds.....	94

## LIST OF FIGURES

Figure 1: Rainfall deficiencies: 7 months (BOM, 2017) .....	2
Figure 2: Rainfall deficiencies: 4 months (BOM, 2017) .....	2
Figure 3: Annual mean temperature changes across Australia since 1910 (BOM, 2016).....	10
Figure 4: Average pan evaporation (BOM, 2006) .....	11
Figure 5: Floating cover (Baillie, 2008) .....	12
Figure 6: Shade-cloth covers (Finn and Barnes, 2007).....	14
Figure 7: Wind breaks (Helfer et al., 2009) .....	15
Figure 8: Destratification systems. Clockwise from top left: 10 bubble plumes, draft-tube mixer and unconfined mixers (Sherman et al., 2010).....	17
Figure 9: Monolayers structure (Toreki, 2015).....	18
Figure 10: Amphiphilic molecules over water surface (Panjabi et al., 2016).....	19
Figure 11: Monolayer is spreading across the surface of water (Craig et al., 2007) .....	20
Figure 12: Mixing hopper (Knights, 2005).....	23
Figure 13: Wave tank setup located at Griffith University (Palada et al., 2012).....	24
Figure 14: Monolayer resistance vs evaporation (Palada et al., 2012). .....	25
Figure 15: Schematic diagram of wind tunnel set up (Prime et al., 2012). .....	26



Figure 16: Mass of water lost over time (Prime et al., 2012).	27
Figure 17: Wind Generate Waves (Sawan, 2003)	28
Figure 18 waves characteristics (Olsen, 2011)	29
Figure 19: wind tunnel and the water tanks (Longo et al., 2012)	31
Figure 20: Experimental setup (Paquier et al., 2015)	32
Figure 21: The experimental facility for a horizontal stratified flow (Bae et al., 2017)	33
Figure 22: Comparison of wave height and velocity correlation with experimental data (Bae et al., 2017)	33
Figure 23: Comparison of the wave frequency correlation with experimental data (Bae et al., 2017)	34
Figure 24: Coordinate system and computational domain (Park et al., 2001)	36
Figure 25: Comparison between the output from buoy and the model where (a) the results of significant wave height ( $H_s$ ), (b) mean wave period (c) mean wave direction (d) buoy and CFSR forced $H_s$ and $T_m$ , and (e) between buoy and ECMWF forced $H_s$ and $T_m$ . (Shanas et al., 2017)	39
Figure 26: Process of Computational Fluid Dynamics (Zuo, 2005)	40
Figure 27: Numerical domain of two turbulent flows (Lin, 2008)	43
Figure 28 : Computational Domain and Sampling Region (Greig, 2013)	44
Figure 29: Computational domain (Williams, 2014)	45

Figure 30: Computational domain (Silva et al., 2015).....	46
Figure 31: Time series of free surface elevation at probe P1 ( $x' = 20\text{m}$ ) .....	47
Figure 32: low field over a simplified car geometry (a) Mean flow; (b) instantaneous flow (Fröhlich and von Terzi, 2008) .....	49
Figure 33 Comparison of mean stream wise velocity profiles in the near-wake region (Nishino et al., 2008). .....	50
Figure 34: DES approach (Fröhlich and von Terzi, 2008) .....	51
Figure 35: first geometry .....	55
Figure 36: the body of influence .....	55
Figure 37 mesh generation.....	56
Figure 38 some results of simulation .....	58
Figure 39: The second model.....	59
Figure 40: Mesh generation for second model .....	59
Figure 41: Reverse flow in the air inlet .....	60
Figure 42 using the fillet for the corners.....	61
Figure 43 Converged results .....	62
Figure 44 Computational domain .....	64
Figure 45 mesh distribution .....	66

Figure 46: velocity magnitude for different mesh sizes.....	71
Figure 47: total temperature for different mesh sizes .....	71
Figure 48: Velocity magnitude for different residence time.....	73
Figure 49: Graph of the temperatures for different residence time .....	73
Figure 50: Final domain.....	76
Figure 51: The elements that have worse skewness quality .....	78
Figure 52: The elements that have worse orthogonal quality .....	78
Figure 53: results of velocity magnitude for different mesh sizes.....	80
Figure 54: results of the temperatures for different mesh sizes.....	80
Figure 55: Sampling region .....	83
Figure 56: Volume fraction of water at wind speed 0.9m/s.....	86
Figure 57: Volume fraction of water at wind speed 1.3m/s.....	87
Figure 58: Volume fraction of water at wind speed 2m/s.....	88
Figure 59: Volume fraction of water at wind speed 3.2m/ .....	89
Figure 60: Amplitude of waves at wind speed 0.9 m/s.....	91
Figure 61: Amplitude of waves at wind speed 1.3 m/s.....	91
Figure 62: Amplitude of waves at wind speed 2 m/s.....	92

Figure 63: Amplitude of waves at wind speed 3.2 m/s.....	92
Figure 64: amplitudes of wave VS wind speeds.....	93
Figure 65: max shear stress at different wind speeds .....	94
Figure 66: Shear stress on the water surface at different wind speeds .....	95
Figure 67: shear stress distribution on the water surface at different wind speeds.....	96
Figure 68: The density of the mixture at the middle of model at wind speed 0.9 m/s .....	114
Figure 69: The velocity magnitude at the middle of the model at wind speed 0.9 m/s .....	114
Figure 70: The velocity in z-direction in the middle of the model at wind speed 0.9 m/s .....	115
Figure 71: The velocity in z-direction at the inlet at wind speed 0.9 m/s.....	115
Figure 72: The velocity in z-direction at the outlet at wind speed 0.9 m/s.....	116
Figure 73: The total temperature in the middle of the model at wind speed 0.9 m/s .....	116
Figure 74: The total temperature at the inlet at wind speed 0.9 m/s.....	117
Figure 75: The total temperature at the outlet at wind speed 0.9 m/s.....	117
Figure 76: The volume fraction of phase 2 (water) in the middle of the model at wind speed 0.9 m/s.....	118
Figure 77: The volume fraction of phase 2 (water) at the inlet at wind speed 0.9 m/s.....	118
Figure 78: The volume fraction of phase 2 (water) at the outlet at wind speed 0.9 m/s.....	119

Figure 79: The strain rate in the middle of model at wind speed 0.9 m/s.....	119
Figure 80: The strain rate at the outlet at wind speed 0.9 m/s .....	120
Figure 81: The density of the mixture at the middle of model at wind speed 1.3 m/s .....	121
Figure 82: The velocity magnitude at the middle of the model at wind speed 1.3 m/s .....	121
Figure 83: The velocity in z-direction in the middle of the model at wind speed 1.3 m/s ....	122
Figure 84: The velocity in z-direction at the inlet at wind speed 1.3 m/s.....	122
Figure 85: The velocity in z-direction at the outlet at wind speed 1.3 m/s.....	123
Figure 86: The total temperature in the middle of the model at wind speed 1.3 m/s .....	123
Figure 87: The total temperature at the inlet at wind speed 1.3 m/s.....	124
Figure 88: The total temperature at the outlet at wind speed 1.3 m/s.....	124
Figure 89: The volume fraction of phase 2 (water) in the middle of the model at wind speed 1.3 m/s.....	125
Figure 90: The volume fraction of phase 2 (water) at the inlet at wind speed 1.3 m/s.....	125
Figure 91: The volume fraction of phase 2 (water) at the outlet at wind speed 1.3 m/s.....	126
Figure 92: The strain rate in the middle of model at wind speed 1.3 m/s.....	126
Figure 93: The strain rate at the outlet at wind speed 1.3 m/s .....	127
Figure 94: The density of the mixture at the middle of model at wind speed 2 m/s .....	127

Figure 95: The velocity magnitude at the middle of the model at wind speed 2 m/s .....	128
Figure 96: The velocity in z-direction in the middle of the model at wind speed 2 m/s .....	128
Figure 97: The velocity in z-direction at the inlet at wind speed 2 m/s.....	129
Figure 98: The velocity in z-direction at the outlet at wind speed 2 m/s.....	129
Figure 99: The total temperature in the middle of the model, wind speed 2 m/s .....	130
Figure 100: The total temperature at the inlet, wind speed 2 m/s.....	130
Figure 101: The total temperature at the outlet, wind speed 2 m/s.....	131
Figure 102: The volume fraction of phase 2 (water) in the middle of the model, wind speed 2 m/s.....	131
Figure 103: The volume fraction of phase 2 (water) at the inlet, wind speed 2 m/s.....	132
Figure 104: The volume fraction of phase 2 (water) at the outlet, wind speed 2 m/s.....	132
Figure 105: The strain rate in the middle of model, wind speed 2 m/s.....	133
Figure 106: The strain rate at the outlet, wind speed 2 .....	133
Figure 107: The density of the mixture at the middle of model at wind speed 3.2 m/s.....	134
Figure 108: The velocity magnitude at the middle of the model at wind speed 3.2 m/s .....	134
Figure 109: The velocity in z-direction in the middle of the model at wind speed 3.2 m/s ..	135
Figure 110: The velocity in z-direction at the inlet at wind speed 3.2 m/s.....	135

Figure 111: The velocity in z-direction at the outlet at wind speed 3.2 m/s.....	136
Figure 112: The total temperature in the middle of the model at wind speed 3.2 m/s .....	136
Figure 113: The total temperature at the inlet at wind speed 3.2 m/s.....	137
Figure 114: The total temperature at the outlet at wind speed 3.2 m/s.....	137
Figure 115: The volume fraction of phase 2 (water) in the middle of the model at wind speed 3.2 m/s.....	138
Figure 116: The volume fraction of phase 2 (water) at the inlet at wind speed 3.2 m/s.....	138
Figure 117: The volume fraction of phase 2 (water) at the outlet at wind speed 3.2 m/s.....	139
Figure 118: The strain rate in the middle of model at wind speed 3.2 m/s.....	139
Figure 119: The strain rate at the outlet at wind speed 3.2 m/s .....	140

## GLOSSARY

BOM	Bureau of Meteorology
CFD	Computational Fluid Dynamics
CFX	Central Florida Expressway Authority
CRC-IF	The Cooperative Research Centre for Irrigation Futures
CSIRO	Commonwealth Scientific and Industrial Research Organisation
DES	Detached Eddy Simulations
DHI	Danish Hydraulic Institute
DPIRD	Department of Primary Industries and Regional Development
h/d	The ratio of the distance between the cylinder and the ground (h) to the cylinder diameter (d)
IIHR	Iowa Institute of Hydraulic Research
LDV	Laser Doppler Velocimetry
LES	Large Eddy Simulation
MAC	Marker-and-cell
NCEA	The National Centre for Engineering in Agriculture



NS	Navier–a Stokes
----	-----------------

PIV	Particle Image Velocimetry
-----	----------------------------

RANS	Reynolds Averaged Navier-Stokes
------	---------------------------------

SST	Shear–stress transport
-----	------------------------

URANS	Unsteady RANS
-------	---------------

USQ	University of Southern Queensland
-----	-----------------------------------

VOF	Volume of fluid
-----	-----------------

# CHAPTER 1: INTRODUCTION

## 1.1 Background

Over the last decade, many studies and reports have shown that the weather is going to be more extreme in the world, rainfall rate will be decreased and more intense hot days. Therefore, the severity of droughts is going to increase and so create a big threaten for the world with the drought. Drought has been cited as the one of the most serious natural disasters in terms of loss of life and its impact on agricultural production, health, ecosystems, economics and urban water supplies. It leads to negatively impact the human health and increases in mortality rates.

One of the continents that is considered the driest inhabited continent on the earth, is Australia which has been suffered from the drought since many decades (Steffen, 2015). Many records have shown that the climate in the different areas cross Australia, is going to be drier and warmer especially over Southern Western Australia (DPIRD, 2017). Moreover, the rainfall is expected to be less by 50% in some areas around Australia by 2070 (Craig et al., 2005). According to Bureau of Meteorology (BOM), the rainfall rate was below average for September 2017 for different areas of Australia such as south of the Cape York Peninsula, New South Wales, northern and far eastern Victoria, South Australia south of Lake Eyre and east of Ceduna, and eastern Tasmania Queensland (BOM, 2017). Figure 1 shows the rainfall deficiencies for 7 months in the west coast of Western Australia between about Exmouth and Perth, While Figure 2 shows the rainfall deficiencies for 4 months in South Australia and western border of New South Wales.

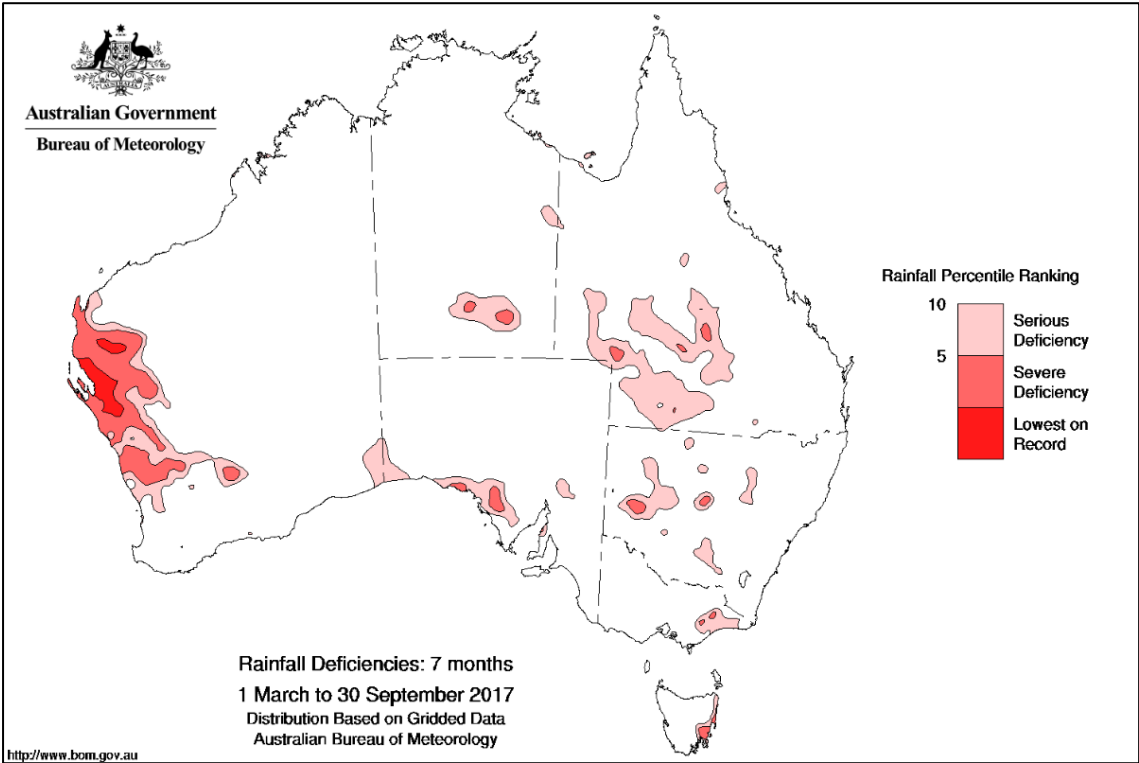


**Figure 1: Rainfall deficiencies: 7 months (BOM, 2017)**

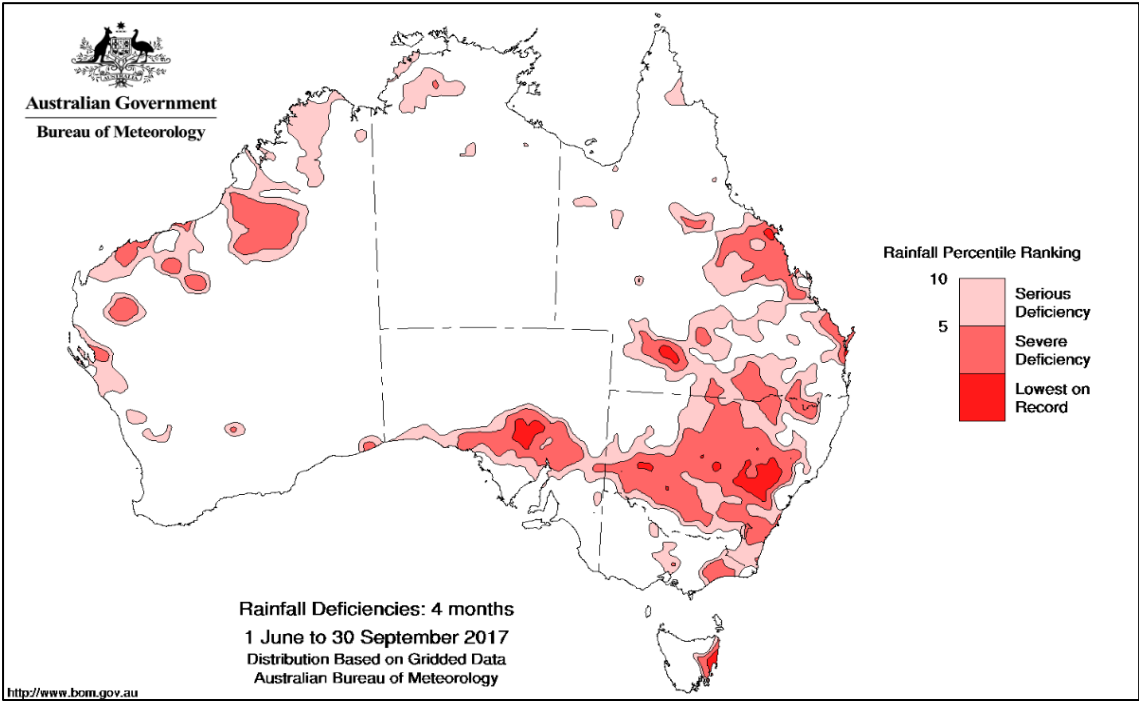


**Figure 2: Rainfall deficiencies: 4 months (BOM, 2017)**

Therefore, drought has received much attention from governments around the world. Many strategies have been developed to overcome drought including decreasing the evaporation rates from open water storage reservoirs since losing water because evaporation is a big problem that has a significant impact on economics and environment of many countries. Evaporation from water resources, is an important issue that have been covered by different researchers as it has a significant impact on the economic growth especially in areas where the climate tends to have a big change. Many attempts to reduce and mitigate the loss of water because of evaporation have been done by using different mitigations

One of the successful methods to reduce the evaporation rate is monolayers. However, this method shows variability of performances since it is broken up and then fail to preform effectively because of wave generated by wind. Therefore, the phenomena of how waves are generated by wind need to study in order to give clear insight on the reason that affects monolayers. This study will determine how the waves are generated on the water surface under the effects of winds. It will include using Computational Fluid Dynamics (CFD)/ ANSYS fluent to develop a three-dimensional model within turbulent flow regime and using detached eddy simulation (DES). The results are obtained from this study can be used in future to help setup the right strategies to mitigate evaporation.

## **1.2 Objectives**

The main objectives of this project are:

1. Research on the theory of wind and water wave.
2. Define the monolayer and the benefits of use it to prevent the evaporation

3. Investigate different models of Computational Fluid Dynamics (CFD) such as Reynolds Averaged Navier-Stokes (RANS) and Large Eddy Simulation LES, and how they produce the Detached Eddy Simulations (DES) model.
4. Investigate different two-phase CFD models to determine the most appropriate for this case.
5. Develop CFD model of problem.
6. Using DES model with a two-phase model from air and water which will be simulated to study the conditions of water surface for a small tank.

### **1.3 Research questions**

Several questions for this research have been raised and thereby created a good motivation to do this project:

1. What are the monolayers and why it has been used widely to reduce the evaporation?
2. What are obstacle that face monolayers to perform effectively on water surface?
3. What is the reason behind formation and growth the waves?
4. What is the relationship between wave and wind?
5. What are previous and current studied to cover wind- wave's phenomena?
6. Has CFD been used to study this phenomenon?
7. What are the expected results of this project?

### **1.4 Project Contributions**

The results of this project will contribute to the current literature by providing and explaining the phenomena for how the waves are generated under the effects of wind. This will be done

by developing a three-dimensional model of CFD to examine and detail the simulations of sub surface layer in wind-generated waves. Getting clear insight about the main properties of waves will help in improving the monolayers to be used for reducing the evaporation even under the wave's conditions that impact them. The model is preliminary which means that is required further studies and development in coming future in order to obtain better results. However, obtaining the results about the important properties of waves such wave height and wavelength in despite of the difficulties, means the project has met all its objective.

## **1.5 Project Rationale**

This research has been done about this topic because there is a big gap in studying the wind generated waves. Although many studies and experiments have been done about different areas related to the waves, they did not cover the waves' phenomena by the way that has been used in this dissertation. This way includes design and optimizing a CFD model to study the properties of the waves on the water surface and the reasons behind the formation and growth of waves by utilizing DES model. Therefore, a significant contribution will help be added to current researches to save the water against the evaporation.

## **1.6 Consequential Effects**

Explaining the consequential effects of this project will include sustainability, ethical issues, and safety and risk issues, as following:

- For the sustainability, in this project, CFD helps to create and design a model that is considered as a simple of the real world without any need to build large physical prototypes. Studying this sample and optimizing it will lead to save money, power

and time. For example, studying the waves in real world required more many and time to get some results even the results might not be accurate as like as the results from the CFD. Moreover, this model gives more understanding of wind generated waves without needing to provide the big effort that used in the experimental studies in the real world. The simulation in this project also has not any impact on the environmental. Briefly, this project will improve the sustainability of water resources.

- Comparing with Engineers Australia Code of Ethics and the policy of the University of Southern Queensland, there were not any ethical issues with this project. For example, the aim of the project will help to save the water resources which are very important for the health and wellbeing of the public.
- The project does not have any risk issues that required more safety steps against them because it does not require any work in the workshop or in the field. It might have some effects on the author's health.

## **1.7 Outline**

The dissertation is divided to five chapters cover all the related information to the topic. All it includes some appendixes that cover more related information. Following an overview for these chapters:

### **1.7.1 Chapter 1. Introduction**

This chapter provides introduce the reader to the topic that have been covered in this dissertation. Then, it covers the objective and aim of the project following by research questions. The project contribution and the reasons behind carrying out this dissertation have

been explained. Information about the consequential effects of the project have been provided. This chapter is included with giving an overview for all the dissertation's chapters.

### **1.7.2 Chapter 2. Background and Literature Review**

This chapter presents a review for previous related works and literatures that have been done on waves generated by wind. It shows the reader the gap and the motivations behind doing such project. It covering different topic including evaporation, monolayers, wind generated waves, computational fluid dynamics (CFD) and detached eddy simulation (DES).

### **1.7.3 Chapter 3. Preliminary model**

In this chapter, the way in which this project has been started will be presented. It includes information about the journey of learning CFD and then the steps that were done before reaching the final model that will give the expected results. This chapter includes different sections such as journey of learning, Preliminary computational Domain, mesh generation, setup and analysing data.

### **1.7.4 Chapter 4. Final model**

This chapter provide information about the final model that have been reached after different steps and changes were undertaken. In this chapter also the obtained results will be presents with analysing them. Moreover, it will include model validation and the limitation that the author suffered from during preparing this project.



### **1.7.5 Chapter 5. Conclusions and Recommendations**

In this chapter, this dissertation will be included to give brief explanation about all important aspect of the project. It also will present the recommendation and the future work required to improve such project.

## **CHAPTER 2: BACKGROUND AND LITERATURE REVIEW**

Chapter 2 has been written to covers different topics that related to the main topic of this thesis. These topics includes evaporation, monolayers, wind generated waves and computational fluid dynamics (CFD).

### **2.1 Evaporation**

Losing water because of evaporation is considered a big problem that has a significant impact on economics and environment of many countries, especially countries who rely on water stored in reservoirs for different uses such as Australia and most semi-arid countries around the world (Helfer et al., 2012). In the next 60 years, it is expected that the evaporation will be increased yearly by around 16% with high increase in the temperature in Australia (Helfer et al., 2012). Bureau of Meteorology in Australia stated some expectations regarding the weather depending on the monitoring and analysing for Australia's climate done by the Bureau of Meteorology and CSIRO (BOM, 2006):

- Since 1910, Australia's climate has warmed by 1 °C in both mean surface air and surrounding sea surface temperature. Moreover, these temperatures are expected to continue increasing in the future (Figure 3).

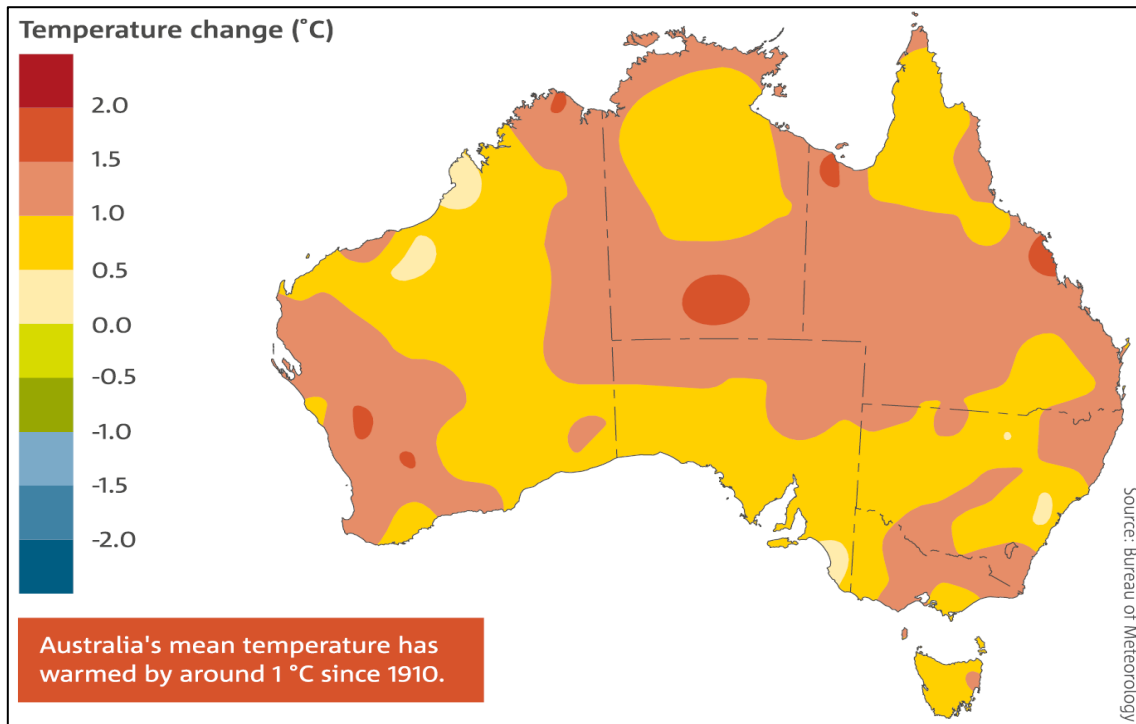


**Figure 3: Annual mean temperature changes across Australia since 1910 (BOM, 2016)**

Since 1970, rainfall has decreased across southern continental Australia by around 19 per cent. It is also expected to decrease during winter and spring with longer period of drought.

Around 40% percent of farm dams and water storages in Australian water could be lost because of evaporation (Considine, 2007). This increase in evaporation rate and decrease the rainfall would have a negative impact on different productions and all uses of water and therefore create. a big challenge (Craig et al., 2005).

Figure 4 shows the average pen evaporation annual across Australia which was done by Bureau of Meteorology/ Australia.

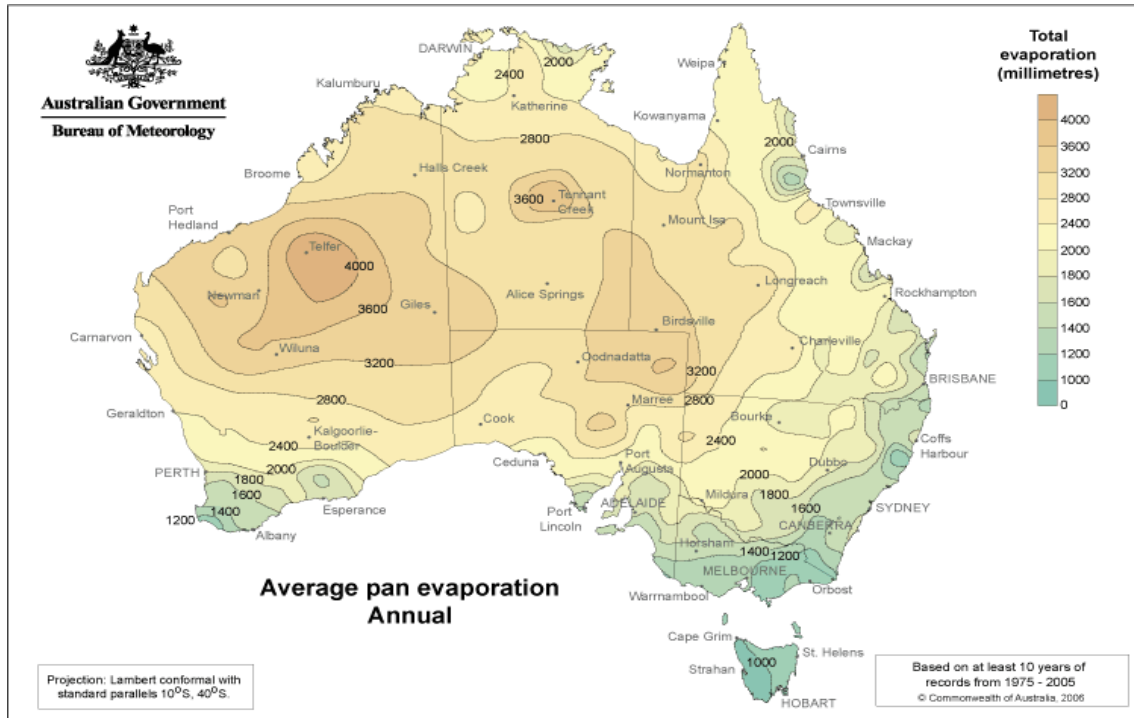


**Figure 4: Average pan evaporation (BOM, 2006)**

Evaporation is likely to decrease the water which is being used in industries, agriculture and other natural ecosystems. Thus, important strategies have been developed in order to face such threat and guarantee availability of water for the life in Australia (Helfer et al., 2012). This issue creates a need to find and adopt different solutions to reduce the evaporation rates from water storages. There are many methods including structural, chemical and physical methods, have been investigated and developed in the last decades to reduce the evaporation such as floating covers, shade cloth, wind breaks, destratification mechanisms and chemical barriers (Jennison (2003); Baillie (2008); Sherman et al. (2010)). Generally, most of these techniques are too expensive, unworkable and have negative impacts on environment (Jennison, 2003).

Floating covers (Figure 5) is considered one of the effective method because it reduces the evaporation losses by 90% with installation cost between \$5.50 to \$8.50 per square metre (Baillie, 2008). These covers float on the water surface and are fixed by some forms of anchoring mechanism to performance as physical barriers that help to prevent the water vapour to pass in any direction (Yao et al., 2010). Finn and Barnes (2007) stated that floating covers helps to reduce the level of solar radiation and wind speed.



**Figure 5: Floating cover (Baillie, 2008)**

However, this method is limited to be used in storages with size less than 2 hectares in surface area (Baillie, 2008). Moreover, floating covers are unable to capture the rain without drainage infrastructure unlike some other evaporation mitigation techniques. Problematic biofilms can grow on internal surfaces of the covers. With floating covers, staff is likely to face difficulty with access or visual assessment of the water storage (Finn and Barnes, 2007).

In addition, Yao et al. (2010) stated that these covers are likely to reduce the level of the dissolved oxygen in the water and reduce the temperatures of water surfaces.

The second method is suspended covers or shade cloth (Figure 6). These covers are installed as a sail to be suspended over water with using poles and steel cable to support it. These covers work to block solar radiation to reach the water and thereby reduces the temperature of water surface and then mitigate the evaporation. It also helps to reduce wind speed (Yao et al., 2010). The installation of such covers positively impacts the quality of the stored water (Craig et al. (2005); Finn and Barnes (2007)). Suspended covers can be used for larger storage sizes of about 5 hectares in surface area (Baillie, 2008).

However, it has less efficiency than floating cover as it reduces evaporation losses by 70% with Installation costs vary from \$7.00 to \$10.00 per square metre (Baillie, 2008). Moreover, installing this method requires high cost, especially for the large reservoirs. It also impacts the life of the organisms in the reservoirs because it leads to reduce the sunlight and dissolved oxygen level and thereby a reduction will occur in local recreational activities including fishing (Yao et al., 2010).



**Figure 6: Shade-cloth covers (Finn and Barnes, 2007)**

Wind breaks is another method that has been used to mitigate the evaporation. Wind breaks consist of shrubs and trees that form barriers to reduce the wind speed (Figure 7). They are usually placed around the area that need to be protected from the effects of the wind such as homes, animals and water storages (Brandle et al., 2004). It plays a good role to reduce the evaporation by reducing the hot wind which passes over the water surface and thereby reducing the humidity gradient between air and water surface. Also, by reducing the speed of the winds, the number and sizes of generated waves on the water surface will be decreased (Helfer et al., 2009). In addition to the benefits of this method on reducing the evaporation, it has other benefits such as decreasing soil erosion, protect the farm animals from the unsuitable weather, and increase crop yields.

However, it might impact the piping and increase the risk of the failure because of planting the trees around the water storages (Jennison, 2003). For example, the roots will grow in deteriorated, damaged and leaked pipes and then affect water, nutrients and oxygen

(CityofSydney, 2015). Moreover, this method has some drawbacks such as growing time for the trees. Furthermore, this method is not preferred to be used on the large dam and the studies have shown that only minor reduction in the evaporation rates will happen. The reductions in annual evaporation levels for 20, 30 and 40m high windbreaks, are only 2.5, 3.6 and 5.6% respectively (Watts (2005); Helfer et al. (2009)). Therefore, it is recommended for just small water reservoirs (Hipsey et al., 2004), despite a large-scale shelterbelt can reduce the evaporation from square waterbodies (waterbody length,  $X = 60$  m) by approximately 20-30% (Hipsey et al., 2004). Moreover, Wang et al. (2001) stated that regional evaporation in China was decreased by using large-scale shelterbelt networks 14%.



**Figure 7: Wind breaks (Helfer et al., 2009)**

Fourth method to reduce the evaporation, is Artificial Destratification which uses the mechanical energy by using devices work to increase the vertical transfer of heat and



dissolved oxygen which helps in reducing the strength of the vertical temperature gradient in the water column. It works to reduce the evaporation by decreasing the saturated vapour pressure of the air as a result of decreasing the surface layer temperature near the water. The most common three mixers that are used in Artificial Destratification are bubble plumes, draft-tube mixers and unconfined mixers .However, practically, results showed that using destratification method is not likely to reduce evaporation in storages with depth less than 20 m due to small volume of cold water that is need for mixing and thus, it will be effective in deeper storages only (Van Dijk and Van Vuuren (2009);Sherman et al. (2010)).



**Figure 8: Destratification systems. Clockwise from top left: 10 bubble plumes, draft-tube mixer and unconfined mixers (Sherman et al., 2010)**

## 2.2 Monolayers

In addition to the small water reservoirs, in large storages, greater than 5 hectares in surface area, chemical barriers (monolayers) are suitable to be used with such size of reservoirs (Baillie, 2008). This layer which is a white powder prior to application, is made up of hydrated lime and an octadecyl alcohol (stearyl alcohol) and hexadecane (cetyl alcohol) which forms a thickness of one molecule (2 millionths of mm) at air/water interface (Figure 9) (Craig et al. (2005); Barnes (2008)). Monolayers are a collection of molecules that have been formed on an appropriate surface spontaneously by chemisorption and self-organization of long series molecules (Prashar, 2012).

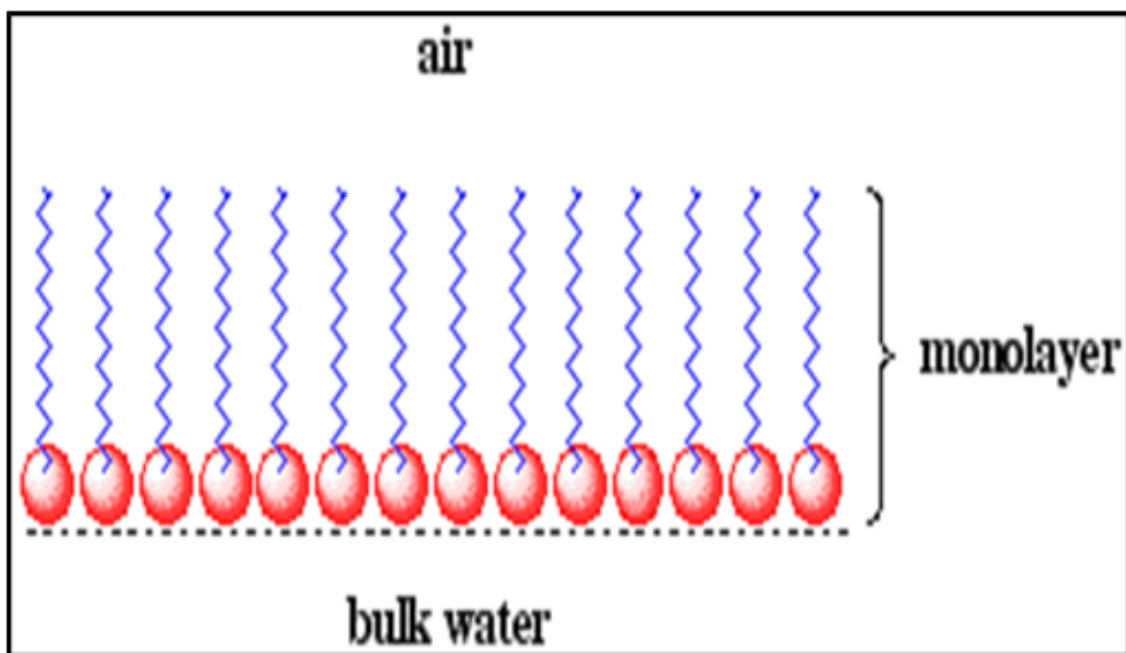


**Figure 9: Monolayers structure (Toreki, 2015)**

Monolayers are amphiphilic (Figure 10) which work as insoluble layers at air- water interface. Such layers have two parts a hydrophobic (water-repelling) part which prevents the molecules to be mixed or dissolved in water while the hydrophilic (water-attracting) part

allows them to be dissolved with water surface and thereby will help to prevent the molecules from piling on top of each other. Monolayers work to increase the thickness of apparent surface layer which leads to reduce the evaporation rate (Hardy (1912); McJannet et al. (2008)).

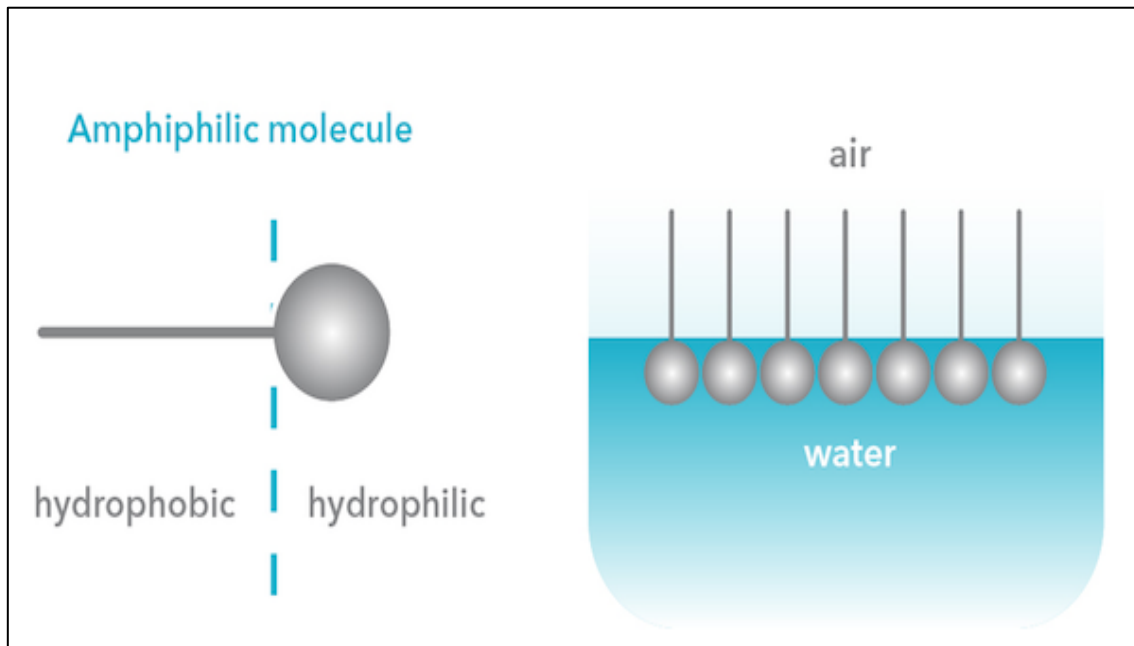


**Figure 10: Amphiphilic molecules over water surface (Panjabi et al., 2016)**

Monolayers are a self-spreading chemical that can be spread at a rate of 0.50 to 0.75 kg/ha, that separates in a few days. For small reservoirs, the common method to spread it is by hand, but in larger reservoirs, there is an automatic applicator which was used for 120 ha storage (Craig et al., 2005).

Chemical barriers are suitable to be used with installation costs vary until \$0.38 per square metre, even it is expected to reduce the evaporation by 40% (Baillie, 2008). Monolayers are considered the best technique to reduce the evaporation among different methods that required higher cost, more time to install and maintain them, impractical and have more environmental deterioration (Schouten et al. (2011); Jennison (2003)).



**Figure 11: Monolayer is spreading across the surface of water (Craig et al., 2007)**

Moreover, these layers have an ability to decrease the penetration of ultraviolet UV into the water which will positively affect the aquatic ecosystem, by reducing the harmful effects on the life in the water (Schouten et al., 2011). Furthermore, monolayers are attractive to be used for different reasons such as, it can be easily prepared, the reasonableness of surface properties through modification of molecular structure, and the ability to be used as building blocks in more complex structures (Schreiber, 2000).

Craig et al. (2005) has done assessment for different technologies that have been used to reduce the evaporation such as monolayers, shade cloths and E-VapCap (floating cover). These assessments have included the impacts of these technologies on the aquatic environment and water quality considering some parameters such as pH, dissolved oxygen, temperature, electrical conductivity and algae. The results show that monolayer is better option comparing with other technologies (Table 1).

**Table 1: Comparing between three evaporation mitigations (Craig et al., 2005)**

	pH	Dissolved oxygen	Temperature	Electrical conductivity	Algae
Monolayer	-	-	-	-	-
E-VapCap	-	↓	↓	-	Not analysed but reducing sunlight will reduce algal populations
Shadeecloth	-	-	↓	-	Not analysed but reducing sunlight will reduce algal populations

Another advantage is that monolayers can be applied when they are required, for example when the rate of evaporation is high, the effects of wind is low and the storage has some water (Craig et al., 2005). Moreover, The National Centre for Engineering in Agriculture (NCEA) at the University of Southern Queensland (USQ) has indicated that monolayers are the best option to prevent the loss in agricultural water in Australia, even it reduce that in lower level comparing with other evaporation mitigations (Craig et al., 2007). Palada et al. (2012) stated that monolayers are highly required to reduce the evaporation due to their comparatively minimal cost and ease of application.

Another study has been done by mixing films of octadecanol and hexadecanol to study the ability of these films to reduce the evaporation and two samples have been taken from

reservoirs to the laboratory in São Paulo (Gugliotti et al., 2005). The study shows high ability of monolayers around 57% to reduce the evaporation from the natural water.

Monolayers have been tested in field and compared to a nearby control lake near Wichita Falls, Texas. The results showed that monolayers are the best with considering the reduced effects on water quality or the environment (Verlee and Zetland, 2014). Much research has been extensively done on monolayers in last decades and most of these studies have shown how the monolayer method can be put on the top of the list of the technologies that have been used to reduce evaporation and save the natural water.

However, many studies have shown variety with the evaporation reduction values between 0% - 43% because of many factors including applying different products, characteristics of water body and climatic conditions. However, this variation at the same time shows the importance of using monolayer to reduce the evaporation (McJannet et al., 2008). Knights (2005) has tested a monolayer product performance on the surface of the 120 hectare storage. Mixing hopper (Figure 12) was used to mix the monolayer and to ensure effective distributed across the water surface of the storage. Other apparatus have were used including a centrifugal pump, a grid distribution system, comprised of poly-pipes, with nine outlets.



**Figure 12: Mixing hopper (Knights, 2005).**

The results showed that monolayers are affected by wind and wave interferences and so it was disrupted and was not able to protect the water against the evaporation until the effect of wind ceased. The reduction of evaporation was about 20%.

Craig et al. (2007) has outlined the research that has recently been done by the Cooperative Research Centre for Irrigation Futures (CRC-IF). They stated that there are deficiencies in current chemical barriers with possibility for significant enhancement. These deficiencies are because of some obstacles such as the effects of wind, waves, solar radiation and bacteria or microlayer impurities in the water. Other studies have been done about controlling the evaporation in reservoirs in New Delhi, these studies included testing monolayers with thickness 0.015 micron on the water surface. The results showed that monolayers will be broken under harsh wind speed (greater than 16 km/ hr) and under the changes in directions of the winds (BPMO, 2006).



Barnes (2008) has reported a summary for some experiments that were done on monolayers. These experiments are based on using the long-chain alcohols, hexadecanol and octadecanol. Monolayers have showed under field conditions to be highly variable, some tests in some fields' shows high ability to reduce the evaporation while in others their effects almost non-existent. The ability of monolayers to reduce evaporation on open water storage decreases quickly and thereby they need to be reapplied every 1 or 2 days. It was stated that monolayers show a poor resistance to the effects of waves and wind. Palada et al. (2012) have done run of simultaneous tests for wind and wave in a controlled water tank with dimensions (15 m×0.46 m× 0.85 m) with octadecanol suspension monolayer. The tank has an automated wave paddle to produce wave height and wave frequency.

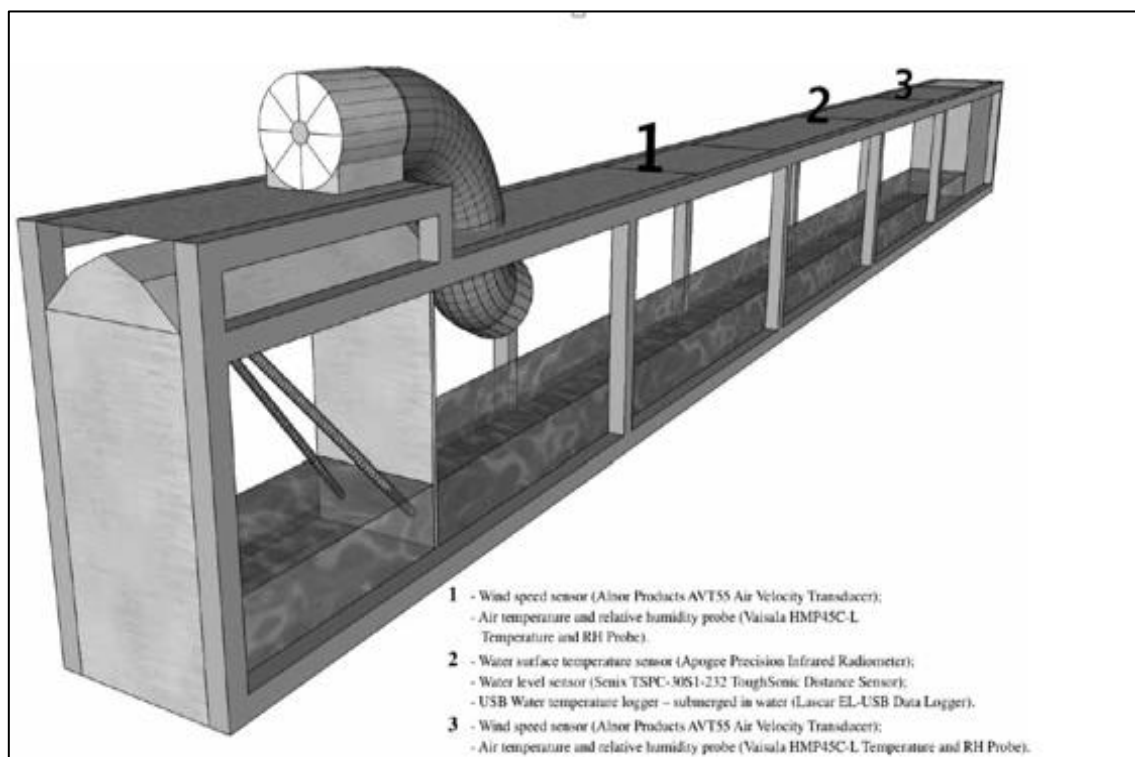


**Figure 13: Wave tank setup located at Griffith University (Palada et al., 2012)**

The effect of monolayers has been tested under different wind speeds (1.3, 0.9, 1.1, 0.6, 0.45, 0.3 m/s) with constant wave height (2 cm) and frequency (6 s). The results showed that monolayers effectively decrease the rate of evaporation at speed below 1.3 m/s. In contrast, higher wind speed will break the monolayers and make it ineffective to reduce the evaporation. Figure 14 shows monolayer resistance against evaporation with different wind speeds.

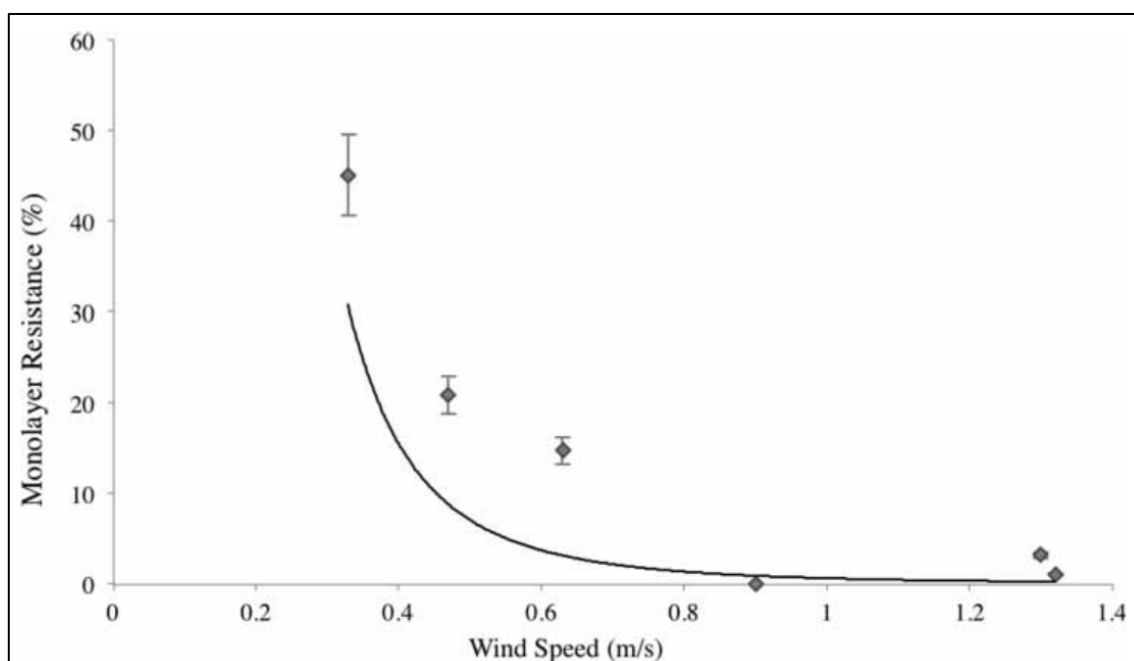


**Figure 14: Monolayer resistance vs evaporation (Palada et al., 2012).**

Furthermore, the performance for a series of chemically synthesized compounds with different head groups were investigated under static and dynamic wind conditions by using a laboratory method to measure the ability of monolayers to reduce the water evaporation under the effect of wind. A centrifugal fan was used in the experiment to generate winds flows out over the water and it was connected to a wind tunnel. A rectangular container (10.5 cm  $\times$  16.3 cm) also was used to contain 800 mL of water as shown in (Figure 15). Schematic diagram of wind tunnel set up (Prime et al., 2012). The results showed that

despite of some groups of monolayers have very short life and they affect poorly under the impact of winds, they still capable to reduce the evaporation even with small rate.

Figure 16: Mass of water lost over time shows the difference between the ability of different groups of monolayers (C16OH and C18OH) compared to the control of evaporation with winds speed 25km/hr with absence of monolayers (Prime et al., 2012).

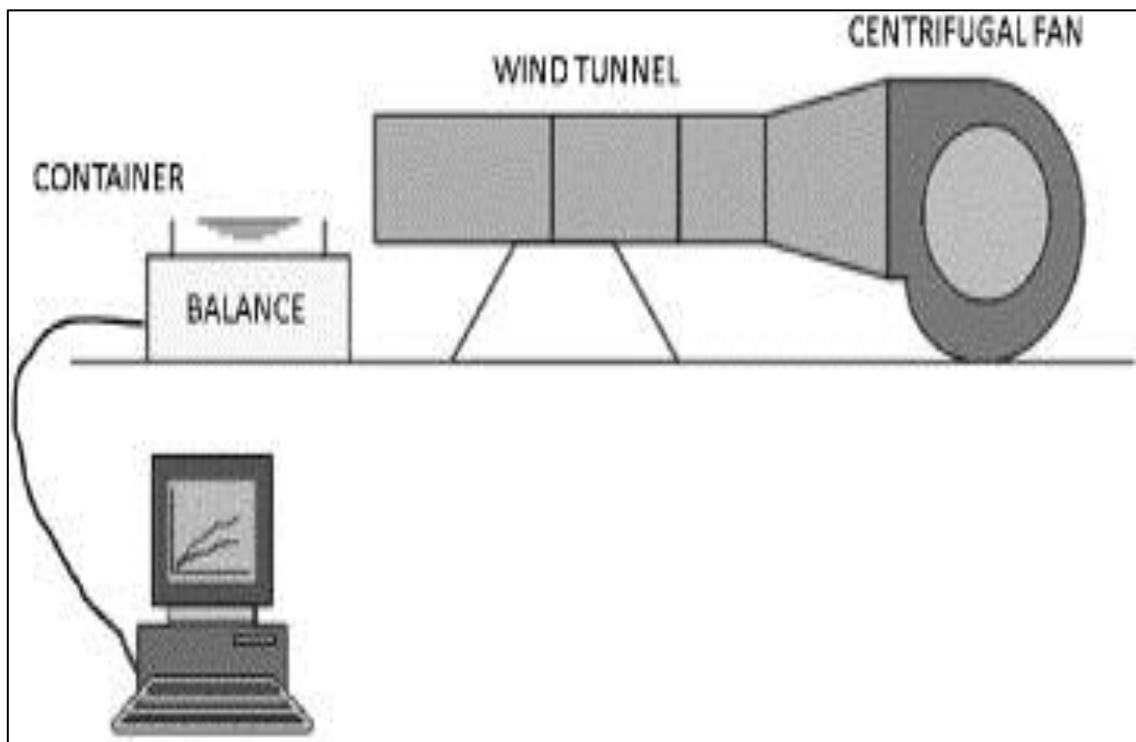


**Figure 15: Schematic diagram of wind tunnel set up (Prime et al., 2012).**

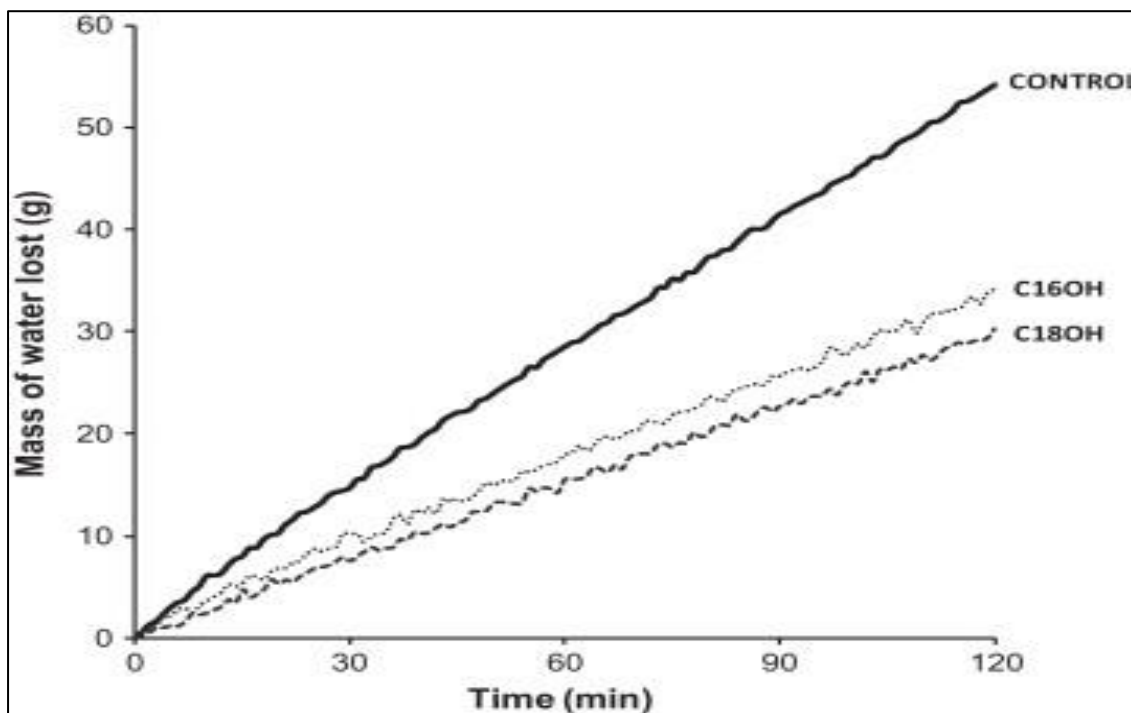


**Figure 16: Mass of water lost over time (Prime et al., 2012).**

Much research has been done on the factors that impact the monolayers and make them ineffective to reduce the evaporation, most of these studies have identified the major factor as the action of winds that break and remove monolayers waves and thereby enforce them to migrate from the surface of open water storages (Crow (1963); Fitzgerald and Vines (1963); Vines (1962); Wandel et al. (2017)). For example, cetyl alcohol monolayers cannot produce any role to decrease the evaporation rate, if it is affected by winds with 24 km/h speed (Vines, 1962). In addition, Craig et al. (2007) demonstrated in his initial investigations, that the most surface films are affected by wind and then it lost its ability against the evaporation. Therefore, wind and waves also need to be studied to understand the nature of them and then it might be important to support such researches.

## 2.3 Wind generated waves

### 2.3.1 General

Although the problem of how the wind generates waves continues to be a significant part of oceanographic research, many studies have been done about it. , Helmholtz and Kelvin tried to explain the formation of wind and wave (Thomson (1887); Helmholtz (1868). However, Sir William was the first researcher that tried in 1874 to put the concept of wind-wave generation on a firm mathematical footing (Thomson, 1981a). Also, Dean and Dalrymple (1991) said that over 150 years, a lot of books and articles have been published in the field of water wave theory. Simply, waves have been defined by (Dean and Dalrymple, 1991) as an action of forces such as wind that deforms water surface against the act of gravity and tension forces. In addition, Sawan (2003) has explained how the wave generated by wind, small ripples start to be formed when the wind passes over the water surface, these ripples will grow and form into fully developed waves (Figure 17).

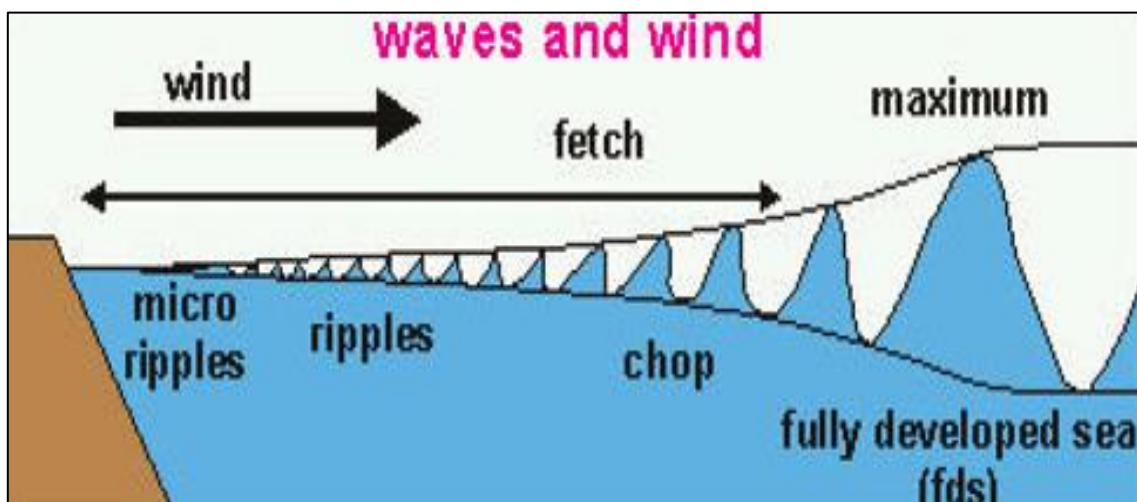
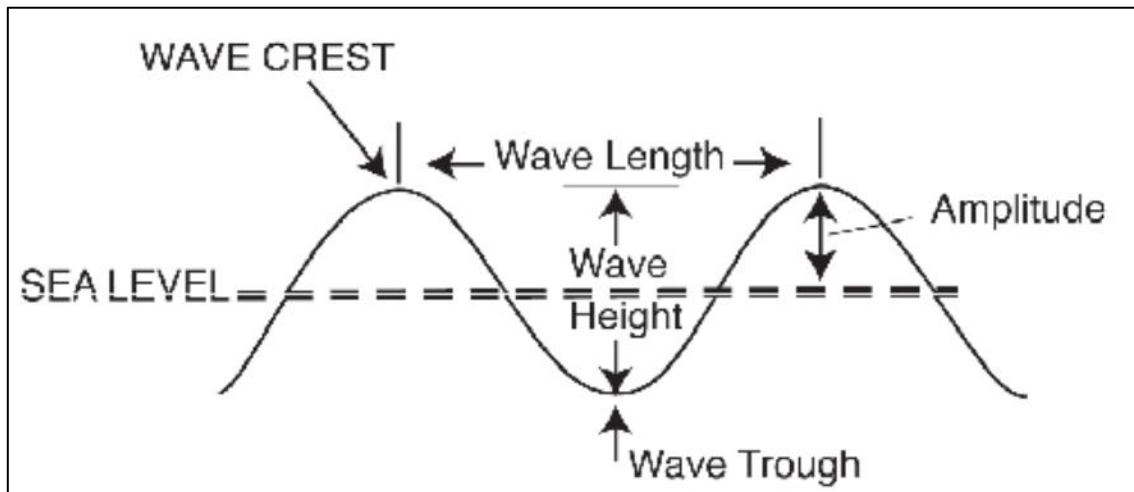


Figure 17: Wind Generate Waves (Sawan, 2003)

The formation of the waves is affected by winds speed, winds pressure, wave fetch and wind period (Deo, 2013). Whatever the type and size of the waves, all waves have the same

characteristics. From Figure 18 waves characteristics can be seen which include wave crest (highest part of a wave), wave length (the distance between two crest), wave height (the distance between the wave crest and trough) and the amplitude (half the wave height) (Olsen, 2011).



**Figure 18 waves characteristics (Olsen, 2011)**

The way that wind creates the waves, have been explained by different ways and by different researchers. The best explanation it was made by (Jeffreys, 1925) by his sheltering hypothesis (Thomson (1981a), Phillips (1957)). Jeffreys (1925) indicated that when the small waves are affected by wind, they will cause separating the pressure to components, one of them which is with the wave slope will develop the wave growth. However, this theory has a lack of how the wave is formed at the first and then developed (Thomson, 1981a). However, Chalikov (1978) mentioned that theories of wind waves that related to wave's generation that were presented by (Phillips, 1957) and (Miles, 1957) are the most important results. These theories give a clear qualitative interpretation of the mechanisms of wave energy exchange and are in satisfactory agreement with experimental data of (Barnett and Kenyon, 1975), but they lead to contradictions.

The understanding of the important processes of winds and waves has faced different challenges including having open-air observations: Platform movement, cost, sensor technology and inconsistency of the atmosphere, wave fields and ocean (Sullivan and McWilliams, 2010). Therefore, different studies whether experimentally or numerically have been done to study the waves generated by winds.

### **2.3.2 Modelling**

#### **Experimental study**

Different studies were carried out regarding how the winds can create waves on the surface of water. Kunishi (1963) was done a study for the physical processes on wind generated waves in a wind flume experiments. Different winds speeds were tested. With lower speed about 50 cm/s, there was no change on the water surface. However, with increasing the speed, small waves started to be formed. Kunishi found that there are three regimes when the waves formed: initial tremor, initial wavelet, and sea wave.

Moreover, Sawan (2003) has completed an experiment in the water Science and Engineering Laboratory at the University of Wisconsin – Madison, to compare between the experimental results with theoretical results regarding the wave growth. The experiment has shown that waves are formed and grown into fully developed waves. However, it has not shown how exactly the waves are grown.

Longo et al. (2012) has present a study about the turbulent structure in the water side of wind generated waves in a laboratory environment. The setup was two-dimensional which leads to some limitation to evaluate some dynamic mechanisms of turbulence. The field of the experiment was made by using water tank figure (13), with blowing air over it. Ultrasound

velocity profiler and Laser Doppler Velocimetry (LDV) have been used to measure the velocity. The results shows that due to micro-breaking, the turbulence is enhanced under the interface of air and water. Also it shows the properties of anisotropic turbulence that made up of a large range of wavelengths.

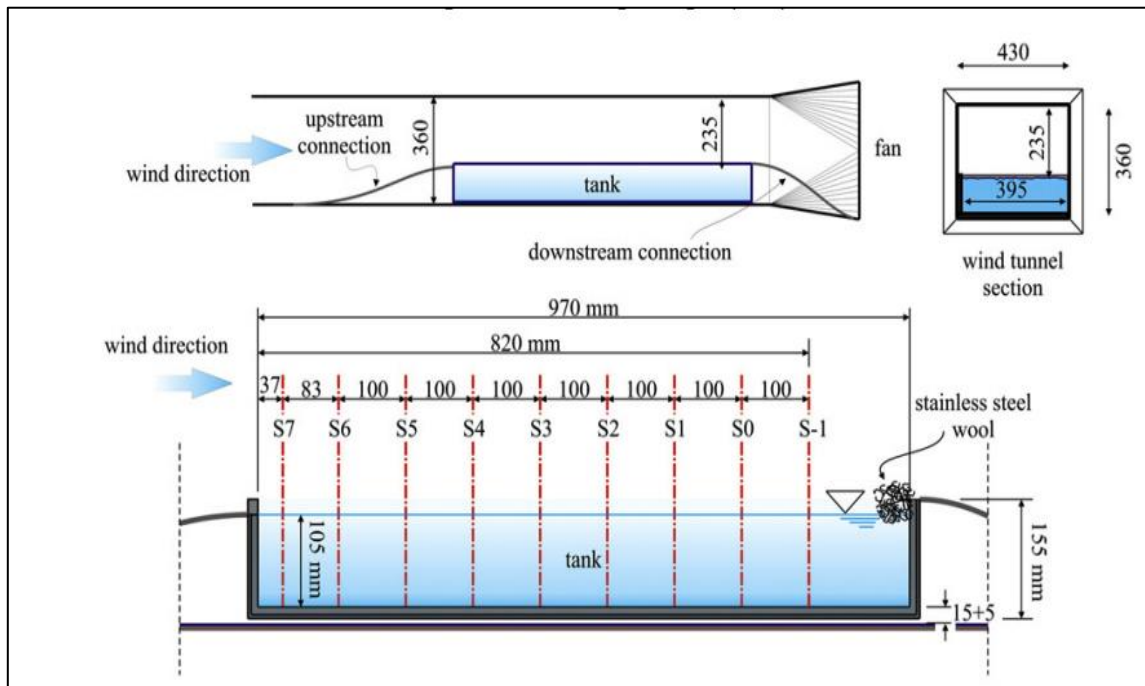


**Figure 19: wind tunnel and the water tanks (Longo et al., 2012)**

Paquier et al. (2015) has done a study on the early phases of wave's formation because of turbulent wind at the surface of a viscous liquid. The experimental field consists of a fully transparent Plexiglas rectangular tank with dimensions (Length = 1.5 m, Width = 296 mm and depth= 35 mm) filled with a water-glycerol mixture. Figure 20 shows the experimental setup.



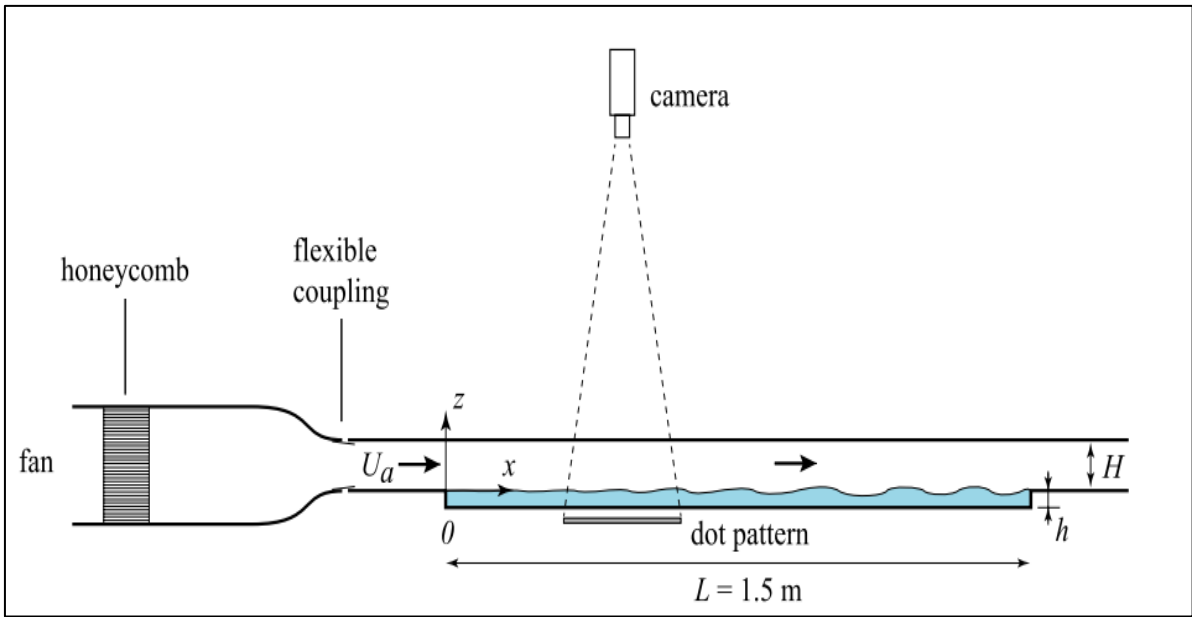


**Figure 20: Experimental setup (Paquier et al., 2015)**

The surface deformations were measured by Free-Surface Synthetic Schlieren (FS-SS). The results show two cases, in the first one with applying low speed, the deformation was dominated by rapidly propagating disorganized wrinkles in the stream wise direction. These deformations increase linearly with wind velocity without any relationship with the fetch. In the second case, with higher wind speed, the wave amplitude increases much more comparing with the first case with.

Another experiment has been carried out in a rectangular channel with dimensions (width = 40 mm and height 50 mm) to investigate and evaluate the parameters related to interfacial wave characteristics in a horizontal stratified flow. These parameters include the wave frequency, wave height, wave velocity, and wave slope. Parallel wire conductance sensors and Particle Image Velocimetry (PIV) have been used to detect the phenomena and to support the results from each other (Bae et al., 2017). Figure 21: The experimental facility for a horizontal stratified flow (Bae et al., 2017) was used in this study shown in Figure 21 .

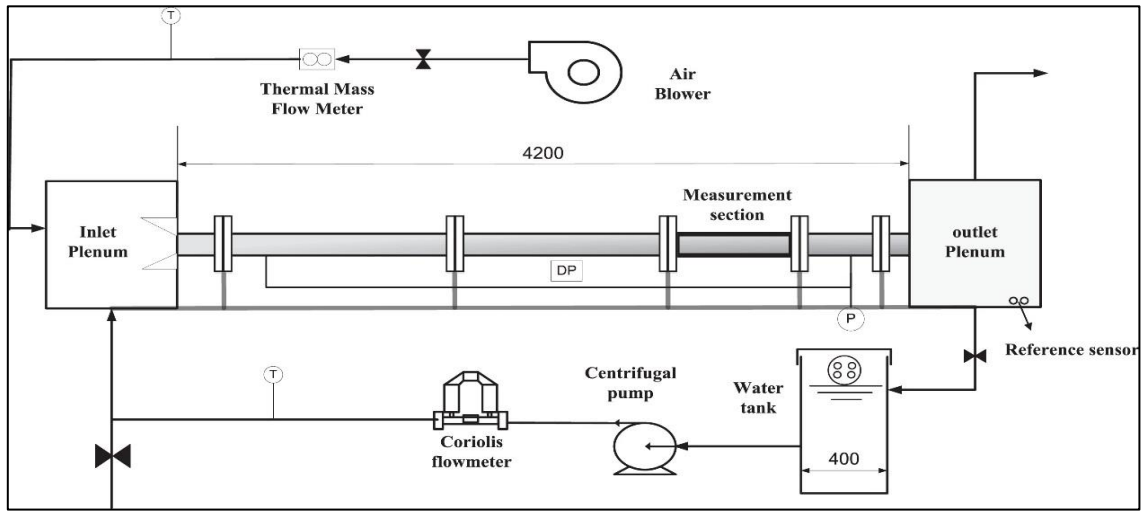


**Figure 21: The experimental facility for a horizontal stratified flow (Bae et al., 2017)**

This study has carried out a comparison with correlation found by (Mantilla, 2008) to determine its validity to the present stratified flow condition (Figure 22)(Figure 23).

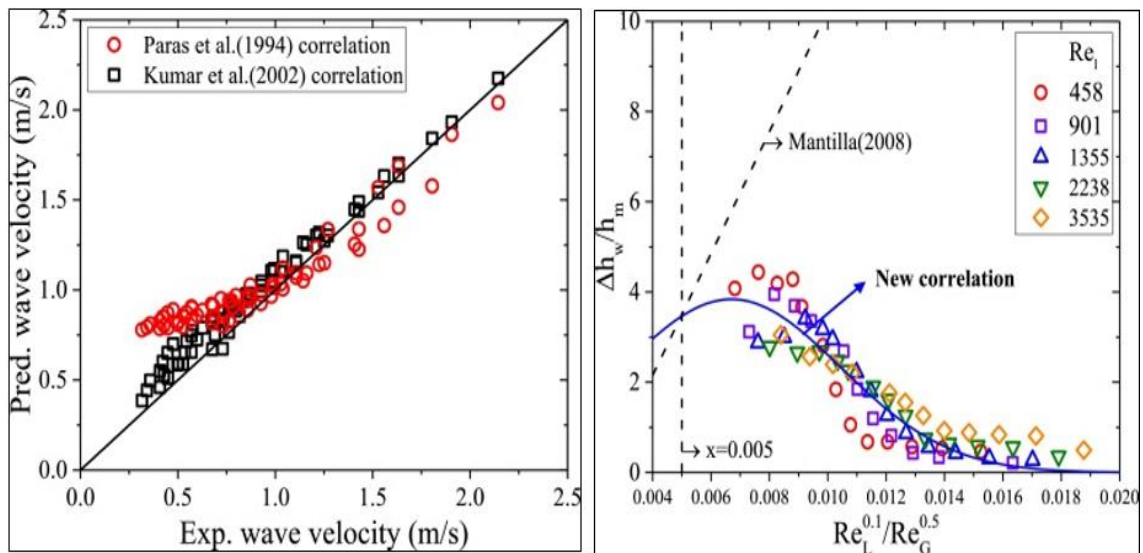


**Figure 22: Comparison of wave height and velocity correlation with experimental data (Bae et al., 2017)**

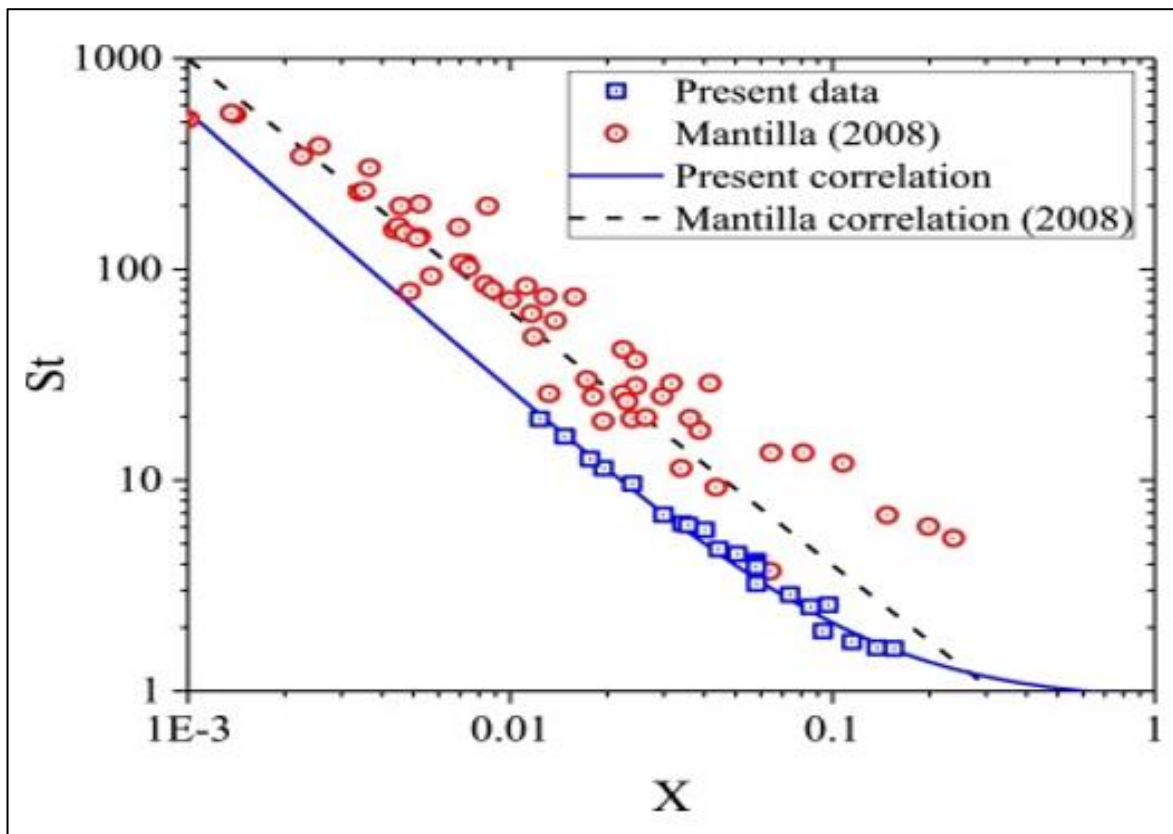


**Figure 23: Comparison of the wave frequency correlation with experimental data (Bae et al., 2017)**

The results show that the types of the present waves are similar to the types which have been detected by (Ottens et al. (1999); Mantilla (2008)) with different pipe dimensions. With respect to gas Reynolds number  $Re_g$  and the liquid Reynolds number  $Re_l$ , the result were obtained which include the parameters of waves. The results show a variation in the wave parameters (frequency, height, and slope) because of coalescence, breakup, and growth of the wave. Also, a direct relationship between the wave velocity and both  $Re_g$  and  $Re_l$  (Bae et al., 2017).

However, the experimental studies for waves generated by wind is not an easy task to measure and indicate the growth rates of waves for different reasons. Firstly, as the time

series of waves can be determined by doing a number of processes including wind input, nonlinear interactions and dissipation, thus, it is hard to find growth rates of waves depending on time series of the surface elevation without accurate assumptions about the causes behind forming waves. Secondly, the ratio of air density to water density is small which leads to small rates of growth and thereby it is required to determine very rigorous amplitude and phase of the wave-induced pressure fluctuations (Janssen, 2004).

### **Numerical study**

In last decades, the demand of numerical modelling for waves have been increased because of a rise in power of computation, the development of numerical algorithms, and increasing the use of open-source and commercial software (Silva et al., 2015). Therefore, different numerical studies have been carried out by different software such as computational fluid dynamics (CFD), MIKE21 and OCEANLYZ.

First of all, Sullivan et al. (2000) have done a study to examine the turbulent flow over idealized water waves by develop three-dimensional direct numerical simulations (DNS). They studied the wave's growth because of winds with setting an eddy-resolving numerical model with low Reynolds number. The results showed the existence of a critical layer a wide range of dimensionless phase speeds.

Park et al. (2001) has developed a finite-difference simulation method by using marker-and-cell (MAC) method and solving the Navier Stokes (NS) equation to study the nonlinear interactions between waves and a three-dimensional body in a numerical wave tank (Figure 24).

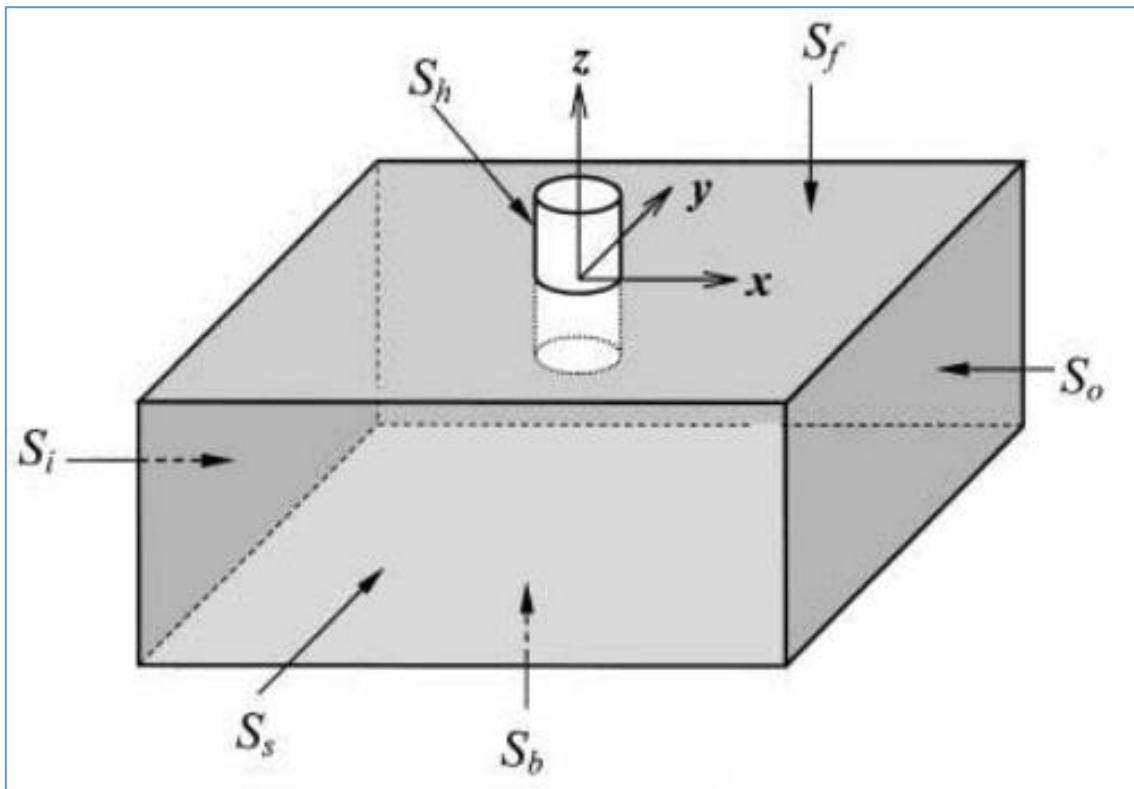


**Figure 24: Coordinate system and computational domain (Park et al., 2001)**

Wave breaking around the body has been simulated. The outcomes from the numerical method was compared with the experimental results of (Mercier and Niedzwecki, 1994). Reasonable results have been obtained for higher-harmonic wave run-up, and horizontal forces which are more sensitive to alterations in the speed than the first-harmonic wave.

Xu et al. (2007) has done numerical simulations for waves generated by hurricane Juan in 2003 by using SWAN (v.40.31) nested within WAVEWATCH-III (v.2.22; denoted WW3) wave models, applied on multiple-nested domains. The results show the effect of translation speed to generate the waves. By increasing the translation speed, both height and length of waves will increase and waves reached the maximum when their speed becomes same as translation speed. However, in this study, there was problem with large waves during and after the peak winds as they are overestimated.

Huang et al. (2011) have developed and evaluated a two-dimensional hydrodynamic model and a spectral wave model in closed dam in a real-world agricultural water reserve in south-east Queensland/ Australia by using MIKE 21 program developed by DHI. However, in comparison to the real-world measurements, the wave's periods have been underestimated. It is also found that monolayer cannot help with reducing evaporation rates at Logan's Dam because of the large waves, although it has better effects with calmer conditions.

Chen et al. (2014) have completed a study for non-linear wave interactions with offshore structures (a vertical surface piercing cylinder) for ranges of wave conditions by using OpenFOAM which it is open-source C++ library for continuum-mechanics problems. A 3D numerical tank have been setup in order to reproduce the experiments performed at Danish Hydraulic Institute (DHI). The total length is 15m and width is 2 m. The modelling was done for two-phase flow based on the unsteady, incompressible Navier–Stokes equations. The numerical results were compared with physical experiments. The comparisons have showed that OpenFOAM has an ability to give accurate results up to 4th order harmonic when used to model nonlinear wave interaction with offshore structures, with correctly captured.

Bühler et al. (2016) have modelled a multiphase system air and water by the two-dimensional incompressible interface Euler equation to find out a mathematically exact answer for the required speed of wind that passing over the water to keep and increase the exciting waves in the quiescent sea. They give a proof of the instability criterion that obtained by (Miles, 1957). Also they showed the ability to connect between the Kelvin–Helmholtz and quasi-laminar models of wave generation by unified a new equation.

Moreover, a study has been done to discuss the required procedure for obtaining a dependable estimation of wave parameters. In this study, the Ocean Wave Analysing toolbox,

OCEANLYZ, has been used. It contains different functions of MATLAB software for wave properties estimation. Sets of data fields have been analysed and developed. The study gives Understandings on parameters that affect a quality of wave data analysis. It also tried to minimize possible errors can happened with during collecting and analysing waves data (Karimpour and Chen, 2017).

Another numerical study has been done by (Shanas et al., 2017) to study the superimposed wind-waves in the Red Sea. This study was carried out by using WAVEWATCH III (WW3) in the Red Sea. Through this study, the variability of waves generated by wind has been studied during the daytime for first time in the Red Sea for a one-year period from December-2009 to November-2010. The outputs of the model (Hs and Tm) linked to the outputs at the buoy location during Dec 2009–Nov 2010. A comparison has been done between the output from buoy and the model as it expressed in Figure 25.

The measurements in buoy agree with both results of the model with CFSR and ECMWF winds. The analysis shows that different areas of the Red sea are dominated by different types of waves. It shows that 58% of area is influenced by non-superimposed waves, 28% area is dominated by superimposed waves and 14% area are dominated by co-existence of both superimposed and non-superimposed waves.

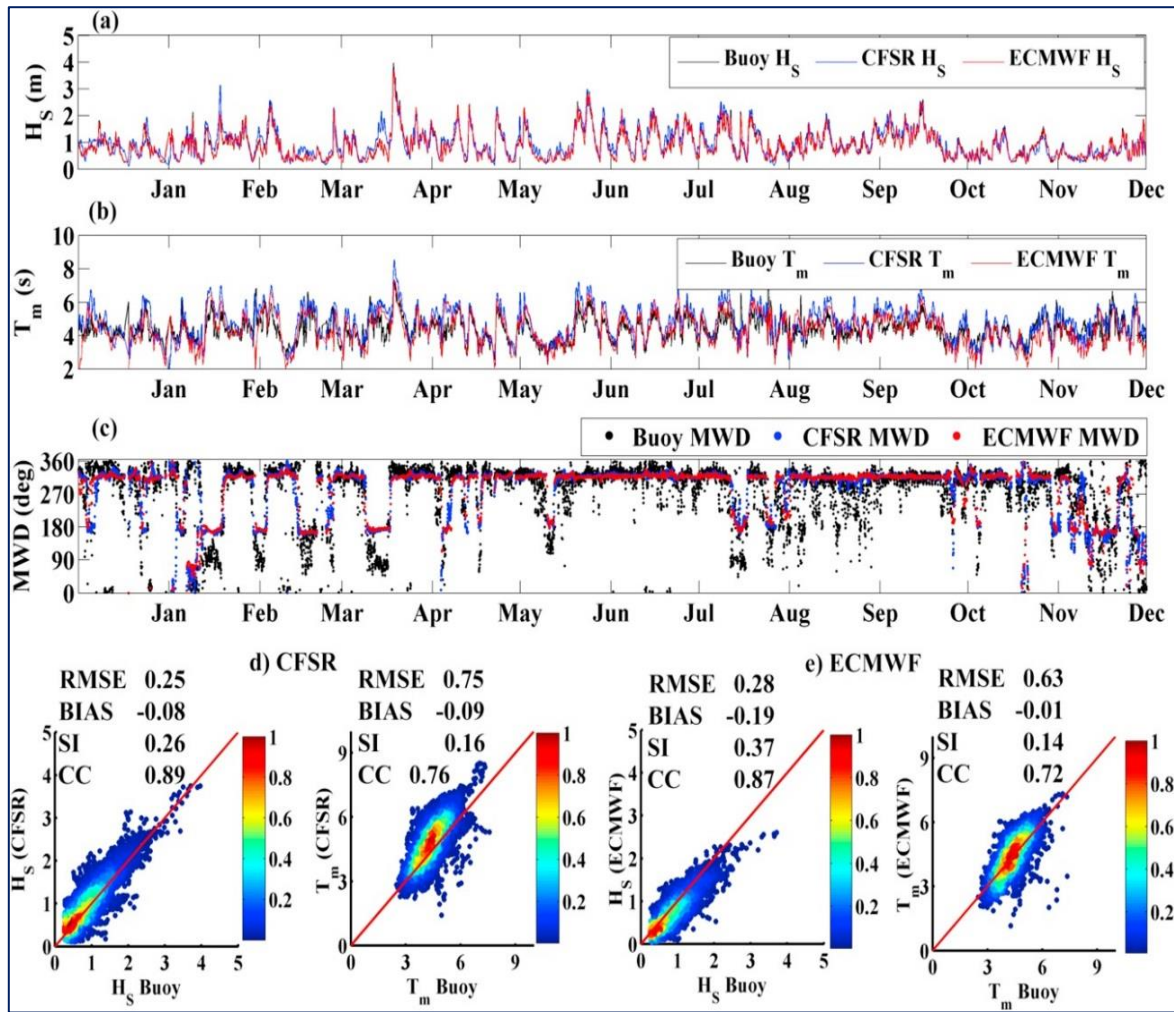


Figure 25: Comparison between the output from buoy and the model where (a) the results of significant wave height ( $H_s$ ), (b) mean wave period (c) mean wave direction (d) buoy and CFSR forced  $H_s$  and  $T_m$ , and (e) between buoy and ECMWF forced  $H_s$  and  $T_m$ . (Shanas et al., 2017)

From above studies, it is obvious that many experimental and numerical studies have been done. Some of them were done with simulating one phase flow (air or water only). Others have been done with multiphase simulation but with lack to explain how the waves generated by wind. Therefore, studies of wind and waves are still partially inhibited because of difficulties with gaining data from laboratory and also field measurements are complicated. Moreover, dealing with highly turbulent flows over complex moving surfaces has



mathematical complications. Another difficulty is, that simulating turbulent flows in both atmosphere and ocean simultaneously has a problem with using an appropriate coupled model (Lin et al., 2008). All that will create good motivation to do the present research by using CFD.

## 2.4 Computational fluid dynamics (CFD)

CFD is considered as a powerful tool that used for modelling and studying the behaviour of different fluids (gas or liquid) in a variety of situations (Morgan et al., 2011). It is dealing with fluids systems whether by modelling (mathematical physical problem formulation) or numerical methods (discretization methods, solvers, numerical parameters, and grid generations, etc.) (Zuo, 2005). The process of the simulation by using CFD can be seen in

Figure 26.

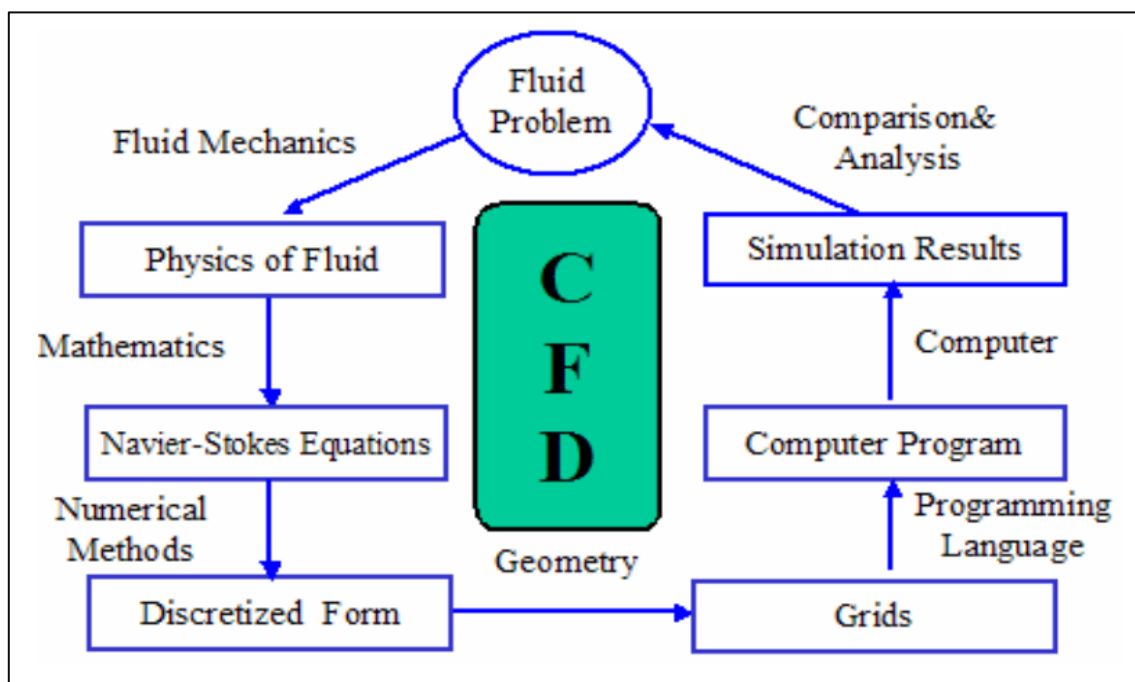


Figure 26: Process of Computational Fluid Dynamics (Zuo, 2005)

It has been used as an important practical design tool for the valuation of coastal, civil and naval engineering problems. Because of the effects of sea level rise and climate change which leads to impact the assumptions behind the design of many of existing sea defences, more accurate and developed design technique need to be applied and used in such areas. Therefore, it is important to use such powerful design tool in the design and assessment of coastal structures. Therefore, and as mentioned above about the processes of the simulation by CFD, it is important to report the governing equations Computational Fluid Dynamics.

### 2.4.1 Governing equation

The governing equation is based on solving Navier-Stokes equations which are the conservation of momentum equations (Zuo, 2005).

Continuity Equation

$$\frac{D\rho}{Dt} + \rho \frac{\partial U_i}{\partial x_i} = 0 \quad (1)$$

Momentum Equation

$$\rho \frac{\partial U_j}{\partial x} + \rho U_i \frac{\partial U_j}{\partial x_i} = -\frac{\partial P}{\partial x_j} - \frac{\partial \tau_{ij}}{\partial x_i} + \rho g_j \quad (2)$$

Energy Equation

$$\rho c_\mu \frac{\partial T}{\partial t} + \rho c_\mu U_i \frac{\partial T}{\partial x_i} = -P \frac{\partial U_i}{\partial x_i} + \lambda \frac{\partial^2 T}{x_i^2} - \tau_{ij} \frac{\partial U_j}{\partial x_i} \quad (3)$$

Where:

$\rho$  :density in kg/m<sup>3</sup>

U: velocity,  $u = (u_1, u_2, u_3)$  in m/s

t: temperature in K

P: pressure in pa

$\mu$ : dynamic viscosity in pa.s

$\tau$ : shear stress  $N/m^2$

g: acceleration  $m/s^2$

((Anderson Jr, 1992); Zuo (2005))

CFD has been used in different fields including the area of this research which is wind generate waves. Different researchers have used CFD in doing their researches about the wind generated waves including (Lin et al. (2008); Afshar (2010); Greig (2013) and (Silva et al., 2015))

Lin et al. (2008) has developed a multiphase direct numerical simulations model (Figure 27), coupled turbulent water and air to study the generation and growth processes of winds and waves.

There was a limitation for the model to be applicable for large-amplitude waves. The results show that the structures of turbulent flow in both air and water is no different from shear-driven turbulent flows on the top of a flat surface at the early period of simulation. In contrast, at the later simulation, motions of waves affect the flow field and also waves grow exponentially. Also, it has been shown that the wave growth can be classified to linear and exponential growth stages which is the same ideas from theoretical and experimental studies.

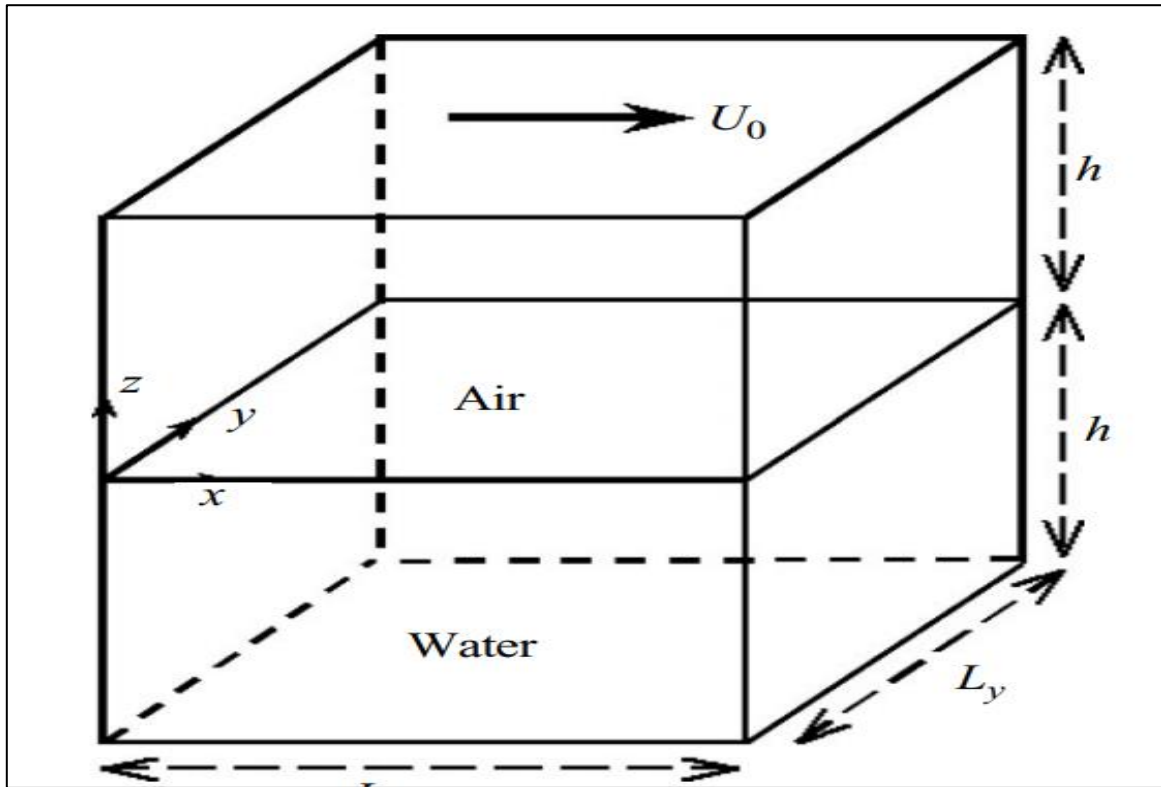


**Figure 27: Numerical domain of two turbulent flows (Lin, 2008)**

Afshar (2010) has completed a study in his thesis in master degree about wave generation. A numerical wave tank has been created by using an open source CFD solver, OpenFOAM. The Volume of fluid (VOF) was used for the free surface modelling. The solution was validated with the test was done by the Whalin shoaling. However, this study has been culminated because of facing some problems with the time and using OpenFOAM-1.6. the run process was stopped unexpectedly after very short time. Another test of whalin was run, but it gave strange results probably because of the mesh independency and so further study need to be done (Afshar, 2010).

Another study has been carried out by (Greig, 2013) by using ANSYS Fluent to develop a multiphase model of air and water to determine the average instantaneous shear stresses due the effect of wind-wave loadings corresponding to observe the restriction of monolayer

performance. The model shown in (Figure 28 : Computational Domain and Sampling Region , was based on the experimental wave tank that was used in the Schouten Schouten et al. (2011) and Palada et al. (2012) study.

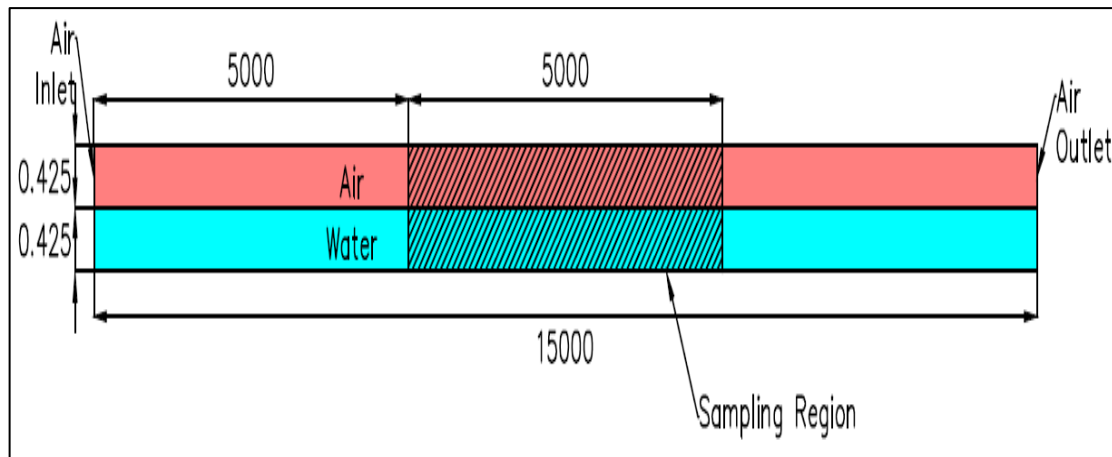


**Figure 28 : Computational Domain and Sampling Region (Greig, 2013)**

Three wind speed (0.89 m/s, 4.11 m/s and 7.33 m/s) were applied. The study found out that wind speed influence the shear stress in which with higher wind speeds, shear stress will be quicker.

Williams (2014) has performed in his dissertation, a numerical simulation for two phases flow (air flowing over water) in 3D rectangular prism (0.500m \* 0.600 \* 0.010m). Figure 29: Computational domain shows the computational domain that was used with showing the location of air and water phases. The aim was determining the effects of waves generated by wind on the temperature distribution next to water surfaces. It also studies the conditions that can help to reduce evaporation form water reservoirs. The simulation was done by utilizing Computational Fluid Dynamics Software ANSYS Fluent. Large eddy simulation (LES) was used to validate the outcomes and conclusions.

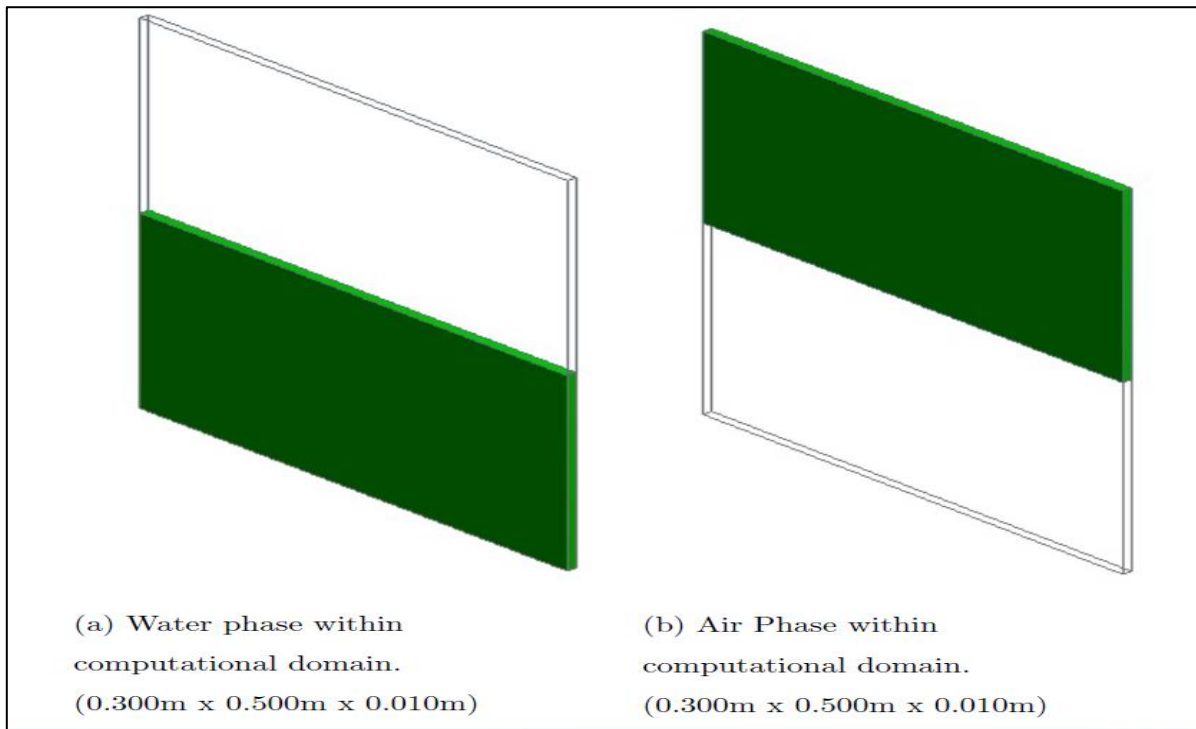


**Figure 29: Computational domain (Williams, 2014)**

The results suggested that aqueous thermal boundary layer has a significant impact on the evaporation. It also showed that the temperature difference is influenced and increased at the trough of waves while it is decreased at the crest.

Silva et al. (2015) have done a numerical study of the generation and propagation of waves in the ocean basin (length 40 m, width 30 m & deep 15 m) of the Ocean Technology Laboratory at the Federal University of Rio de Janeiro. A multiphase model which it was created by using ANSYS-CFX has been used in this study (Figure 30: Computational domain .

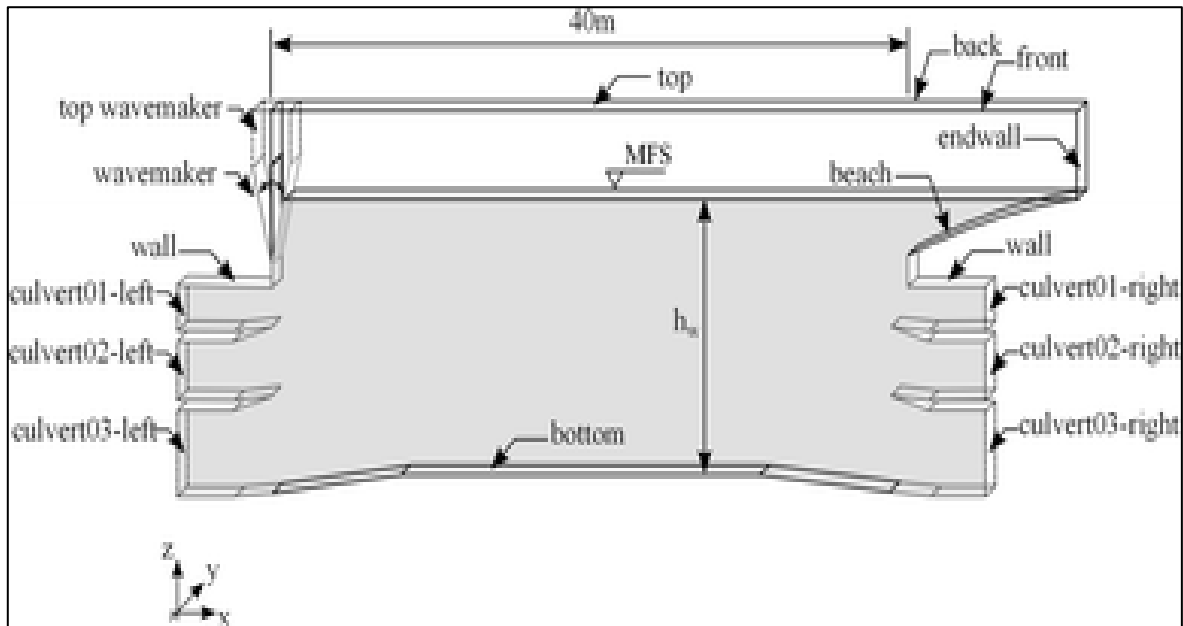


**Figure 30: Computational domain (Silva et al., 2015)**

A comparison between the theoretical and experimental data, which were obtained for waves with steepness from 0.005 to 0.033 has been done. Wave behaviour, mean wave period and height, and wave attenuation along the basin were investigated. Some differences between numerical and experimental data have been shown in the results. For example, the results of free surface elevation along the basin shows that the numerical waves arrive earlier than the experimental waves do (Figure 31). Moreover, the paper has neglected the impacts of the three-dimensional effects which probably help to found out the reasons behind these differences in the results.

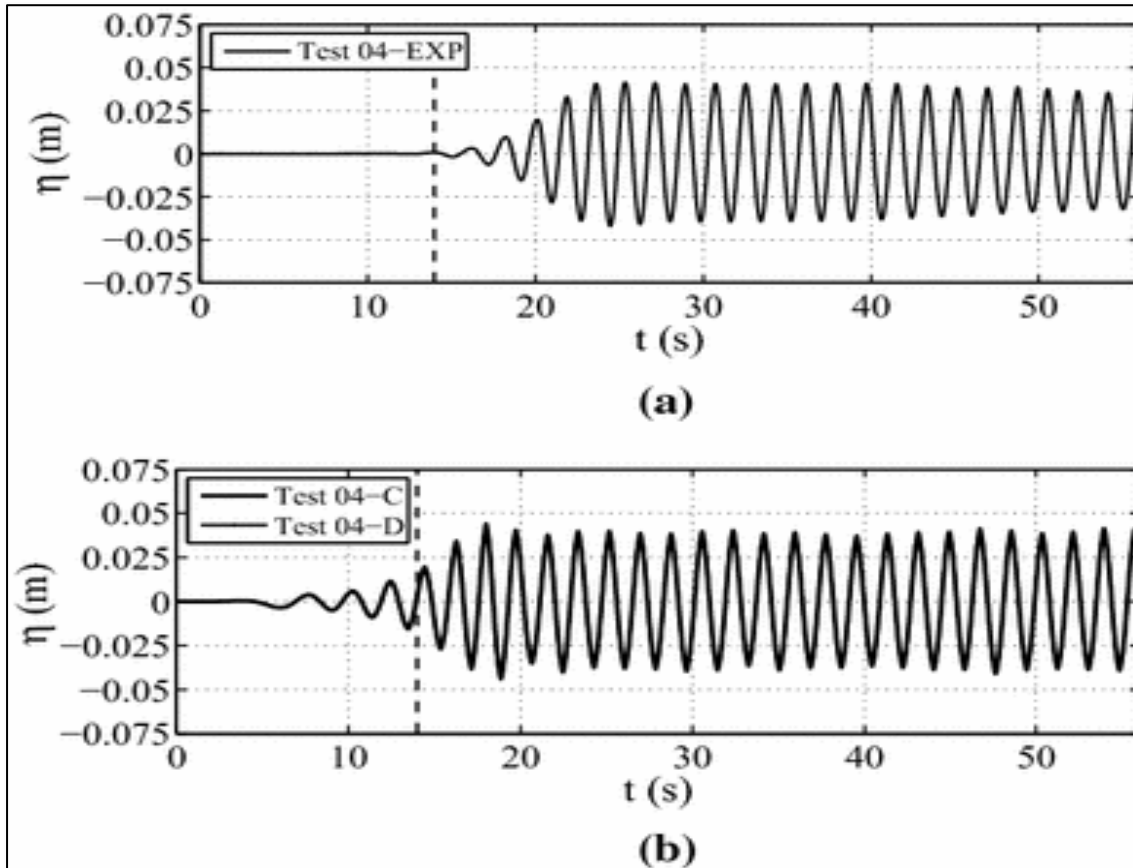


**Figure 31: Time series of free surface elevation at probe P1 ( $x'=20m$ )**

**a) Experimental data      b) numerical data**

#### **2.4.2 Detached eddy simulation**

Detached-Eddy Simulation (DES) is a hybrid technique from large-eddy simulation (LES) and the Reynolds-averaged Navier-Stokes (RANS), was first proposed by (Spalart et al., 1997) to predict the behavior of turbulent flows at high Reynolds numbers (Squires, 2004). Due to some challenges of high-Reynolds number separated flows that have to be addressed in some areas of study including aerospace, atmospheric studies and ground transportation, DES was created to help in addressing these challenges (Spalart, 2009). Other issues with both LES and RANS have led to create DES. For LES, it is required using high resolution in the boundary layers when it is applied to configure elements at high Reynolds numbers and



thereby it is required very high cost (Squires, 2004). Moreover, LES has problems with simulating wall bounded flows (e.g. channel flow) as it is required big grids to give an accurate solution. However, the structures are very small near wall region which required finer mesh to resolve such structures (IIHR, 2012). LES becomes impractical for resolving wall-bounded flows at high Reynolds number as the scaling of the computational solving depends on this number Chapman (1979); Spalart et al. (1997).

While the RANS or what is called unsteady Reynolds-averaged Navier-Stokes URANS also has disadvantages which make it needs to be improved. RANS model has difficulties with providing accurate results for mean quantities at the regions where large-scale anisotropic vortical structures are dominated (Fröhlich and von Terzi, 2008). Another problem with RANS that is required unsteady information for engineering purposes such as vibration and noise (Spalart, 2009). **Error! Reference source not found.** a good example about the behaviour of the RANS simulation. A simulation has been done for the flow around a simplified car geometry called Ahmed body. It shows the flow around the body and especially at and behind the trailing edge where the flow is very complex and then RANS method is not applicable in this area. Therefore, LES needs to be used to simulate this region (Fröhlich and von Terzi, 2008).

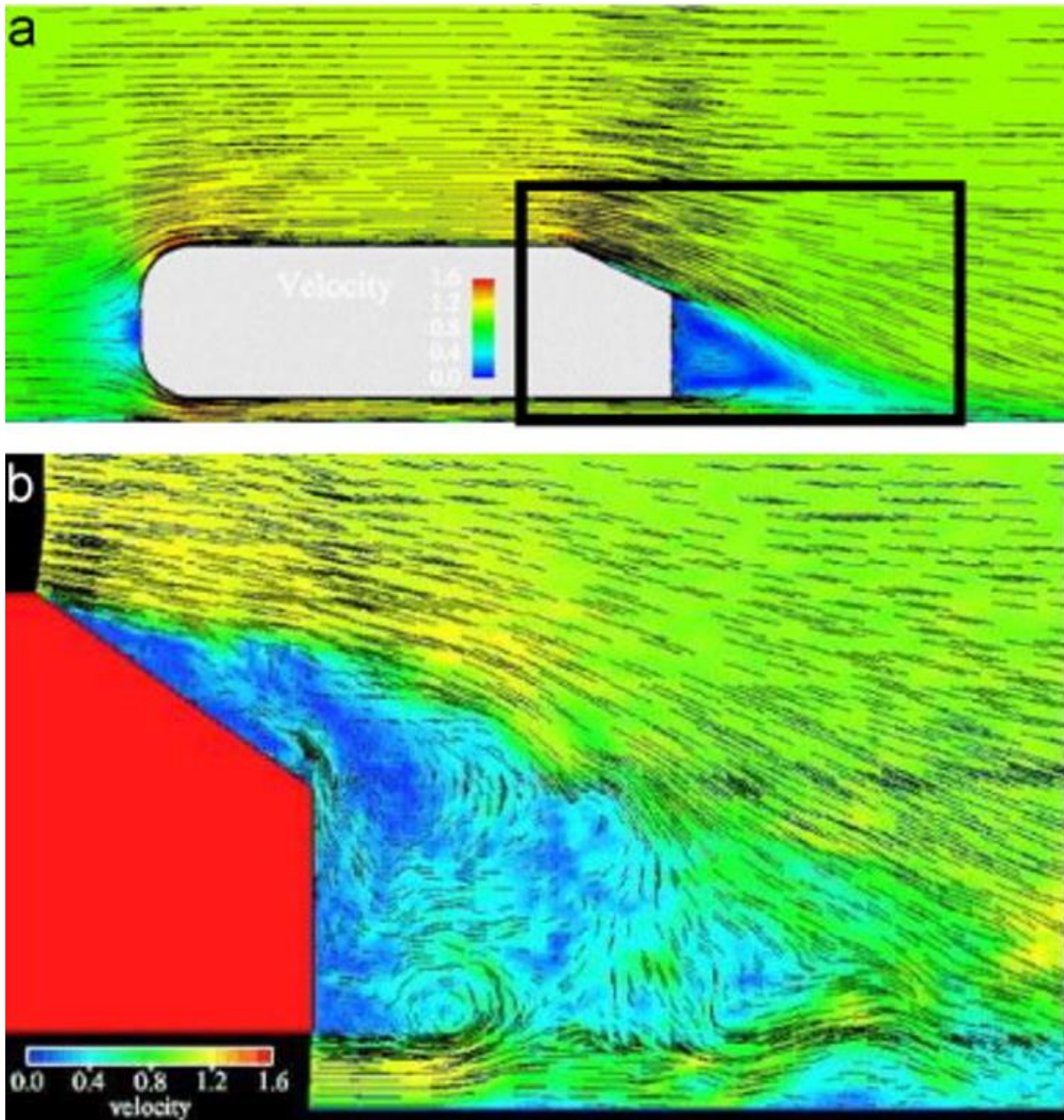


**Figure 32: low field over a simplified car geometry (a) Mean flow; (b) instantaneous flow (Fröhlich and von Terzi, 2008)**

Nishino et al. (2008) has used URANS and DES to simulate a subcritical flow ( $Re=4.0 \times 10^4$ ) around a circular cylinder placed near wall. In a three-dimensional domain, the DES model based on a modified version of S-A model was used. While in both two and three-dimensional domains, URANS was used. It is based on a low-Reynolds-number  $k-\epsilon$  model of

Launder and Sharma (Launder and Sharma, 1974). The results of the simulations show that the DES has captured the features of the flow with higher accuracy than the URANS. Moreover, the cessation of the large-scale von Kármán-type vortex shedding has been predicted at the back side of the geometry for the ratio of the distance between the cylinder and the ground ( $h$ ) to the cylinder diameter ( $d$ ) which was between two  $h/d$  (0.4 - 0.3) with DES, while by URANS was  $h/d$  of 0.2–0.1. It also shows that the near-wake profiles was unstable with URANS comparing with DES (Figure 33)

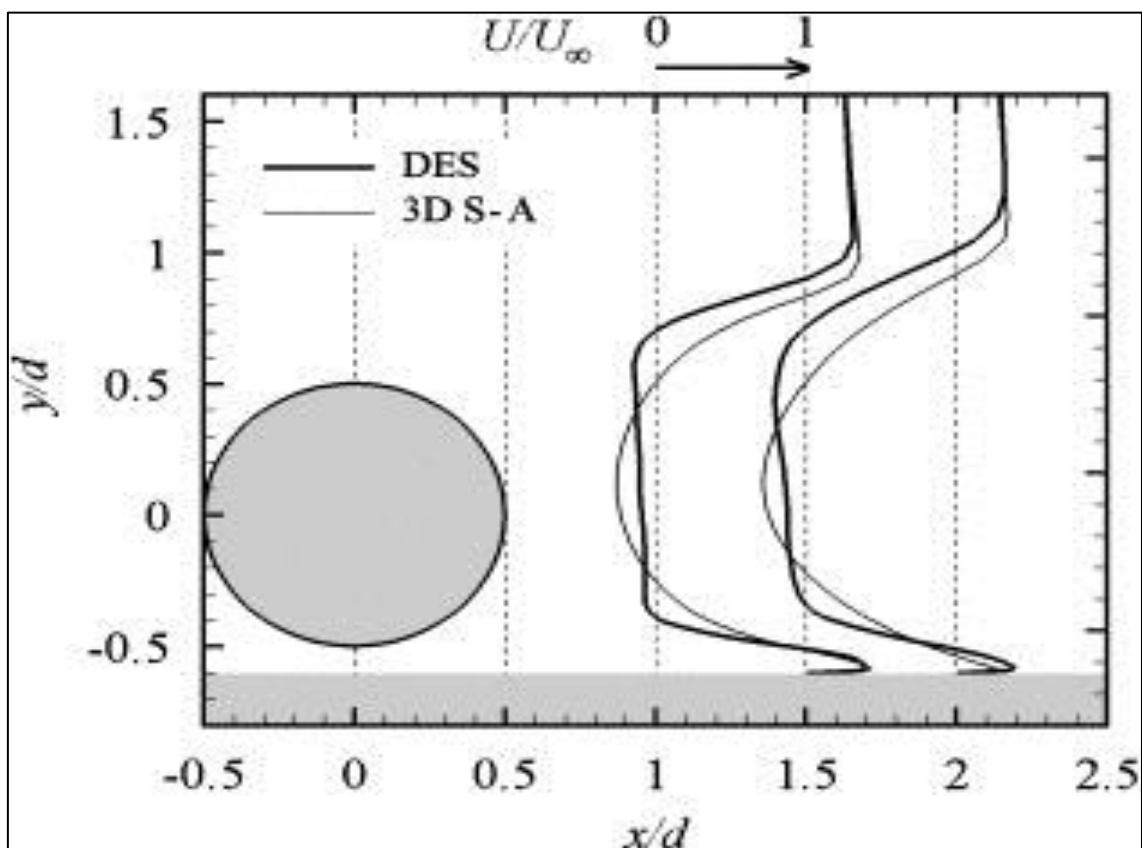


**Figure 33 Comparison of mean stream wise velocity profiles in the near-wake region (Nishino et al., 2008).**

DES has been implemented in different studies with obtaining satisfactory results in different engineering fields such as vehicle (Kapadia et al. (2004), Sreenivas et al. (2006), Deck and Thorigny (2007), Trapier et al. (2008)).

From above, it is obvious there is a need to create a new approach that can overcome the challenges with using whether LES or RANS. DES is the solution for that, which includes using full RANS model the simulation near the wall region while it will turn into LES to be used for the simulation in regions of massive separation in despite of the problems that might happens in the space between these areas which called the grey area (Fröhlich and von Terzi (2008); Spalart (2009)). Figure 34 shows the work principle of DES. Near the wall when the wall distance ( $d$ ) (coefficient in vortex method) less than step size of the grid ( $\Delta$ ) ( $d < \Delta$ ), the RANS model will be employed. Then, when ( $d > \Delta$ ), the model will switch into LES model (Fröhlich, 2008). There are many examples of using DES including flow around non-aerodynamic obstacles (e.g. buildings and bridges), separated flow around transport vehicles (e.g. cars and trucks), noise generating obstacles (e.g. car side mirrors) and massively separated flow around stalled wings (Ansys, 2015).

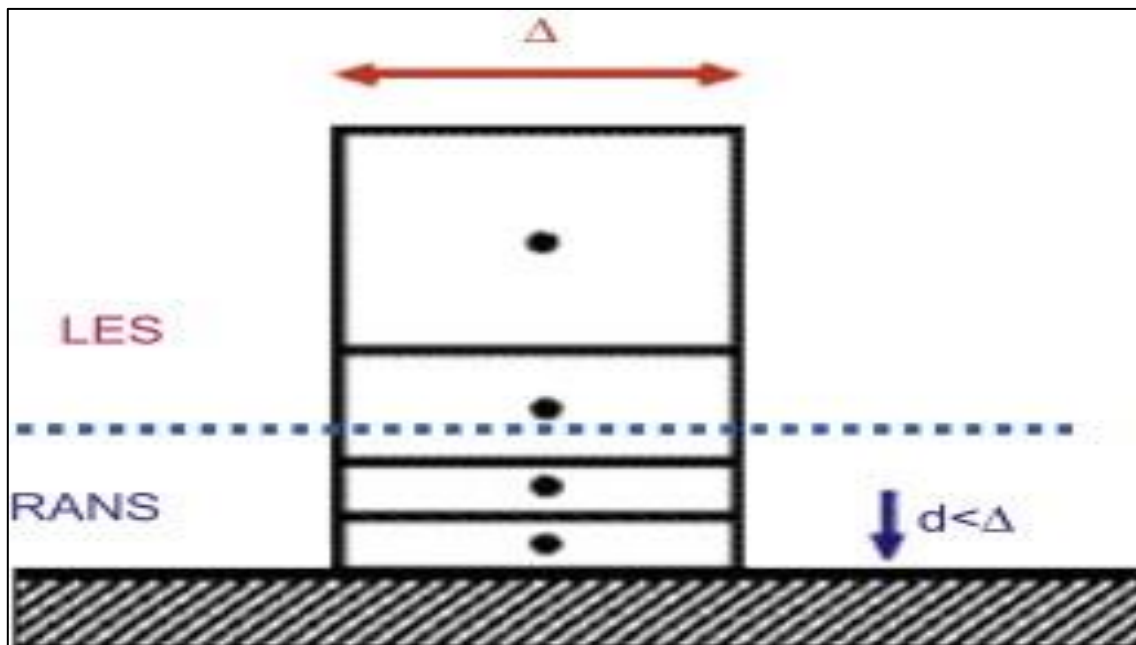


**Figure 34: DES approach (Fröhlich and von Terzi, 2008)**

## **2.5 Summary**

The literature review showed and found that many mitigations have been used to reduce the evaporation. It also showed that monolayers are the best method to be used for such purpose comparing with other evaporation mitigations. However, these layers are become ineffective under the effects of harsh winds and waves. Different studies have been done to study the waves generated by winds. These studies still have lack with explaining the phenomena of how the waves generated by wind. It also has been shown that using numerical study by CFD will be better choice to study the waves. Detached eddy simulation will be better to give clear results about the waves especially with no study has been done before with DES on the waves.

## CHAPTER 3: PRELIMINARY MODEL

### 3.1 Introduction:

This section will explain and describe the methods and software that have been used to prepare and complete the preliminary model. The methodology will cover the main instrument which is Computational Fluid Dynamics Software ANSYS Fluent that has been utilized to produce the required simulations in order to study the sub surface of water where waves can be generated by wind. Fluent was used as it is applicable to have a detached eddy simulation while CFX does not have DES just RANS solver. As mentioned above, the numerical simulation has been used because it is much easier to be used in a field where an experimental study cannot reach such area and especially in the waves' study as it is hard to collect correct data from large reservoirs where monolayers might be used.

The resources that were used, are provided by USQ including the software, computers, libraries and other important requirements. The project has been completed by different basic steps which are summarized below:

- Create a three-dimensional rectangular tank with dimensions (15 m × 0.092 m × 0.85 m) which contains multiphase model water and air, by using ANSYS Design Modeller which allows to create and modify any geometry to be used for the analysis in ANSYS Workbench.
- Create a mesh for the model with tetrahedral type to have higher quality that will influence the results.

- Create finer mesh around the subsurface between air and water as it is the interesting area for the research. Thus, will help to obtain better resolution.
- Choosing the suitable setup for the simulation and as will be explained later.
- The sampling region where the data will be calculated, have been chosen over the area where the waves can be formed to ensure less effects of the waves on the results.
- Post processing has been used to study the results.
- MATLAB and Microsoft Excel have been used for the analysing.

## **3.2 Software ANSYS Fluent**

### **3.2.1 Journey of learning**

Before the main model was created, some models were created to help in being familiar and mastering the important aspects of CFD. The journey of learning CFD has been started with using Design Modeller to create a three-dimensional rectangular tank with dimensions (length = 6m, width= 3m, height= 2.5). Two rectangular prisms were used with different height, one for water with 1.5m height and another one represents air with height 1m. These prisms represented together two-phase model for both air and water (Figure 35). Also by using Design Modeller, another body has been created in order to help meshing the subsurface between air and water. This body represents the body of influence which is an arbitrary body that intersects with the interested area for meshing and helps to control the size of area where the refinement will be done. It was created with random dimensions (Figure 36).

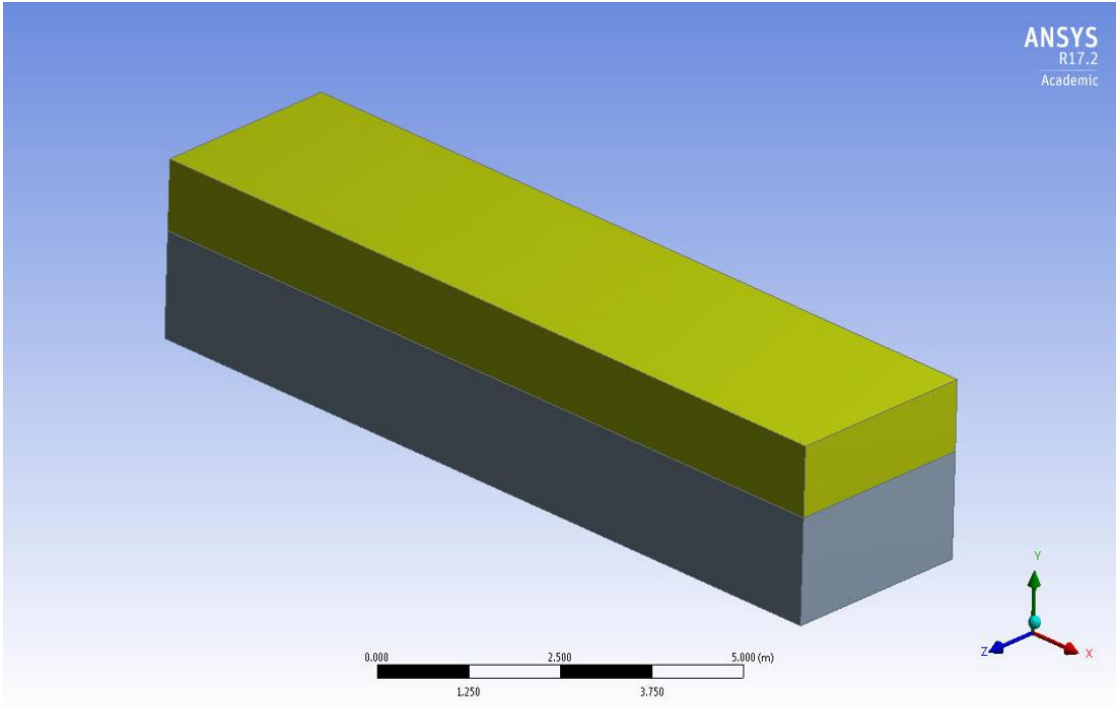


**Figure 35: first geometry**

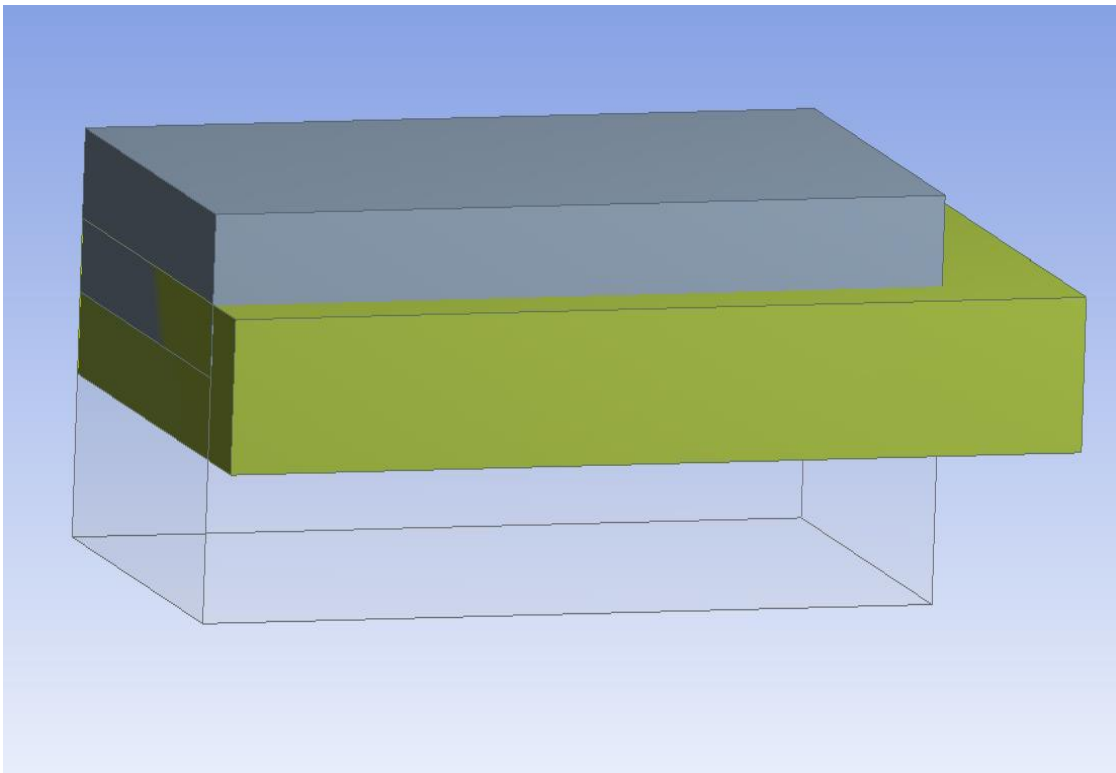


**Figure 36: the body of influence**



The model has been meshed with different sizes of mesh. First of all, the mesh has been created for the whole model by using hex dominant method with default setup. This method was used as it creates hex meshes which are more efficient and controllable than others (CAEAI, 2013). However, for the interesting area where the waves are formed between air and water, the meshes has been refined by using the body sizing method of mesh and by the help of the body of influence to get more accurate results with higher resolution. Figure 37 shows the mesh generation. Names for the faces and bodies have been selected. One face has been named (air inlet) and another one is (air outlet). Other faces have been named (wall). Upper body has been named (air) while the bottom one has been named (water).

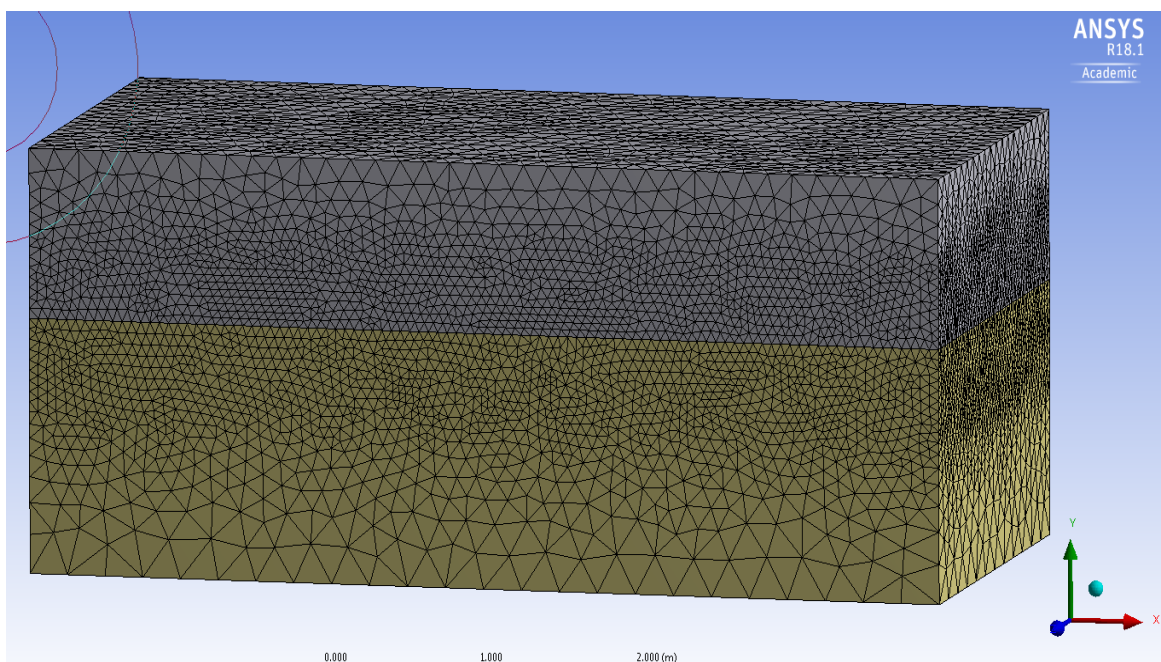


**Figure 37 mesh generation**

For the setup, following setups have been done to run the simulation:

- a) The flow is transient.

- b) Gravity is in y-axis =  $-9.81 \text{ m/s}^2$
- c) The model has been setup as a multiphase. Phase 1 is air while phase 2 is water.
- d) Detached eddy simulation (DES) has been used as it will be better model for the simulation and study the formed waves. Default settings were used.
- e) For the boundary condition, at the air inlet, the velocity has been set as  $2.5 \text{ m/s}$ . while the air outlet is pressure outlet ( $P = 0$ ).
- f) Transient formulation has been setup as second order implicit.
- g) The volume fraction of water has been set as 1.
- h) The time step size was fixed as  $(10^{-5})$
- i) Number of time steps is 40 and the iterations are 20.

The results of the residuals of the simulation were not good and divergence was happened and thereby more setup needs to be done in order to get better results (Figure 38).

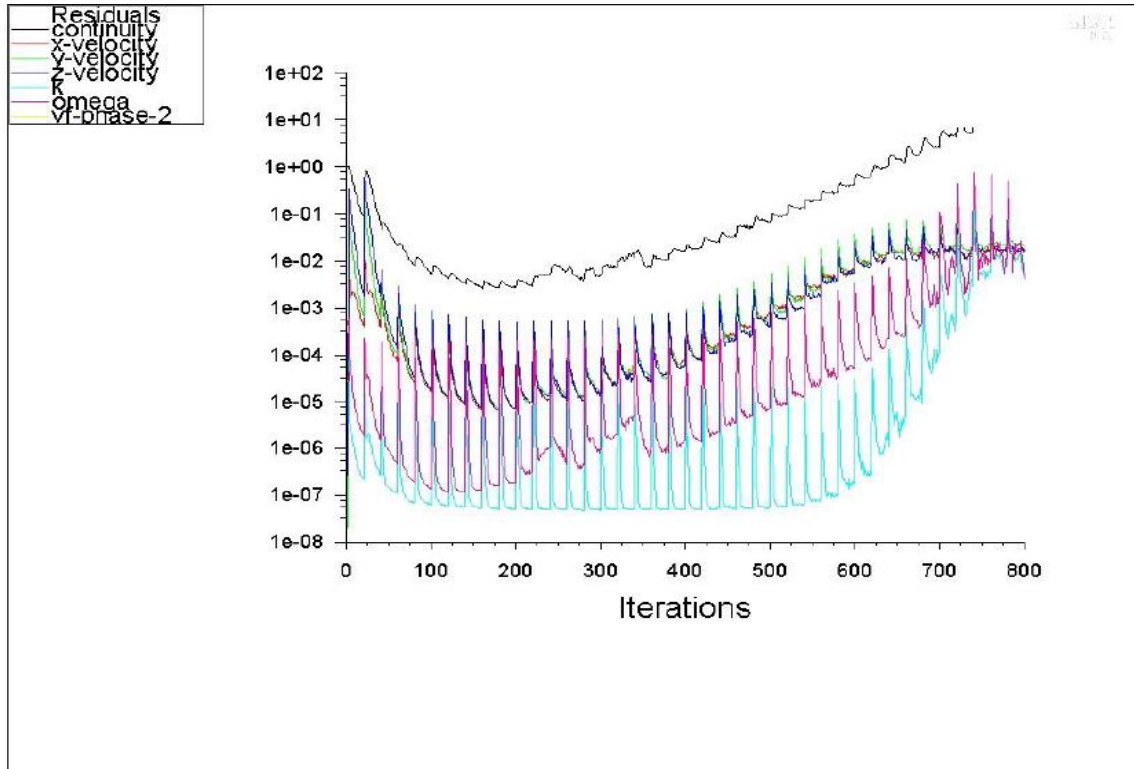


**Figure 38 some results of simulation**

After that, more changes have been done on the geometry, mesh and setup. The model was created with smaller dimensions ( $0.8 * 0.8 * 0.8 \text{ m}^3$ ) (Figure 40). The reasons for that, first steps were just to be familiar with CFD as well as reaching some important stages before the final model. However, using a large model will lead to waste more time for the simulation while the size of the model was not very important. Therefore, this will help in avoiding the disadvantages with using finer mesh in a large computational domain, including accessing the limitation of academic version of ANSYS in the USQ labs because the available software allows to run simulation for a maximum 500,000 elements only. Moreover, another disadvantage is being very expensive model, in terms of computer processor and required time to do the simulation. Thus, the mesh has been generated for the second model (**Error! Reference source not found.**

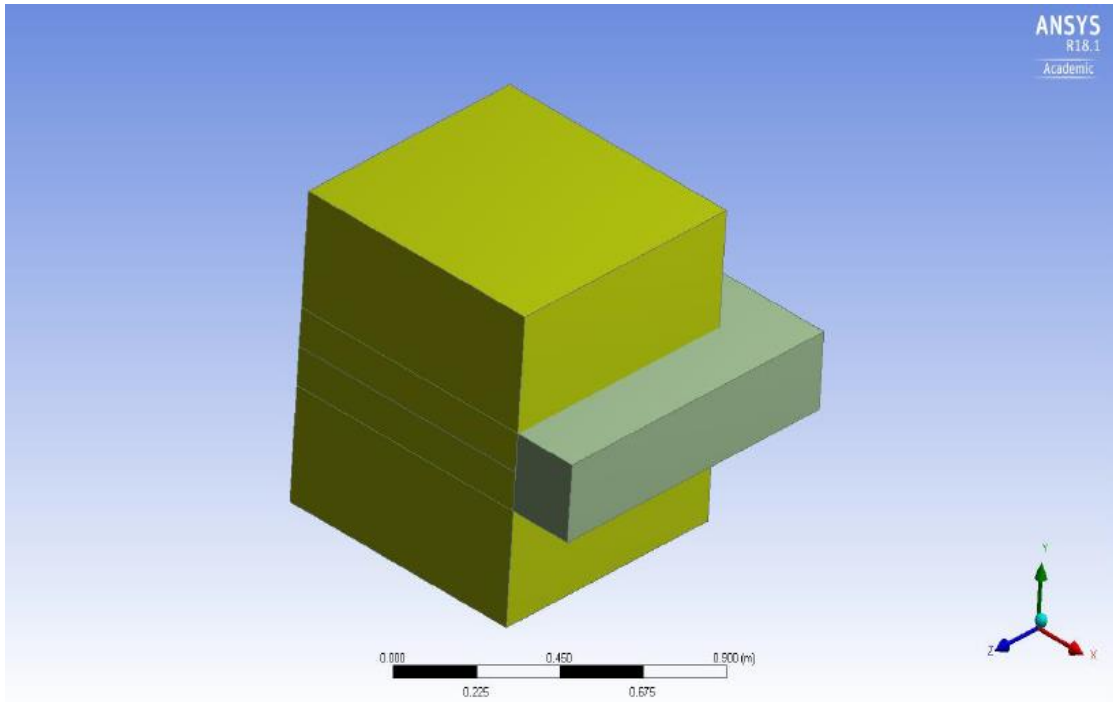


**Figure 39: The second model**

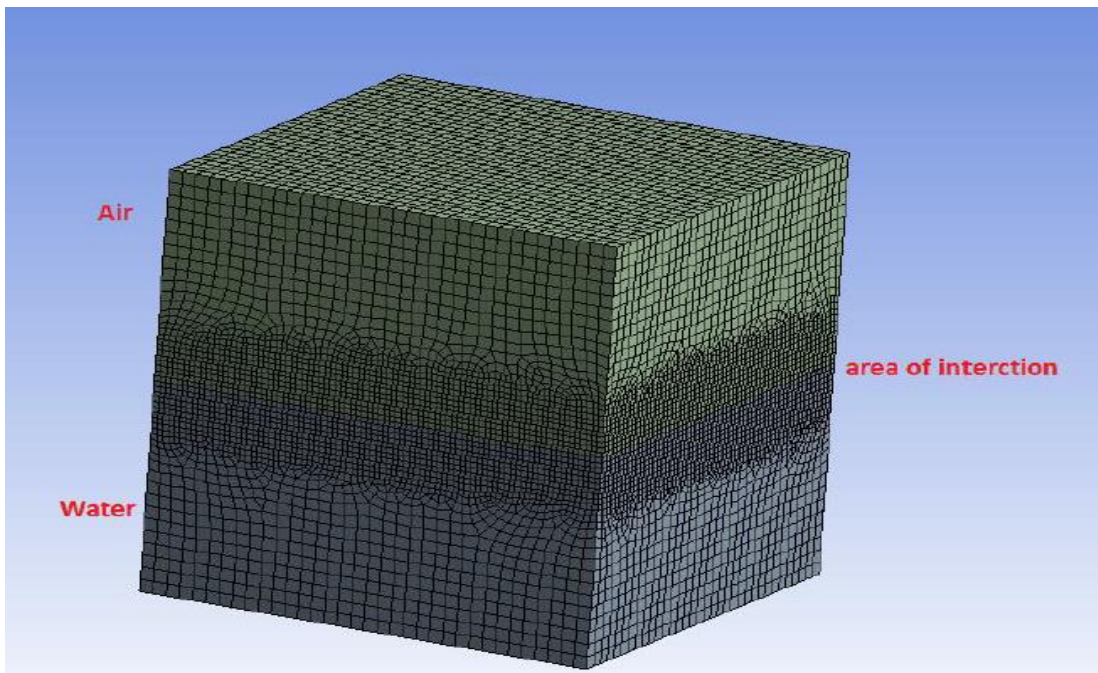


**Figure 40: Mesh generation for second model**

After running the simulation also, the results were not good. Moreover, an error happened which is 'reverse flow occurred in x faces'. Reverse flow, which means there is a flow in the opposite direction, were happen in the inlet and outlet as it is illustrated in Figure 41: Reverse flow in the air inlet.

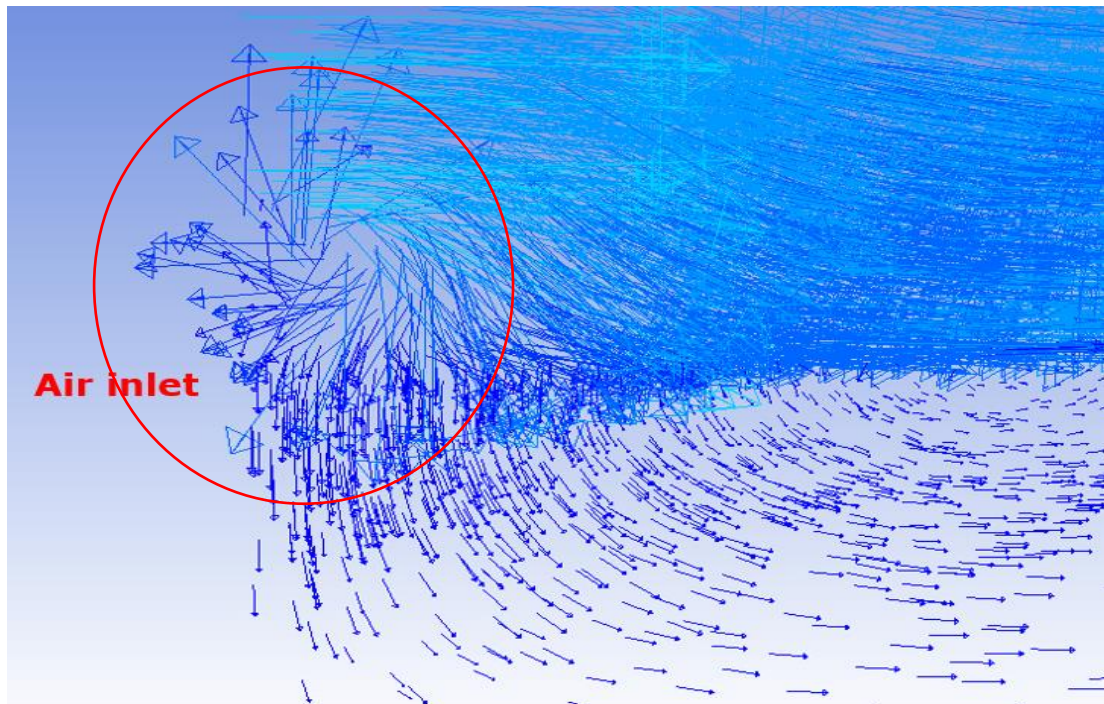


**Figure 41: Reverse flow in the air inlet**

To avoid that, different steps have been done and as following:

- The location of the inlet and outlet has been changed to be far from the recirculation regions which lead to reverse flow at the inlet and outlet faces. Therefore, the generated waves will be independent from the effects of the inlet and the outlet.
- Changing the outlet setup from pressure outlet to outflow.

- The chamfer and fillet were used to create the corner between the new two phase's air and water. Figure 42 using the fillet for the corners. For the chamfer, the solution was divergent. However, fillet, Figure 42 using the fillet for the corners, was the better solution for the corners as it helps to reduce the circulation.
- The water level has been set to be lower than the wall
- Mesh type have been changed from hex method to tetrahedron. Although hex method is considered the best mesh type because it is efficient and controllable comparing with other types (CAEAI, 2013), the quality of the mesh was not good because of the maximum skewness was 0.99 and the minimum orthogonal quality was less than 0.1. More detailed will be illustrated later.
- Run simulation by using transition SST and then another simulation by using DES.

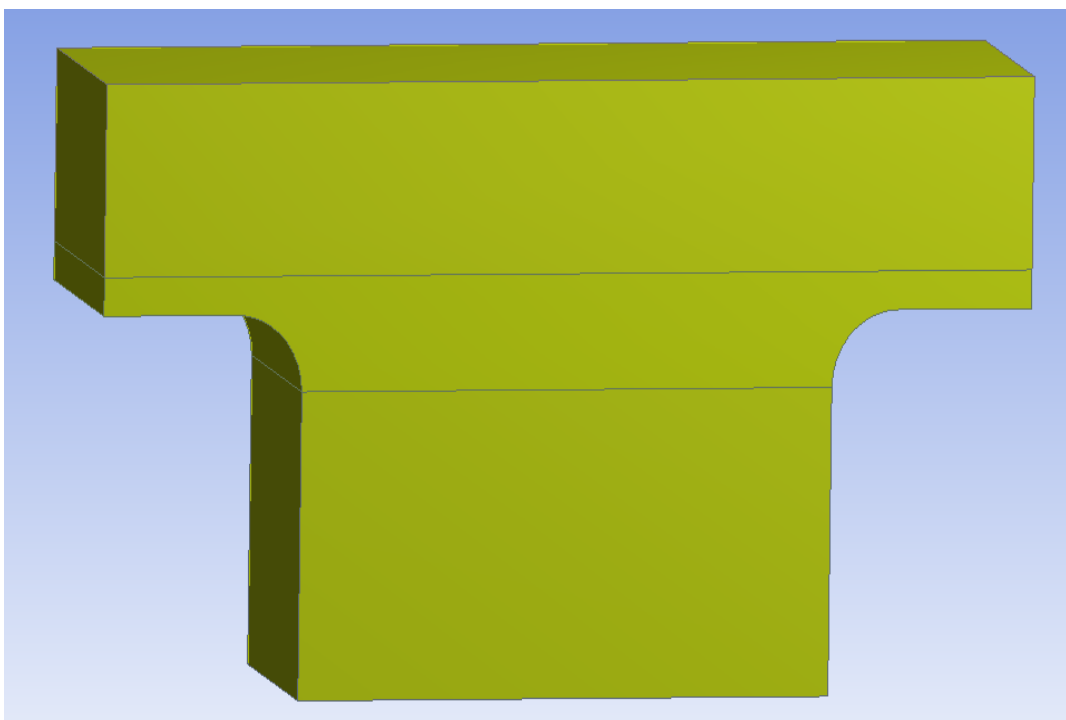


**Figure 42 using the fillet for the corners**



For the setup, dynamic mesh was used. Time stepping method was chosen as variable more details about the reasons for choosing above setup will be explained later in this chapter. The solution was converged which means the setup are more suitable to be used with last model that were created later to be validate with experimental date. Figure 43 Converged results of the simulation.

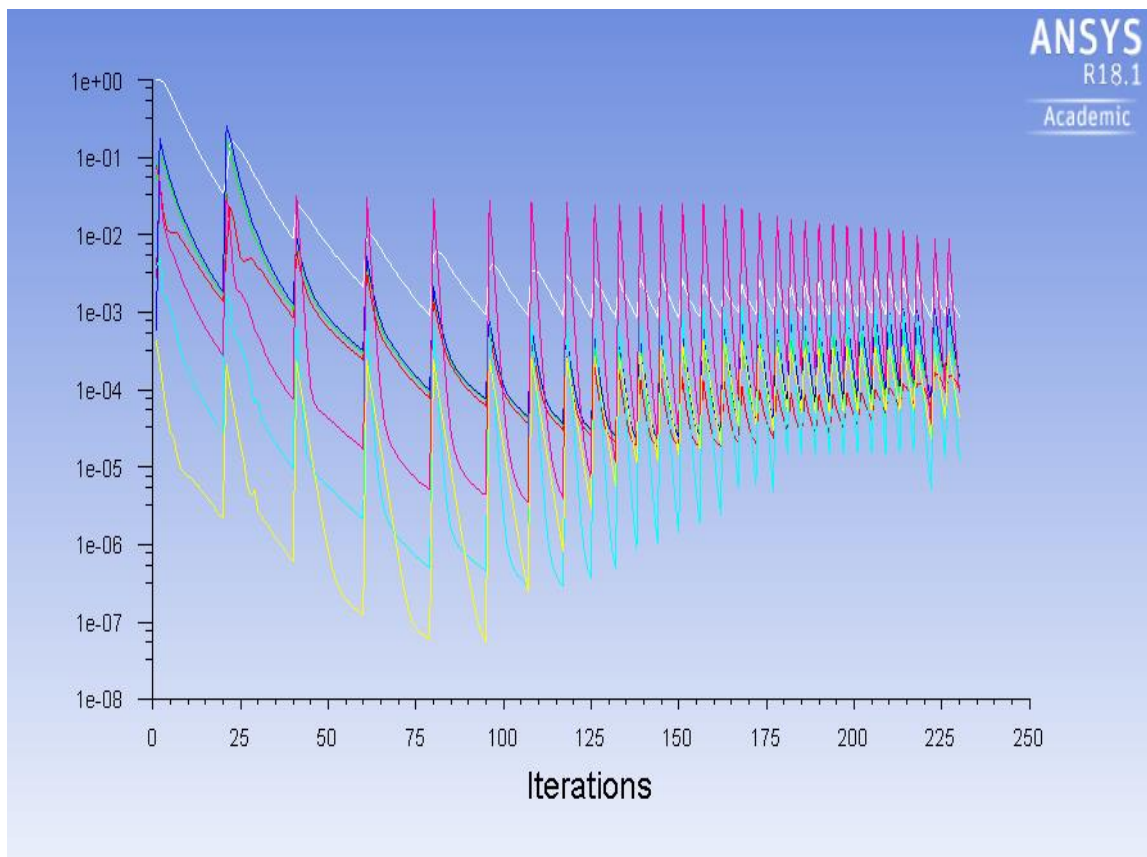


**Figure 43 Converged results**

### **3.3 Preliminary Computational Domain**

Due to the waves cannot be created independently in small domain without the effects of the walls, a long model have to be used to study the independent domain waves. Therefore,

ANSYS Fluent was used to create a three dimensional rectangular tank with dimensions (15 m× 0.46 m× 0.85 m) which was based on an experimental tank that was used in an experiment done by (Palada et al., 2012). This tank was developed with some change in the design to obtain better results from the simulation. The locations of the inlet and outlet have been moved further for 1 m in each direction. As mentioned above, this will help to reduce the reverse flow and then reducing the effects on the results. Three rectangular prisms were put together to form the geometry of the model. The upper one represents the air and has the inlet and outlet (length 17 m, width 0.46, height 0.325). The second one in the middle also represents air but with wall faces (length 15 m, width 0.46, height 0.2). The reason for that, is to make the water level lower than the wall. The third one represents the water with dimensions (length 15 m, width 0.46, height 0.325). All three prisms have been set as fluid. The fillet radius has been chosen as 0.3m. Other changes were the same changes that have been explained above regarding second model (Figure 44).



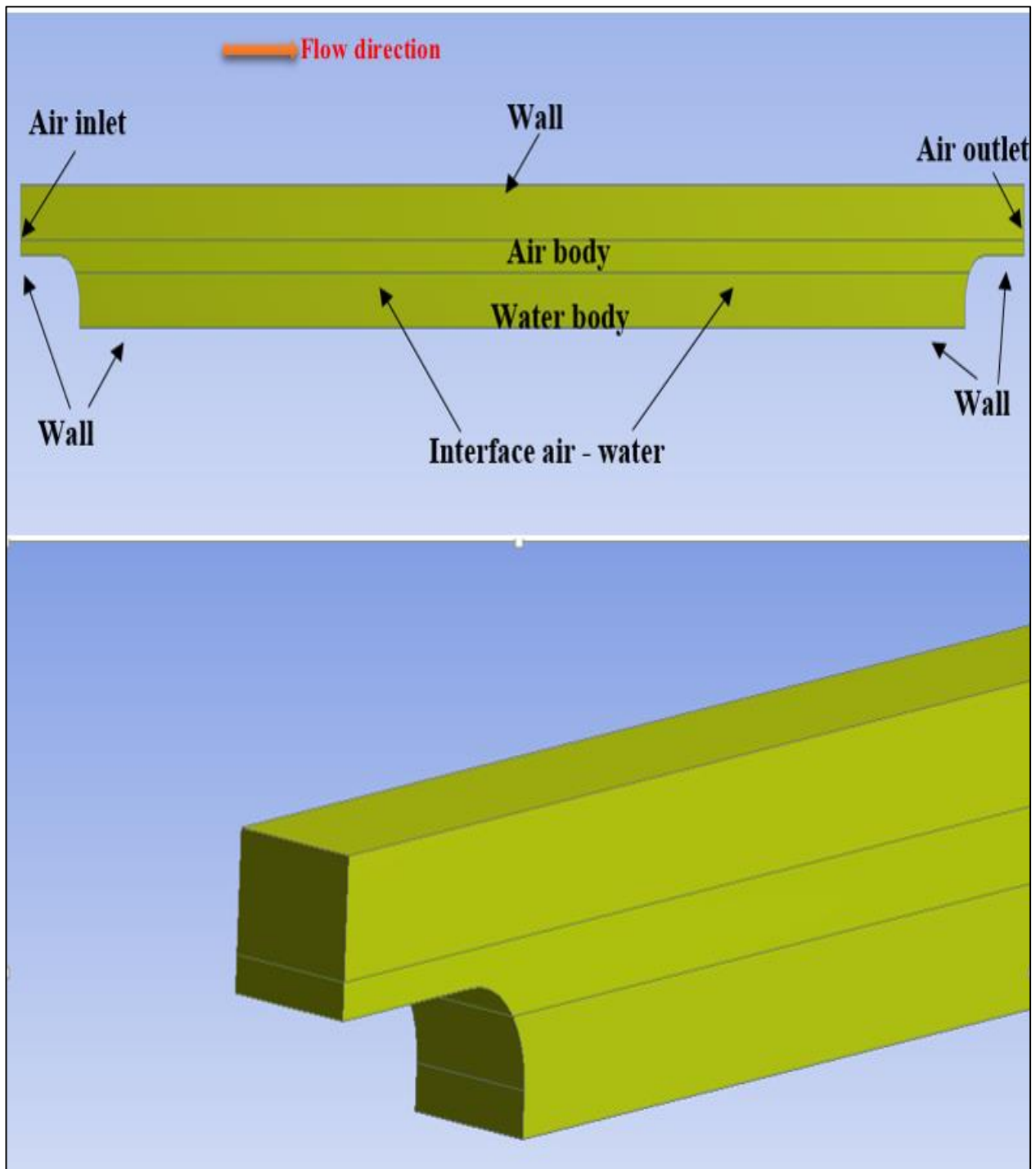


**Figure 44 Computational domain**

### **3.4 Mesh generation**

Mesh generation is considered one of the most critical stage in the simulation. Mesh properties have a very big impact on the results of the simulation especially in the interaction area between air and water. High quality mesh is required to obtain more accurate and converged results which forms a big challenge with available limitations such as the cost and time. Therefore, as previously stated above that the type of mesh was chosen as tetrahedron to allow for smoother transitions between the cells where there are changes in mesh size (Horko, 2008). Although, using tetrahedral mesh will lead to increase the number of elements, the quality of the mesh is within mesh quality recommendations which stated that minimum orthogonal quality should be less than 0.1 while maximum skewness less than 0.95 (GroupSSC, 2014). Therefore, the minimum orthogonal quality is 0.15388 and maximum skewness is 0.846. At the first, mesh generated for all three bodies with coarse size. Then, using body sizing method and body of influence to refine the mesh in the middle. This will help to obtain a sufficient accuracy and adequate capture for the flow. As it was stated above that all faces have been named as wall except two faces as air inlet and outlet. The upper two prisms have been named as air while the lower one as water (Figure 45).

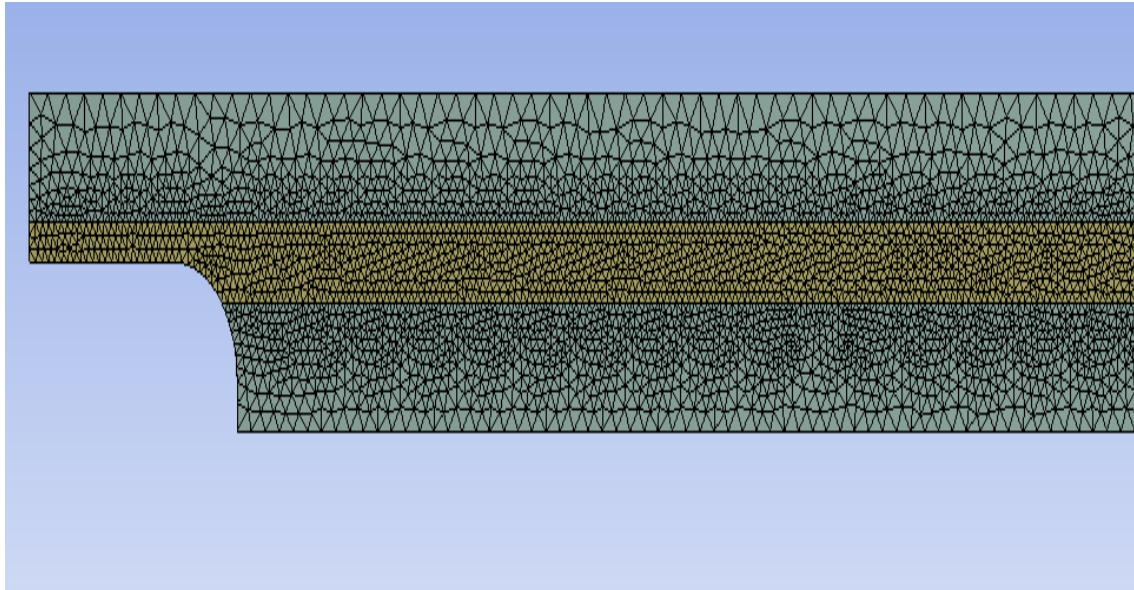


**Figure 45 mesh distribution**

### **3.5 Setup**

Transient flow has been set for this simulation. For the models, volume of fluid has been chosen as a multiphase model with implicit formulation to allow ANSYS Fluent to achieve better numerical accuracy especially with higher-order transient. To allow for the heat transfer between air and water, energy has been activated. Detached eddy simulation has been set to be used as mentioned earlier to allow for obtaining accurate results in all subgrade in the interface area whether near the wall or far from it. DES uses the large eddy simulation model to study the flow in the area far from wall, while it switches to use Reynolds Averaged Navier Stokes simulation in the wall bounded flows. Others setup for the models have been left as default.

For the materials, they have been set as fluid including water and air. Their properties have been left as default as in Table 2 while monolayers have not been included in this model.

**Table 2: The properties of air and water**

Fluids	Density (kg/m <sup>3</sup> )	Specific heat (j/kg-k)	Thermal conductivity (w/m-k)	Viscosity (Kg/m-s)	Molecular weight (kg/kmol)	Reference temperature (k)
Air	1.225	1006.43	0.0242	1.7894e-05	28.966	298.15
Water	998.2	4182	0.6	0.001003	18.0152	298

The boundary conditions are very important to direct the motion of flow. They are very important for any governing equations to be solved. For the model used in this project, they have been set as air inlet, air outlet and wall.

For the air inlet, the type has been chosen as velocity inlet with velocity magnitude equal to 1.3 m/s. this velocity has been chosen according to the Beaufort scale of wind force which stated that small ripples will be formed with appearance of scales with air velocity between 0.5-1.5 m/s (Thomson, 1981a). The temperature was assumed as 298 K for the air. Fluctuating velocity algorithm has been set as vortex method with default setup which allow to consider all the perturbations that happen in the domain. While for the outlet, the type is outflow as it mentions earlier that outflow will help to reduce the effects of reversed flow.

Dynamic mesh has been activated in interior air – water to simulate all the grid of flow that can be changed with the time. The mesh method is layering and the zone of interior air – water is deforming.

For the initialization, hybrid initialization has been used to avoid the error message (temperature divergence in AMG solver). Hybrid initialization is combine of instructions and boundary interpolation methods. It finds out the velocity and pressure by solving Laplace's equation, while other variables including temperature, volume fractions and Turbulent Kinetic Energy can be automatically patched (ANSYS, 2016). Table 3 shows the values that have been used.

**Table 3: Initialization values**

Fluids	Z velocity (m/s)	Temperature (K)	Volume fraction of water
Air	1.3	298	0
Water	0	288	1

The simulation has been run for 30-time steps and 20 iterations with activating variable time stepping to find the more appropriate time step for each speed and mesh size to use. Using variable time stepping will make the time step more flexible to be automatically changed to give more accuracy of the solution. For example, when the solution is changing slowly, larger time steps will be chosen, while the solver will use smaller time steps when the solution is varying rapidly (ANSYS, 2009);(Piché). Residence time for the flow which

is define by the required time for the air to travel from the inlet to the outlet, has been calculated by using the below formula

$$t_{res} = L_{tank}/U_{inlet} \quad (4)$$

Where

$t_{res}$ : the residence time of the flow in s

L: length of tank in (m)

U: the velocity of air in m/s

Table 4 shows all the calculations for time residence, time steps and the appropriate time step that has been found when variable time stepping been used.

**Table 4: calculations for time residence, time steps and the appropriate time step**

	U <sub>inlet</sub> m/s	L <sub>tank</sub> m	t <sub>res</sub> s	Time steps	Time steps size
1	1.3	15	11.53	2641	0.006312022
2	0.9	15	16.67	2434	0.00473999
3	2	15	7.5	2718	0.002759985
4	3.2	15	4.688	2713	0.001728168

Then, the simulation has been run to for different velocities, different mesh sizes and different residence time to examine the data in order to obtain the more appropriate results and as it will be explained in the nest section.

## **3.6 Analysing data**

### **3.6.1 Simulation for different mesh sizes**

Mesh independency is very important for any problem that an engineer deals with. As the mesh size has an influence on the results, it is important to run many tests on different mesh sizes until reaching the size where the results will not be effected even if the mesh become finer. Reaching mesh independency will make the results more credible and sufficient. Therefore, in this study, the simulation has been run with velocity with 1.3m/s for different mesh sizes. This process show whether the solution is independent from the mesh resolution or not. Three sizes of mesh were chosen in this project, a coarse mesh with 451,346 elements, a medium mesh with 1,116,870 elements and a fine mesh with 2,693,194 elements. The results were exported by creating a line In the middle of the domain where is the best place where the lowest level of the effects of wall. After exporting the data, it has been manipulated by creating Matlab codes which includes dividing the data in z direction to equal spaces and then taking the average for each space to give smoother plots in despite of the effects of transient flow. Appendix C.1 and C.2 show the codes. Plots of the velocity magnitude and total temperature are shows below:

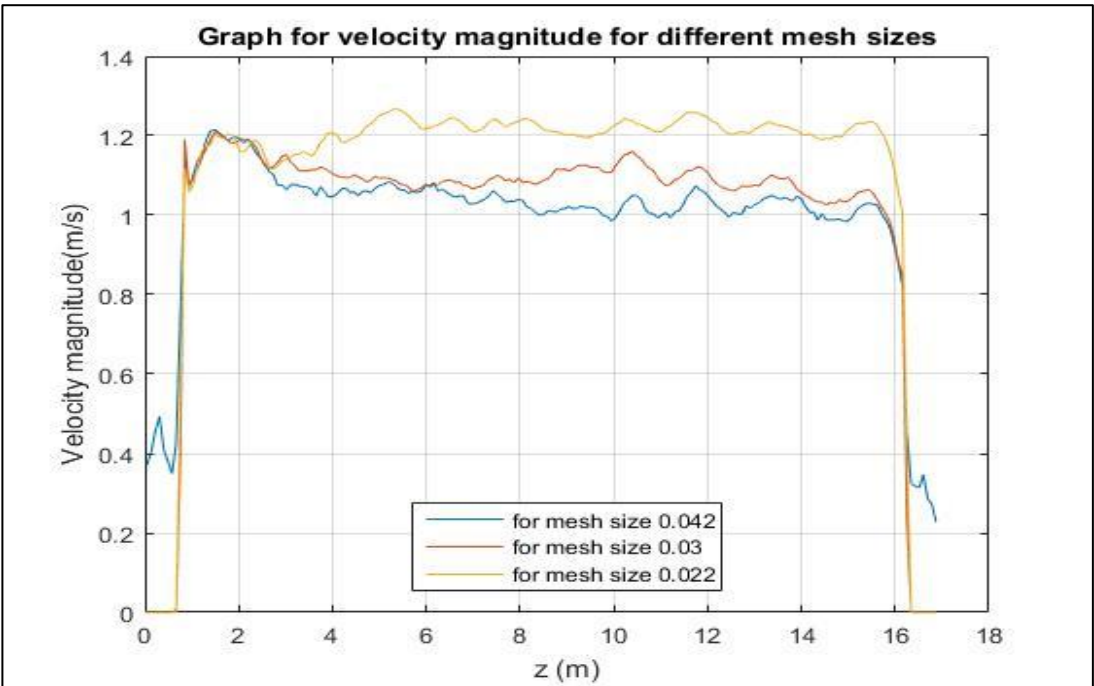


**Figure 46: velocity magnitude for different mesh sizes**

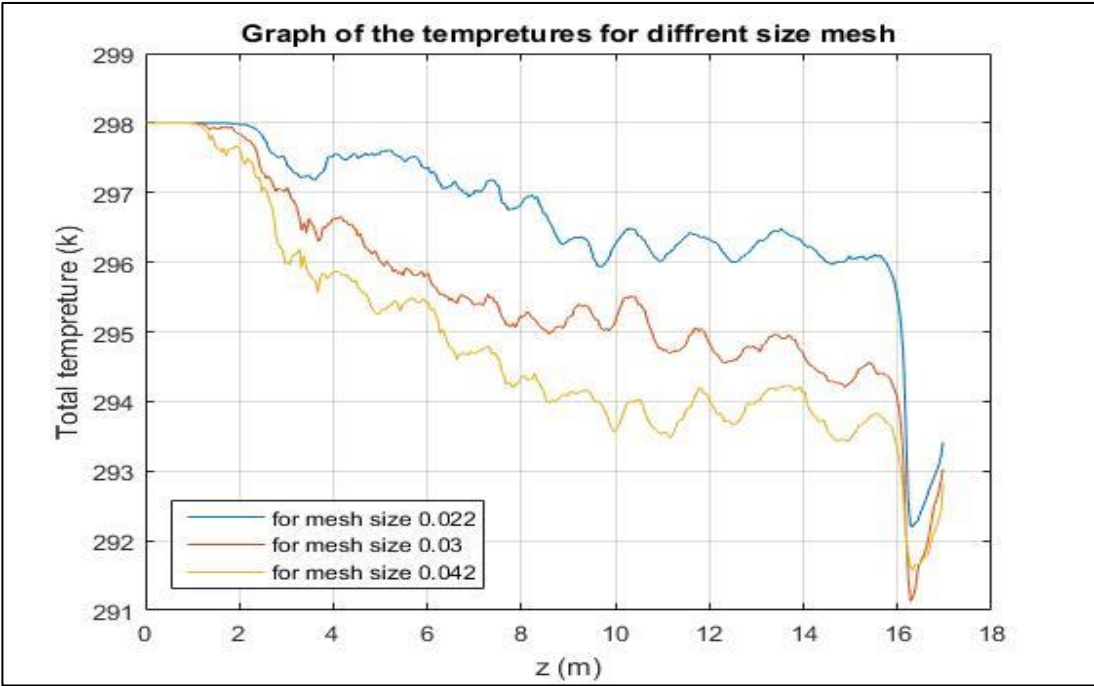


**Figure 47: total temperature for different mesh sizes**



From the above plots, it is obvious that the solution does not independent for the mesh effects which means finer mesh need to be tested. However, due to the limitation with the time and required licence of CFD to do the simulation, it was hard to go ahead with finer mesh. Moreover, one simulation for finer mesh was taking more than 2 weeks which make getting results are impossible for student who has very limited time. Therefore, more changes in the design of the model were required which will be explain in next chapter.

### **3.6.2 Simulation for different residence time**

This simulation has been carried out in order to reach a solution independent of the initial conditions and then to determine the statistics of the flow field. The coarser mesh with 451,346 elements, has been used to run the simulation as other two meshes will be complicated to be simulated with the available limitation. Therefore, the simulation has been run for four residence times. Then, data of the velocity and total temperatures were exported as ASCII file and then modified by creating Matlab codes. These codes have been created to take the average of data in each space to give smoother plots. Also, these codes have found and plotted the average of the data from all 4 residence time. Appendix C.3 and C.4 show the codes.

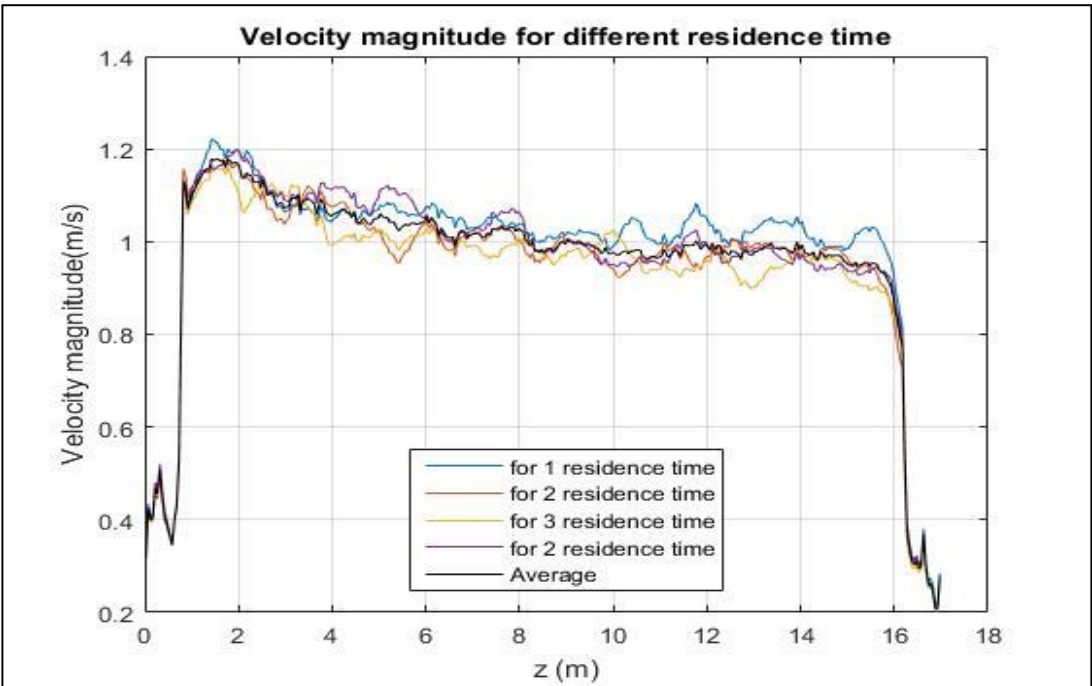


Figure 48: Velocity magnitude for different residence time

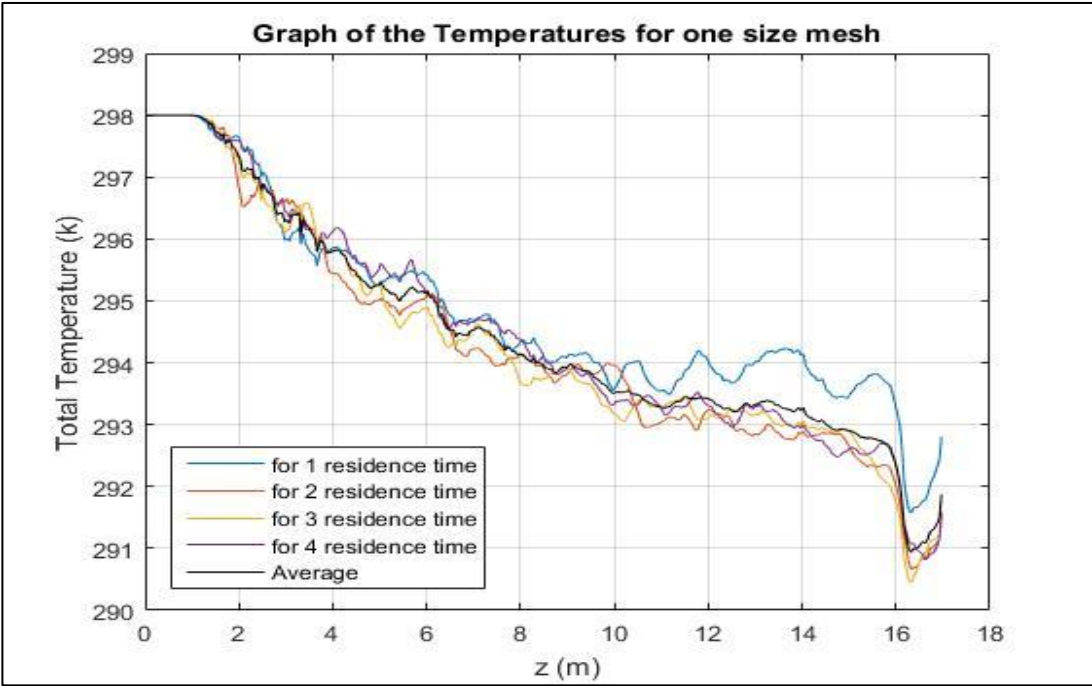


Figure 49: Graph of the temperatures for different residence time

From Figure 48 Figure 49 which show the plots for the data after the simulation, it is obvious that the solution after 1 residence time cannot give statistically stable data comparing with other plots. It is higher than other plots which mean a big difference between the data from 1 residence time simulation and others. Therefore, the data will be obtained after two residence time as it gives initial condition independent solution.

### **3.7 Summary**

Different models have been created and developed in order to help the author to be familiar with the software of ANSYS. These model have been developed systematically in order to obtain the better solution of the simulation. Many changes have been done for the models. After the simulation were run, results showed that more changes are required. Last model has given good results in this study. However, the limitations make this model useless especially with the problem with the available licenses of CFD in the university which restrict the author to run simulation for mesh elements less than 500,000 only. Therefore, a change in one of the dimension of the tank will be done to make the number of mesh elements within the academic license. More information will be provided in the next chapter.

## **CHAPTER 4: FINAL MODEL**

### **4.1 Introduction:**

In this chapter, more information about the final model will be given. These information will cover many important steps including the way in which the model was created, the required changes in mesh generated and in the setup as well. Then, it will produce analysis for the obtained results from the simulation.

### **4.2 Final Computational Domain**

Design modeller was used to create a three dimensional rectangular tank with dimensions (15 m× 0.092 m× 0.85 m). The width of the preliminary domain was changes from 0. 46 m to 0.092m to make the number of the elements less than 500,000 with the finest mesh size 0.022m. Thus, more simulation with different velocities have been done with less time as the simulation done within the limitation of the CFD licences. No more changes on the domain have been done. Figure 44 Computational domain after applying the changes.

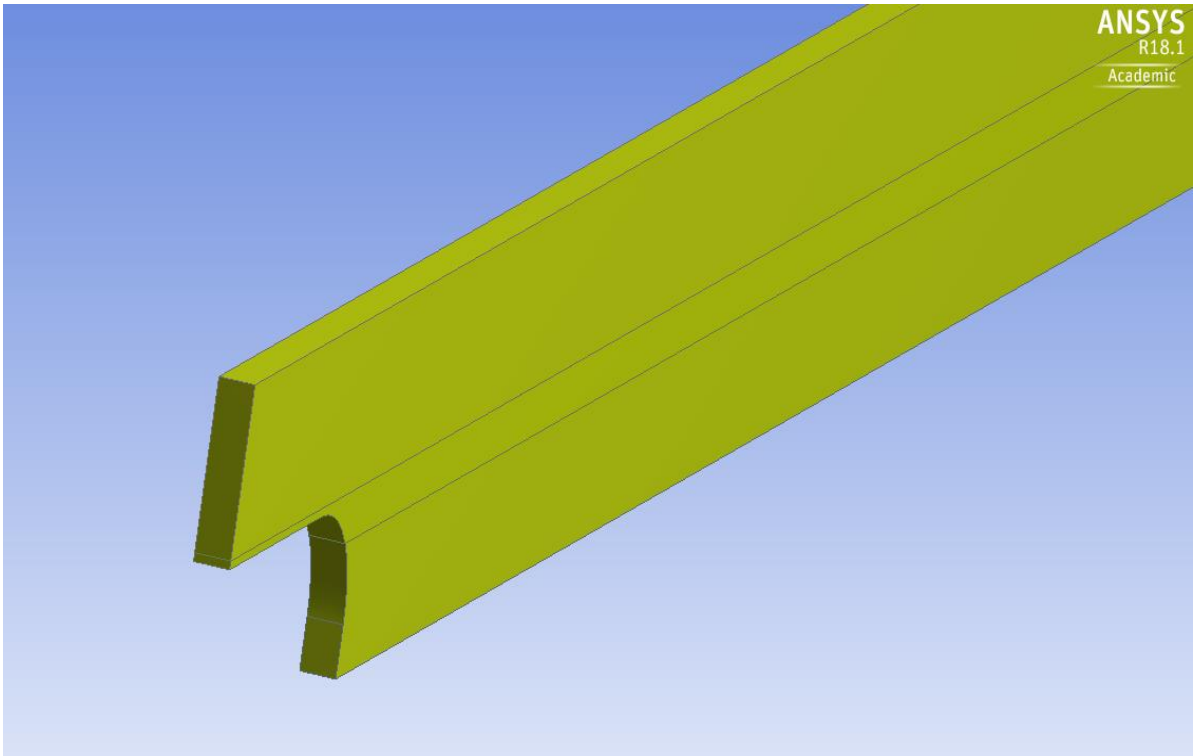


**Figure 50: Final domain**

### **4.3 Mesh generation**

Mesh generation also were included some changes in order to get less number of mesh element with better resolution. In the preliminary domain, the height of the body of influence was 0.35 m which is much higher than expected wave's height under such conditions of winds. The expected height of waves has been seen from the previous simulation. Therefore, the height of the body of influence have been reduced to cover exact area where the waves can be generated. It becomes 0.25m. In this domain, also three mesh size have been chosen for the interesting area around the interface air water as in Table 5, which shows three types of mesh sizes with the number of nodes and elements for each mesh in addition to the quality of them.

**Table 5: Comparison for different mesh sizes**

	Finer mesh size (m)	Elements	Nodes	Quality	
				Max Skewness	Min Orthogonal quality
	0.022	429367	87788	0.89422	0.10578
	0.032	175762	39293	0.85248	0.14752
	0.042	92283	21844	0.80029	0.19971

Form Table 5, it can be seen that the quality of mesh size 0.022 is lower as the max skewness is 0.89422 and the Orthogonal quality is 0.10578. However, the elements that cause this low level of quality are not in the interesting area around the water surface and then it is not likely to impact the required results. Figure 51 shows the elements that have worse skewness quality in the domain with red circle. While, Figure 2 shows the elements with worse orthogonal quality in the domain.

In despite of that, the quality still within the range of the recommendation level (GroupSSC, 2014). The named selections of the faces and prisms have not been changed.



**Figure 51: The elements that have worse skewness quality**

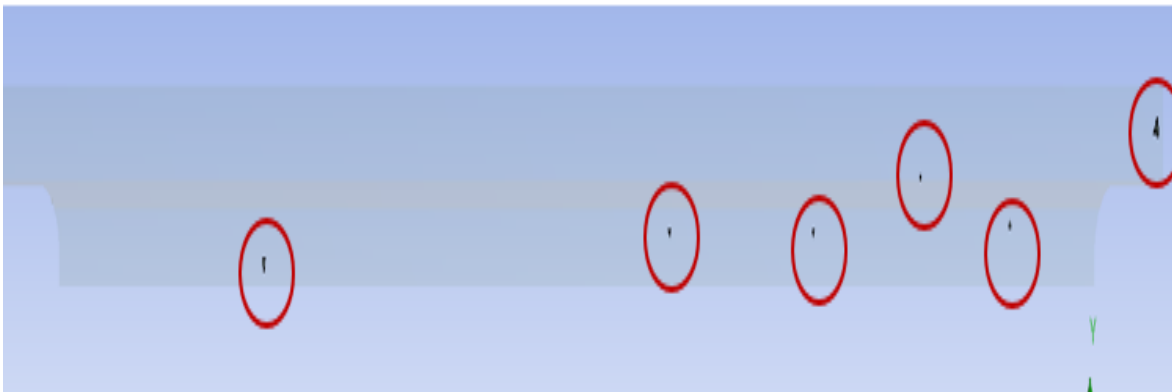


**Figure 52: The elements that have worse orthogonal quality**

#### **4.4 Setup**

The same setup steps of the preliminary domain have been used with this model with no any changes. Simulation have been run for variety of velocity magnitudes (0.9, 1.3, 2 and 3.2) m/s. for (0.9 and 1.3m/s) were taken from the experiment that was done by (Palada et al., 2012) while the other velocities (2 and 3.2 m/s) have been taken as the range of the velocities between them will include small wavelets, crests appear glassy and waves will not be broken under such a wind speed. (Thomson, 1981b). Therefore, there are not any

effects of broken waves on the results. The simulations have been run for two residence time for each speed in order to obtain a solution independent of the initial conditions as it mentioned earlier in previous chapter..

#### **4.5 Flow Field Data Analysis**

Before exporting any data, another mesh independency test has been done to find whether there is effect of the mesh size on the solution or not. After getting the results and plotting the data, it is obvious that the mesh independency has not been reached. Therefore, mesh need to be finer for better results. However, it is impossible to go finer than 0.022 at this stage as it will require more than the academic licence that is available for master student. Therefore, the solution and results will be exported from the simulation of mesh with size 0.022 after two residence time as the best solution at this stage. Figure 53: results of velocity magnitude for different mesh sizes.



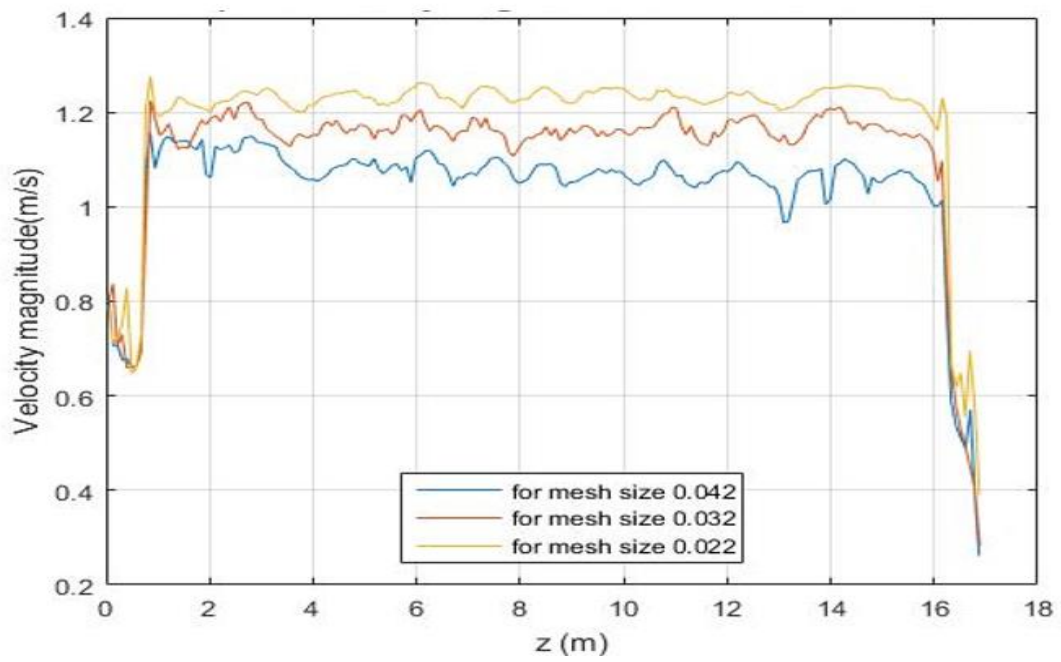


**Figure 53: results of velocity magnitude for different mesh sizes.**

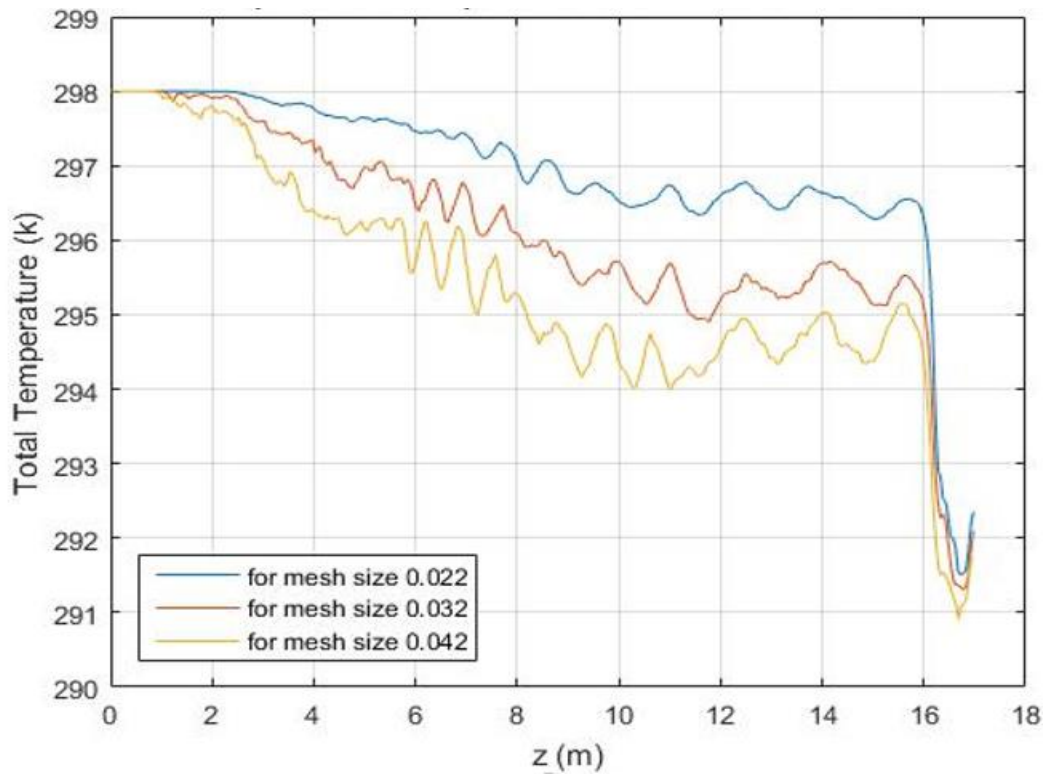


**Figure 54: results of the temperatures for different mesh sizes.**

The simulation data has been exported after 2 residence time as it will be independent from the initial conditions. Minimizing the effect of the wall boundaries is very important because it might lead to incorrect results that does not much the real environment. It is considered one of the common problems with using computational simulation. Therefore, better results will be obtained with minimizing the effect of the boundaries in the domain and so a plane with the dimensions showed in **Error! Reference source not found.** was created to export the data far from the wall boundaries. These data will be manipulated latter with mat lab to get rid of the effects of the inlet and outlet boundaries.

**Table 6: Dimensions for the plane**

Point 1	X <sub>o</sub>	Y <sub>o</sub>	Z <sub>o</sub>
	0.046	0	-1
Point 2	X <sub>1</sub>	Y <sub>1</sub>	Z <sub>1</sub>
	0.046	0	16
Point 3	X <sub>2</sub>	Y <sub>2</sub>	Z <sub>2</sub>
	0.046	0.85	16

The data shown in Table 7 have been exported with ASCII format form nodes. Then, the date have been manipulated by using MATLAB, although there was an attempt to use Microsoft Office Excel 365 to manipulate the exported data and plot some figures, but Excel showed difficulty to deal with large number of data. Some codes of MATLAB have been used to analysis and plot the results and as it will be shown in Appendix C.

**Table 7: Exported data**

	Data	Reason for exporting
1	x-coordinate	To identify and determine the position of nodes in x-axes in the computational domain
2	y-coordinate	To identify and determine the position of nodes in y-axes in the computational domain
3	z-coordinate	To identify and determine the position of nodes in z-axes in the computational domain
4	Velocity magnitude	Used to provide an information about the velocity profile in the domain
5	dX-Velocity/dx dY-Velocity/dx dZ-Velocity/dx dX-Velocity/dy dY-Velocity/dy dZ-Velocity/dy dX-Velocity/dz dY-Velocity/dz dZ-Velocity/dz	These velocity gradients will used to calculate shear stress on the water surface.
6	Volume fraction of phase 1 (Air)	To identify the interface between air and water in the domain
7	Volume fraction of phase 2 (Water)	To identify the interface between air and water in the domain

To avoid and minimize the effects of the wall, air inlet and air outlet boundary conditions on the results, a sampling region was chosen by using Matlab to be from (5-10m) in z-direction and from (0.25-0.45m) in y-direction. Figure 55 shows the sampling region that is illustrated by the red rectangle.

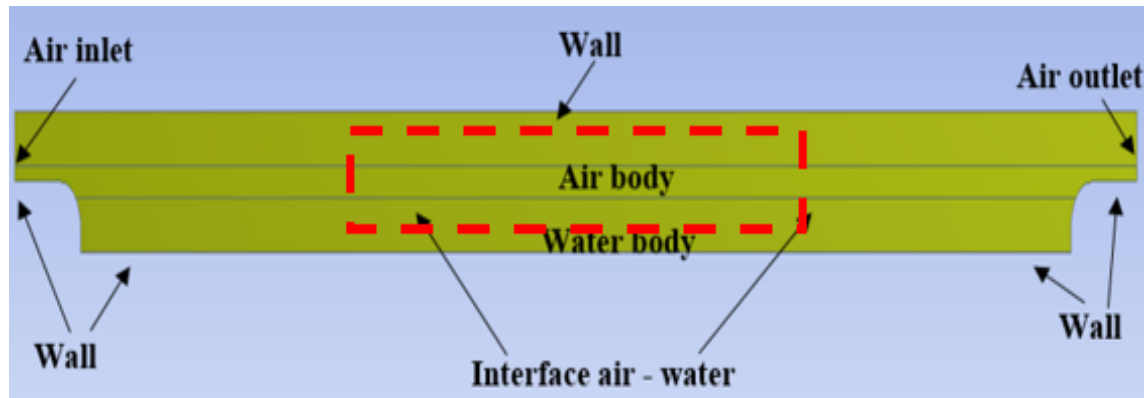


**Figure 55: Sampling region**

The data were exported for four winds speeds (0.9, 1.3, 2 and 3.2m/s) for two residence time. Using Matlab has helped to done the following tasks:

- Exported data have been sorted and organized by using interpolation functions family.
- Contour function was used for the plotting.
- The data of the velocity magnitude was sorted and plotted to check the velocity profile in the domain (Appendix C.6).
- Volume fraction has been plotted in order to identify the interface between air and water in the domain (water surface). (Appendix C.7).

- From the velocity gradients in y and z direction, shear stress has been find in z-direction and y-direction by using the equation (5). As the required shear stress is for water surface, the dynamic viscosity of water has been taken to calcite the shear stress. It has been taken as (0.001139 kg.m/s) at 15 C° which is the initialization temperature of water.

$$\tau_{zy} = \mu \left( \frac{\partial v_y}{\partial z} \right) \quad (5)$$

- Then the shear stress on the water surface was found by solving (6) in Matlab.

$$\tau_{yz} = -\frac{\sigma_y - \sigma_z}{2} \sin 2\theta + \tau_{yz} \cos 2\theta \quad (6)$$

Where:

$\tau$ : shear stress N/m<sup>2</sup>

$\mu$ : dynamic viscosity pa.s

$\sigma$ : normal stress N/m<sup>2</sup>

- Shear stress was plotted (Appendix C.8).
- The wavelength, amplitude and frequency of the waves were calculated. (Appendix C.9). More details will be illustrated in next section.

## **4.6 Results and discussion**

### **4.6.1 Volume fraction Plots**

The volume fraction of water has been plotted under the effects of wind with different speeds of air inlet including 0.9m/s (3.24 km/h), 1.3m/s (4.68km/h), 2m/s (7.2 km/h) and 3.2 (11.52 km/h). These plots of volume fraction will provide observation and derivation of the results. It will help to show the location of the waves, wave's frequency and wavelength. From Figure 56, Figure 57, Figure 58, Figure 59, it can be seen that the waves were happened in the interface between air and water. In this study, the water surface is more stable with lower wind speed and tend to be instable at higher speed, where the wavelength is longer and the frequency is higher. Therefore, higher wind speed would affect monolayers on the water surface. The code of Matlab that has been used to obtain these plots is shown in appendix C.7.

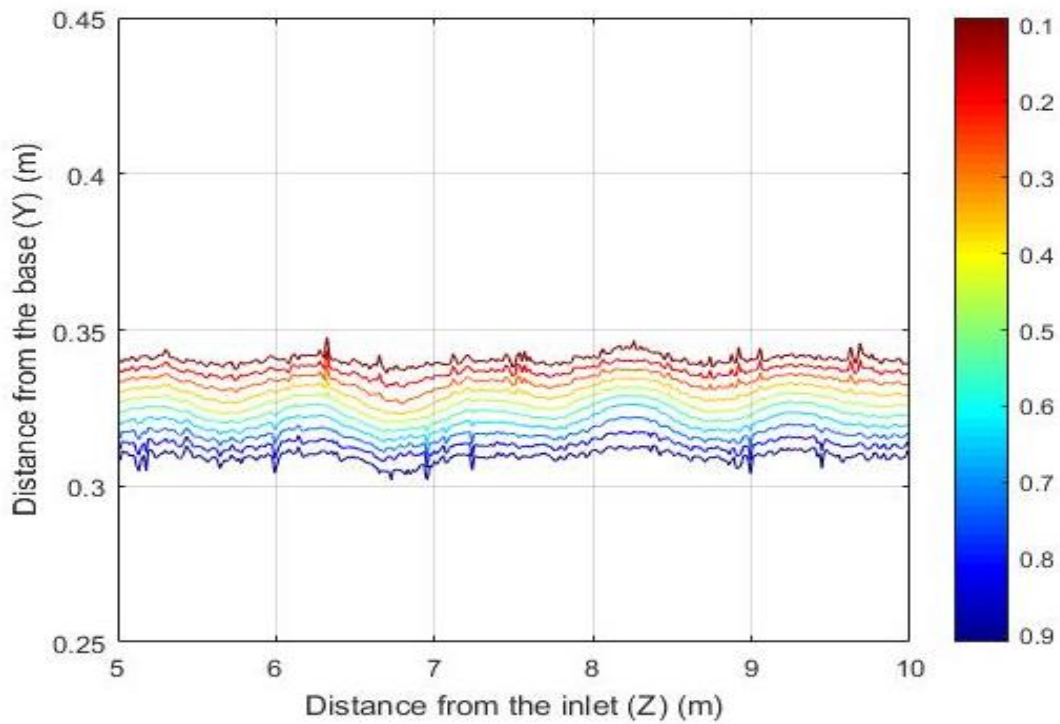
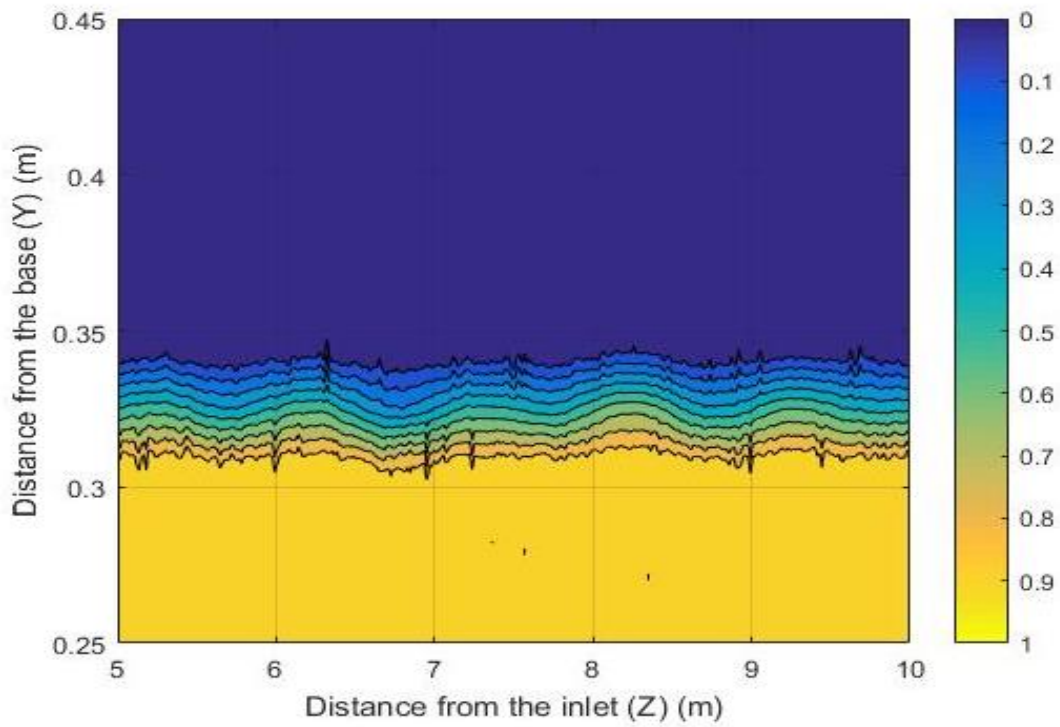


**Figure 56: Volume fraction of water at wind speed 0.9m/s**

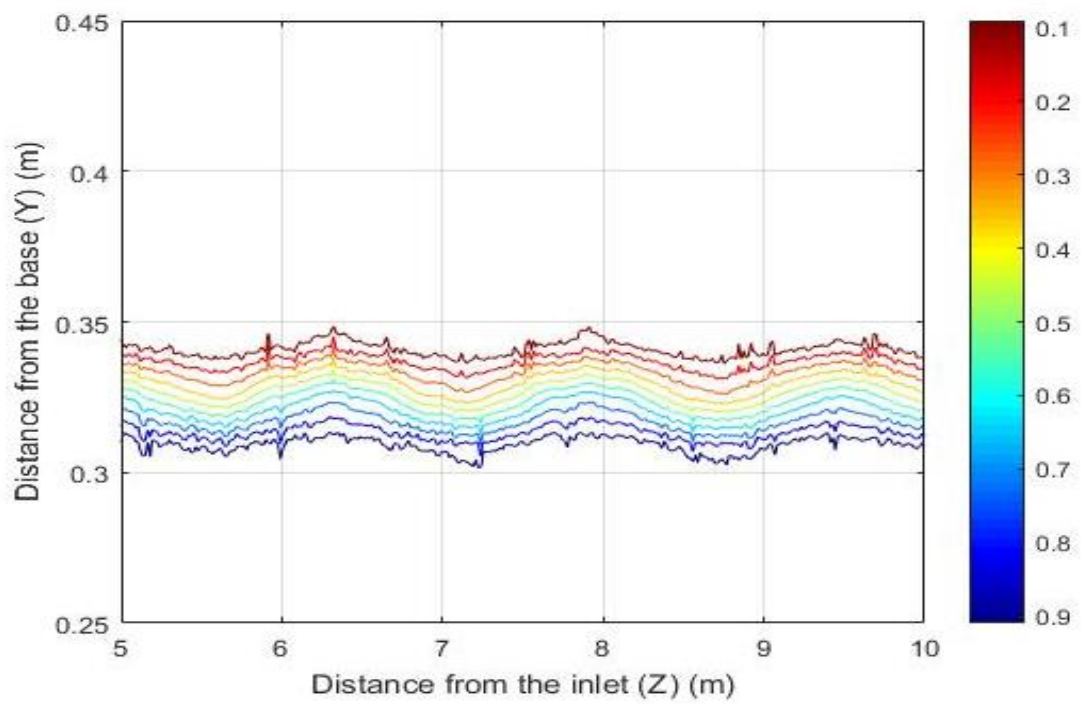
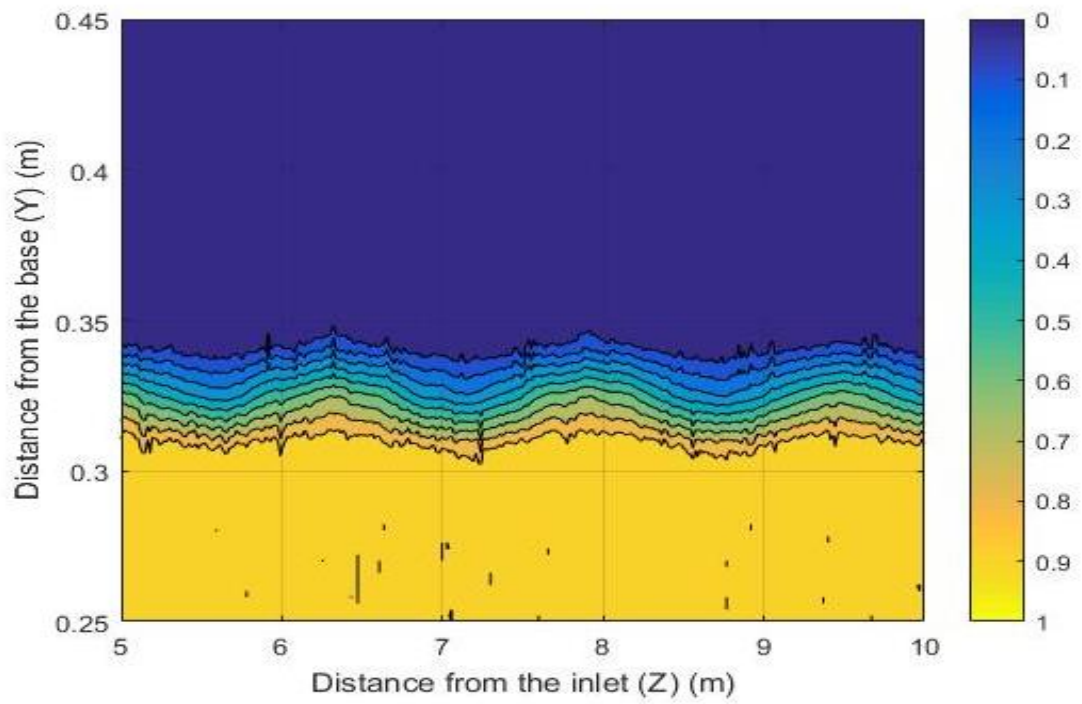


**Figure 57: Volume fraction of water at wind speed 1.3m/s**



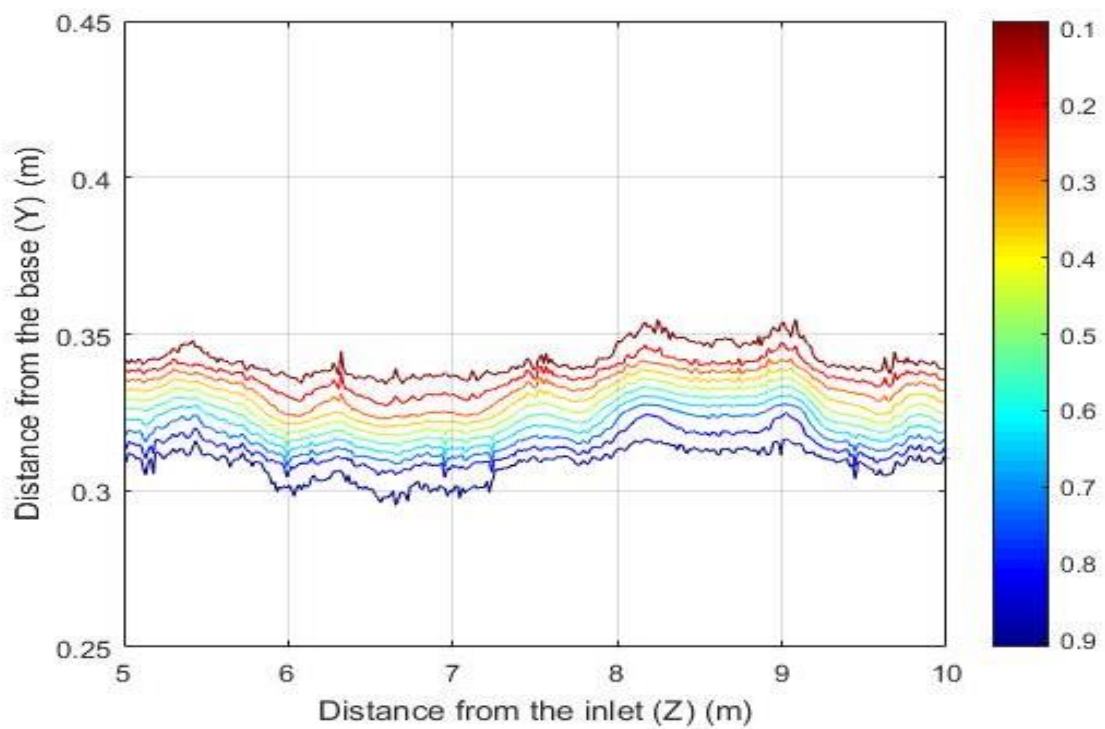
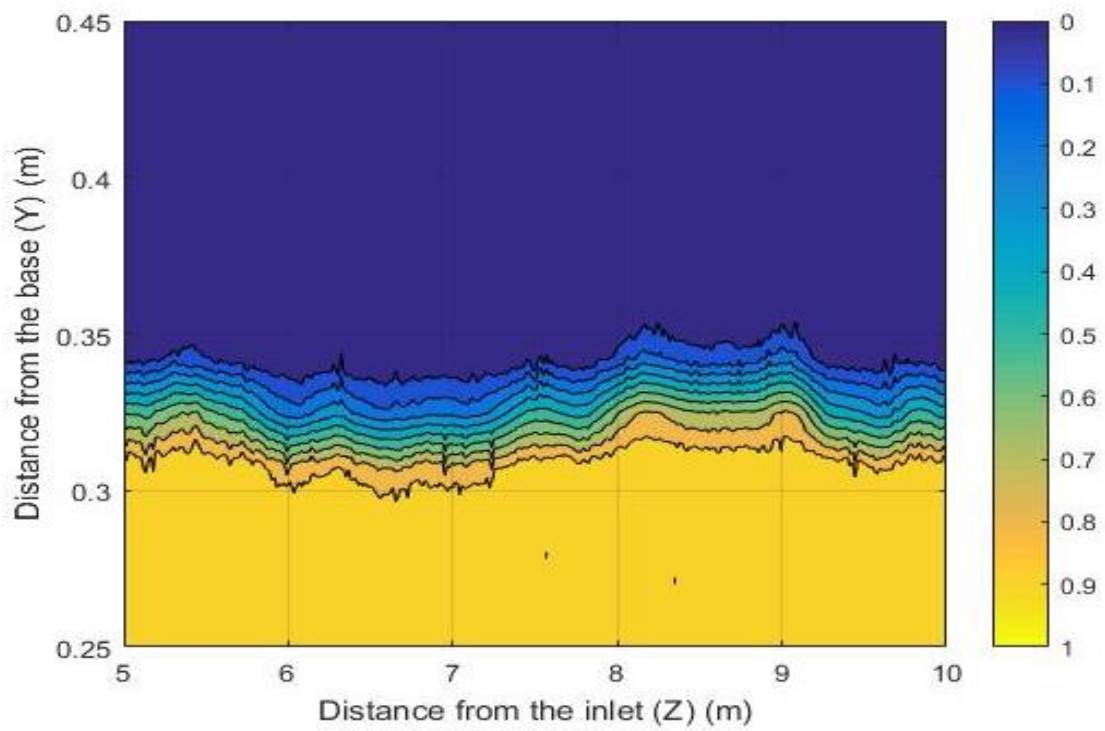


**Figure 58: Volume fraction of water at wind speed 2m/s**

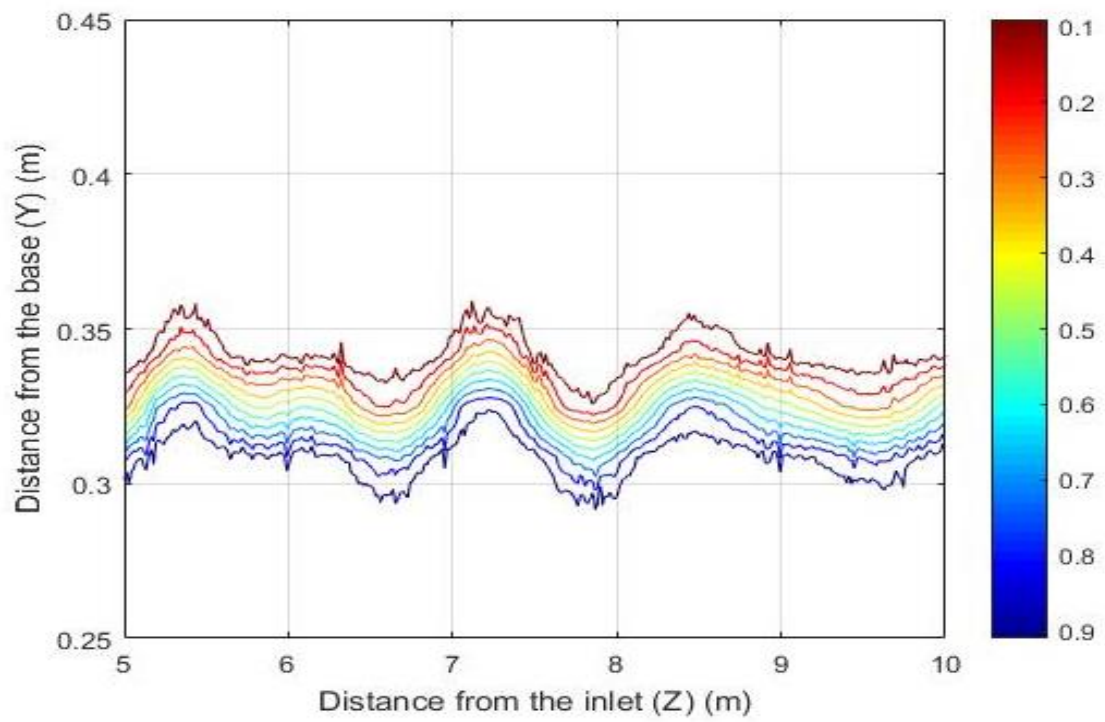
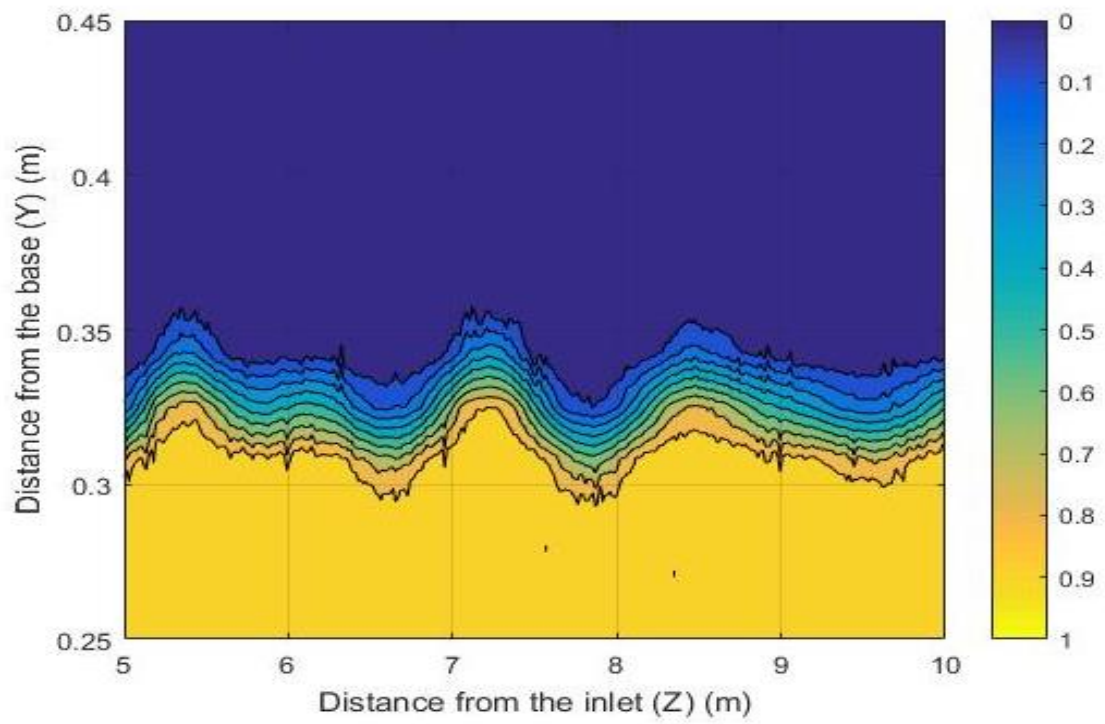


**Figure 59: Volume fraction of water at wind speed 3.2m/**

#### 4.6.2 Waves' frequency and amplitude plots

The parameters of waves have been determined and plotted by using Matlab codes (Appendix C.8). From the exported data of volume fraction, the results were obtained. For wind speed (3.2 and 1.3m/s) the sampling region allow for capturing the results while at wind speed (0.9 and 2 m/s) the dimensions of the sampling region in z-direction were changed to be from (5-12m) and (3-11m) respectively. Table 8) shows the values of the amplitude under the effects of different wind speeds.

**Table 8: wave's amplitude**

Winds speed (m/s)	Amplitude (m)
0.9	0.001509
1.3	0.004801
2	0.005339
3.2	0.007294

It has been found that at different wind speeds the waves' amplitude was affected. When the speed is increased, the amplitude of waves is increased proportionally. Thus, when wind speed increase, monolayers will be impacted. From (Figure 60-Figure 63) it have been shown the amplitudes of waves separately. These figures need to be normalized in order to get proper z - axis values from 0 – 1, which will help to get better understanding of the amplitude of the waves.

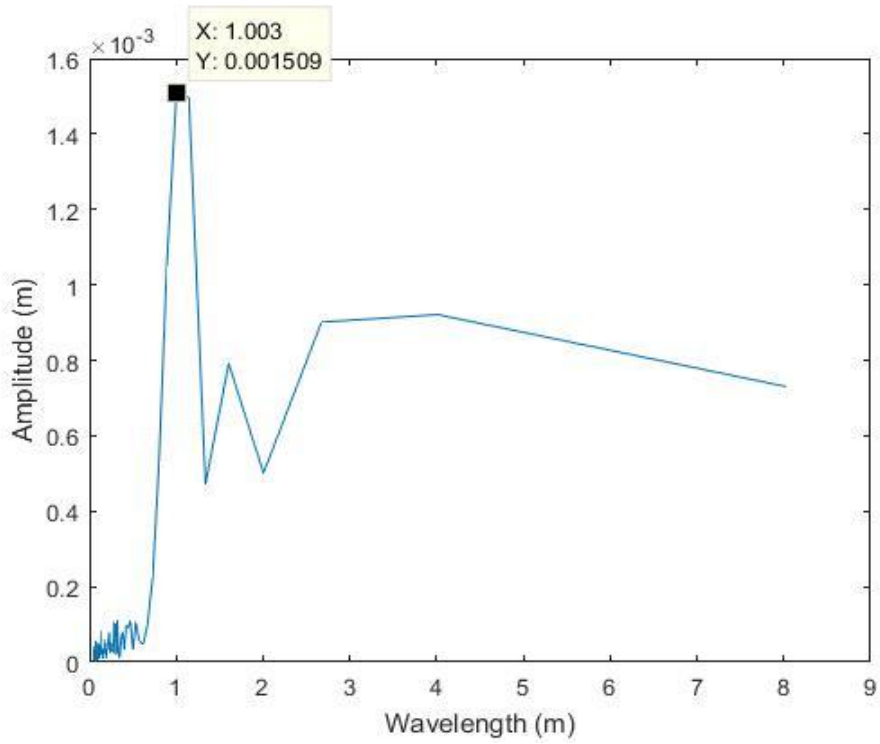


**Figure 60: Amplitude of waves at wind speed 0.9 m/s**

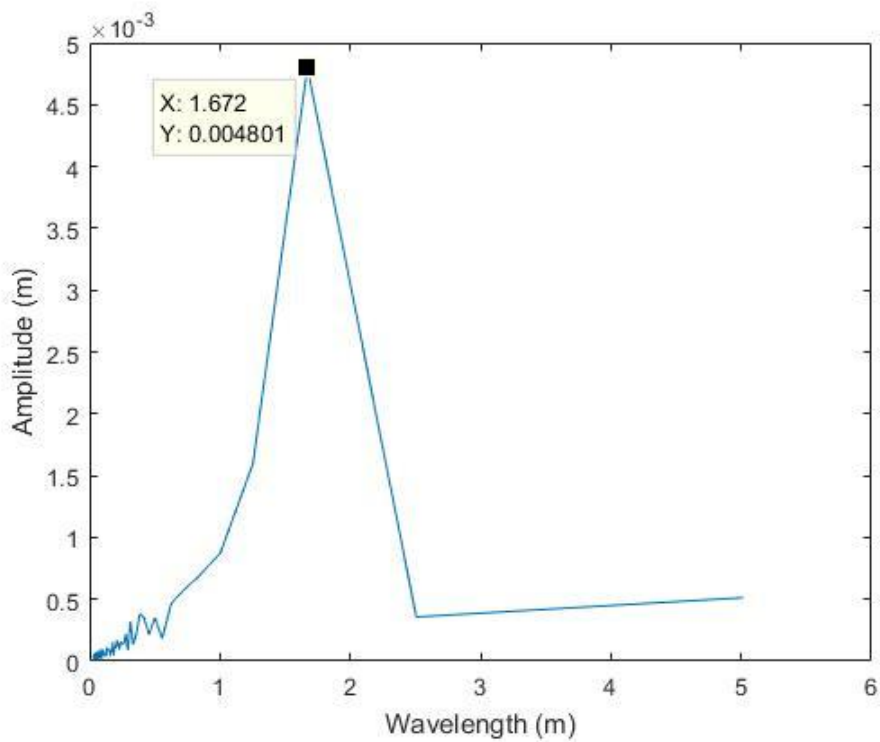


**Figure 61: Amplitude of waves at wind speed 1.3 m/s**

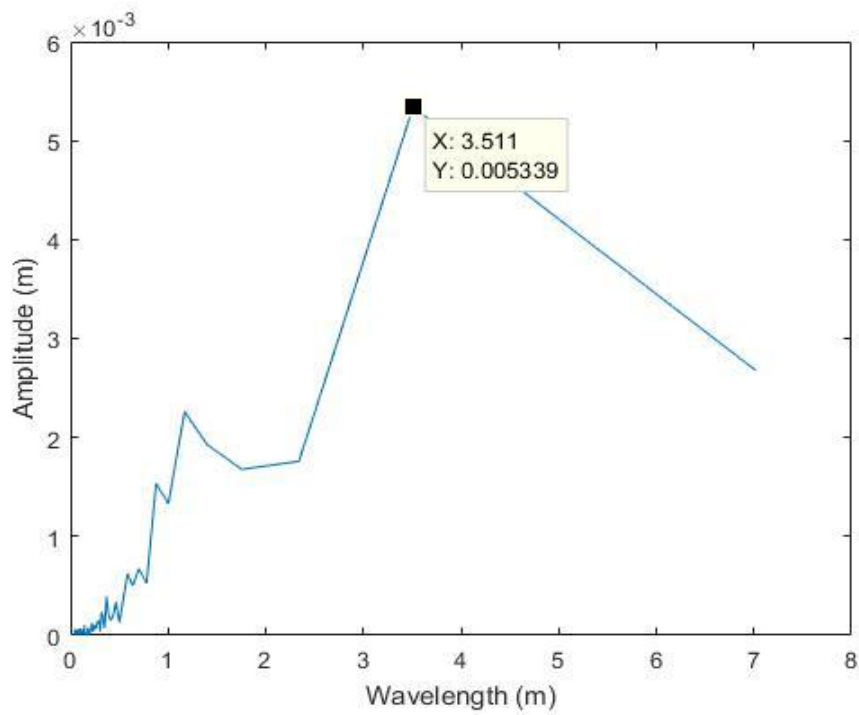


**Figure 62: Amplitude of waves at wind speed 2 m/s**

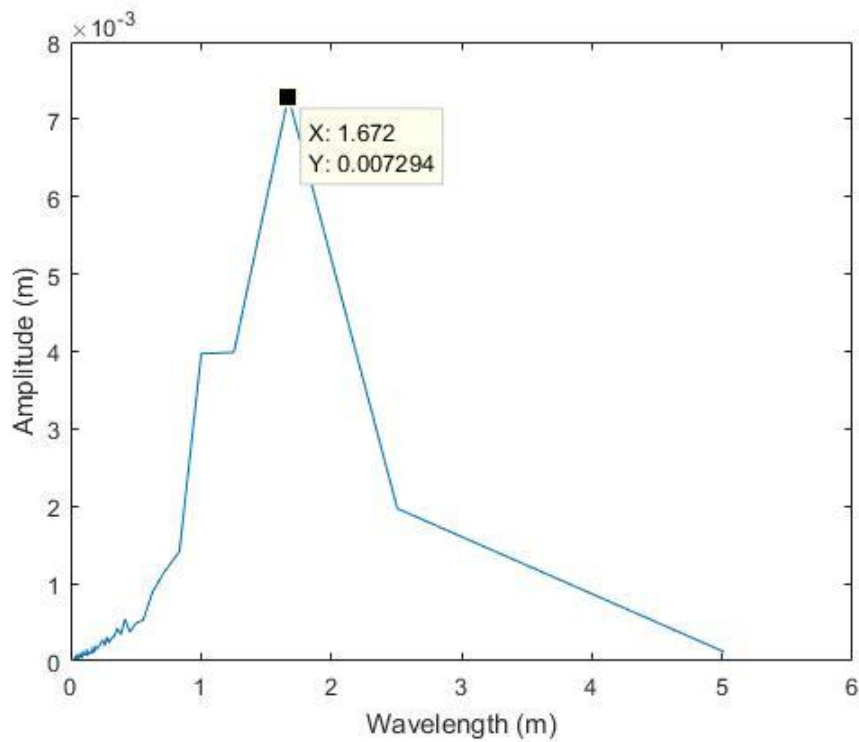


**Figure 63: Amplitude of waves at wind speed 3.2 m/s**

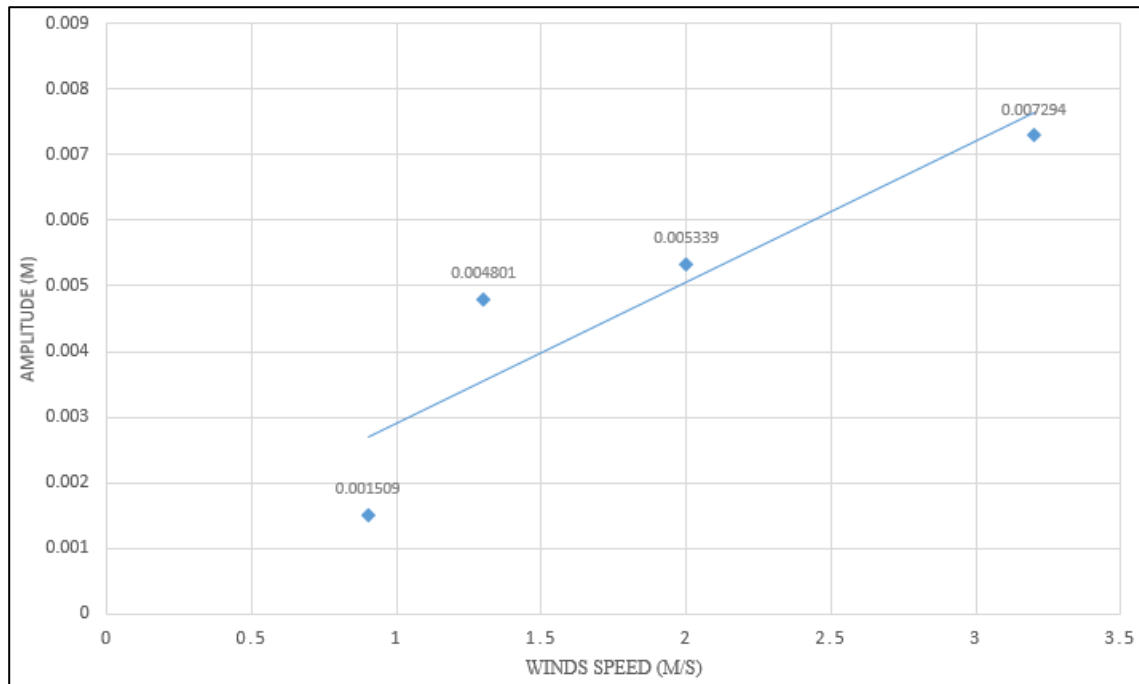


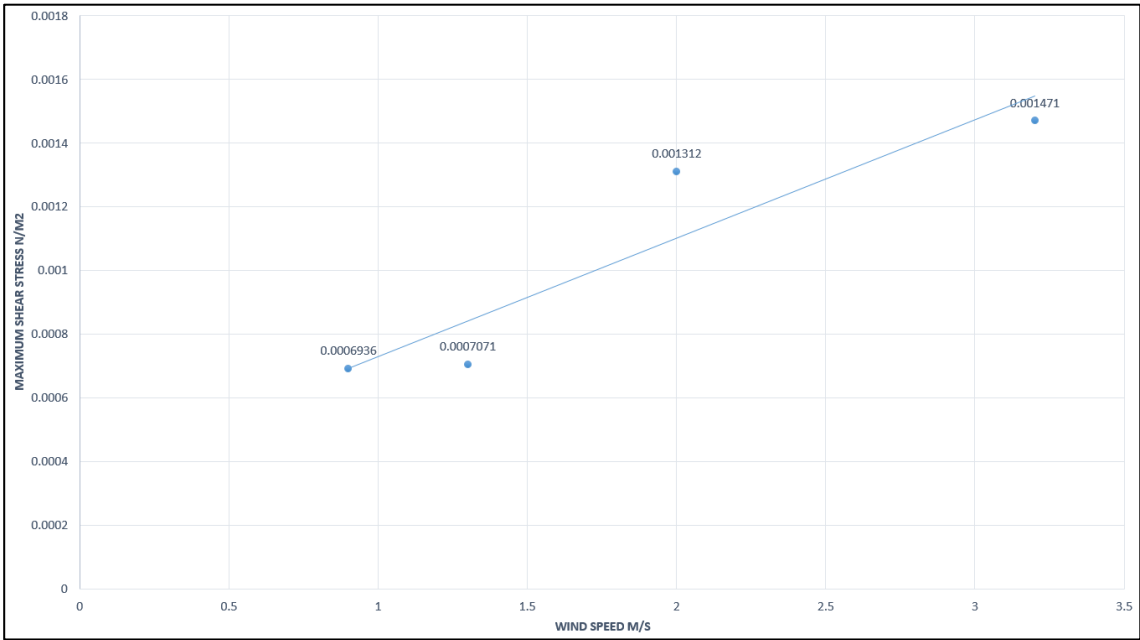
**Figure 64: Amplitudes of wave VS wind speeds**

#### 4.6.3 Shear Stress plots

Shear stresses of water surface have been found by the way that explained in the methodology of this chapter. As the model is a three dimensional, velocity gradients will be variable in x, y and z axis. However, while the wind speed is predominant in z-direction, velocity gradient in z-direction will have more influence on the shear stress of water surface. As it was expected that shear stress of the water surface will increased with increasing the wind speed. When the air passes over the water with a high speed, more energy will be transfer to the water surface and thereby forming bigger waves, which have higher shear stress. Table 9: max shear stress at different wind speeds.

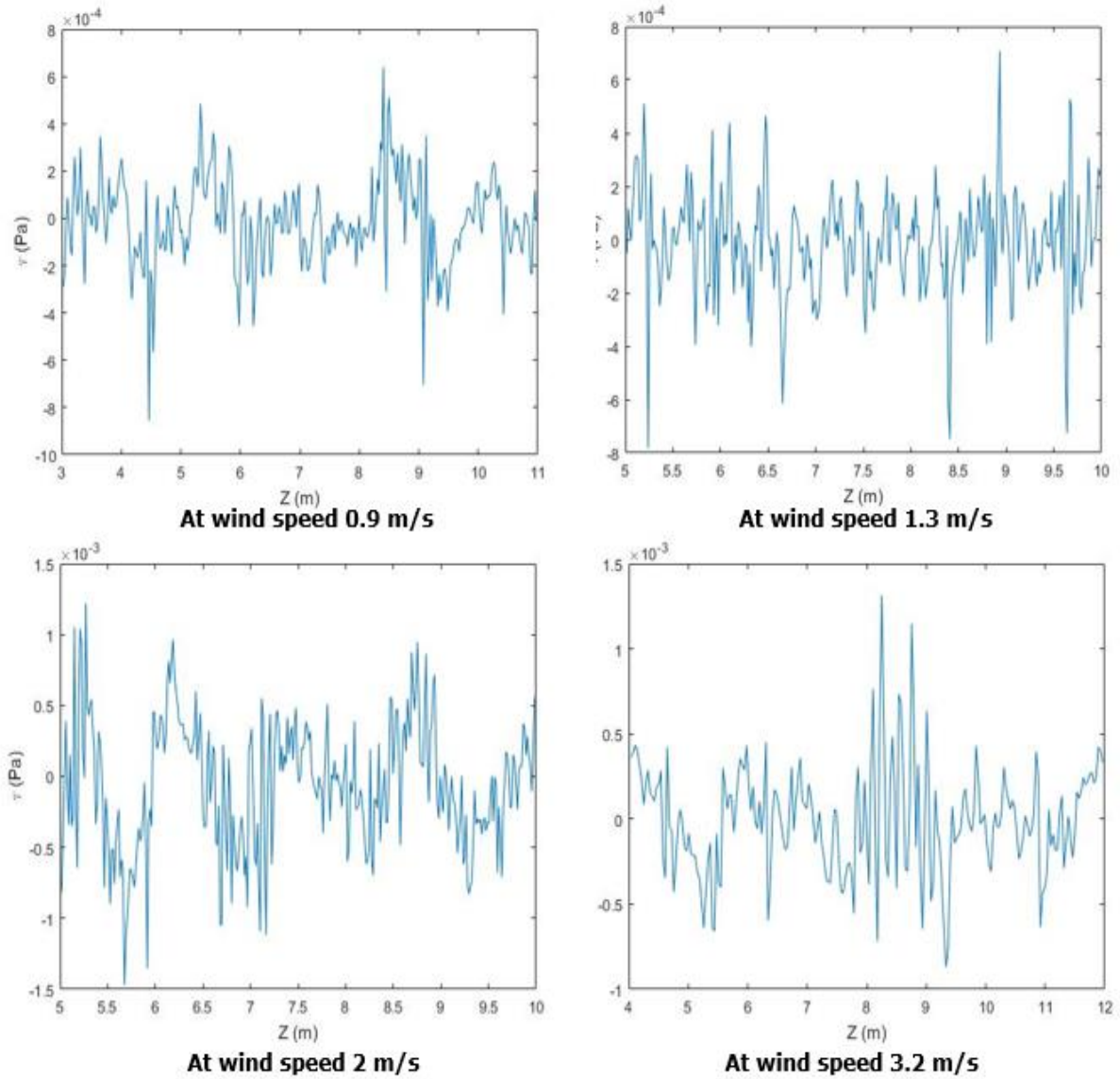
**Table 9: max shear stress at different wind speeds**

Winds speed (m/s)	Max shear stress (pa)
0.9	0.0006936
1.3	0.0007071
2	0.001312
3.2	0.001471



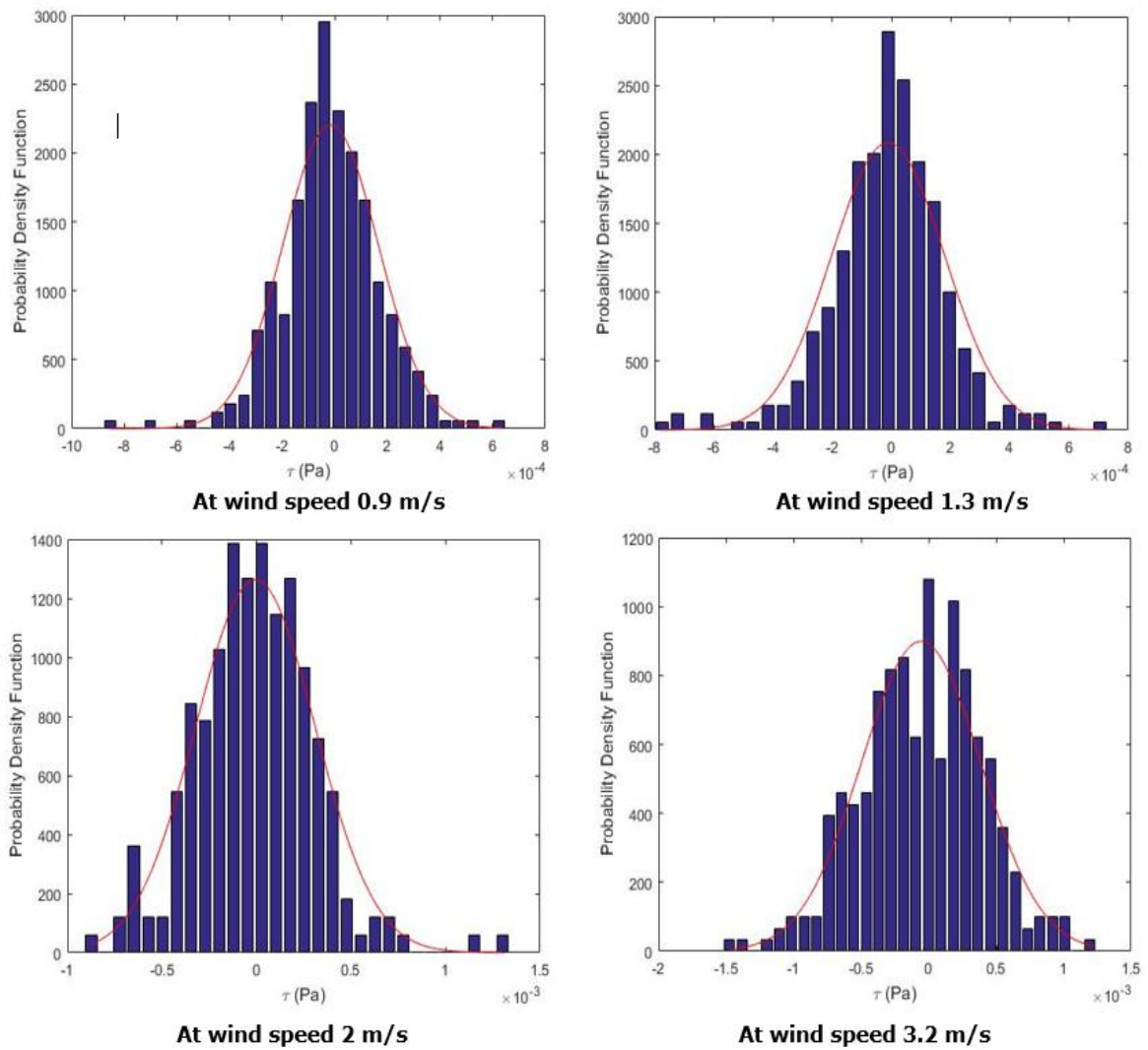
**Figure 65: max shear stress at different wind speeds**

Figure 66: Shear stress on the water surface at different wind speeds from the change in the shear stress under the wind speeds, it can be understood that higher speed will lead to destroy the monolayers as it a very thin film that will be affected by higher shear stress.



**Figure 66: Shear stress on the water surface at different wind speeds**





**Figure 67: shear stress distribution on the water surface at different wind speeds**

#### **4.7 Limitations of this study**

Although there are many tasks remain to be done in the future, this study has done many important steps in studying wind generated waves. There are different limitations that have been faced during this study and caused difficulty in completing all the tasks. Then, they affected the accuracy of the results. The main limitations are time limit of the study, the

student overloaded study, number of elements and grid resolution, simulation run-time, available licence of CFD, and computer processor.

The time was one of the problems that faced the author to not complete all the tasks of this study. The specified time for completing all the dissertation was two semesters (around eight months) which is not enough to have sufficient results.

Moreover, doing research at the same time with studying some courses put the author under overloaded study which will definitely impact the research and thereby impact obtaining better results.

A grid independency which is another significant problem, has not been completed because the difficulty with having finer mesh. The more accurate and sufficient results require creating extremely small and fine element size. Thus, the problem was created as finer mesh will increase the number of the elements within the domain and so a research licence of CFD is required to do that. However, this was not available for the author as only academic version were used which allow for maximum 500000 elements to be simulated. Moreover, finer mesh required large amount of the time steps which mean longer run time around weeks which is very difficult with the fixed time of this study. In addition, using detached eddy simulation model in this study which include switching between RANS and LES has increased the complexity of the simulation especially with the available computer processor. Therefore, it is obvious that the unavailable computer resources for the study (e.g. software, more than one computer and licences) has prevented the implementation of this dissertation completely.

Finally, because of the above reasons and because of unavailability of an experiment that done the same procedure to study the waves, the model has not been validated within this dissertation. The validation is recommended in the further work.

## **4.8 Summary**

This chapter showed the steps that have been undertaken to development the final model that helps to obtain sufficient outcomes. It shows the final design with final setup. The flow field that has been chosen to export the data and the way in which these data were exported were explained in this chapter. The obtained results from the simulation including volume fraction, wave's amplitudes and shear stress have been illustrated and discussed with their plots. The limitations with the study have been mentioned and explain in this chapter

## CHAPTER 5: CONCLUSIONS

Evaporation is one of the most significant factors that threaten the existence of the water in the world. Different techniques have been used to reduce the evaporation rates such as the chemical layers (monolayers). Monolayer is considered the best technique to reduce the evaporation. However, it is disturbed by harsh wind and waves, and then broken up and becomes ineffective. Therefore, wind-generated waves phenomena have to be studied in which the reasons behind destroying the monolayers can be known.

In this study, the idea of how wind-generated waves has been carried out. Prior to simulations being run, a study was done about the background and all related work that have been done about the evaporation, monolayers, waves and CFD. A three-dimensional rectangular tank model has been developed with two phases (water and air). Detached eddy simulation model was used in this study. Mesh independency test has been done but unfortunately the independent solution has not been reached because of the limitations. Simulation has been run for four speeds (0.9, 1.3, 2 and 3.2).

The results that were obtained from this simulation include the volume fraction, waves' amplitude and frequency and the shear stress of water surface. The results show a clear and direct relationship between wave's properties and wind speeds which is the expected. Waves with longer wavelength and higher frequency will be formed when the wind speed increased. Also, the amplitude of the waves has been found at each speed. The study found that waves' amplitude will increase with increasing wind speeds. Moreover, this study

shows how the shear stress will be generated and increased on water surface under the effect on different wind speeds.

Due to some limitation, the study has not been done completely and further work is required. These limitations can be expressed as follow: time limit, overloaded study, mesh independency, long run-time, licence of CFD and computer processor.

More tasks need to be done in order to complete this research and getting better and more accurate results. These tasks can be expressed as follow:

- Refinement of the mesh need to be done on the domain especially the area where the waves are formed until reaching the independent solution of the mesh.
- Obtaining the result and validating them with results that obtained from an experiment.
- Running the simulation for at different speeds and longer time steps to get clearer idea about the properties of the waves under different conditions.
- Changing the boundary conditions and the area of research to bigger area with longer tank that allow the flow to be fully developed.

Moreover, the main recommendations for any improvement might be carried out in the future to develop this dissertation are:

- Using more than one computer to run more than one simulation and then saving more time.

- Using computer with larger memory and faster processor that is able to run such simulation.
- Model should be developed with the finest mesh.

## REFERENCES

- AFSHAR, M. A. 2010. *Numerical wave generation in OpenFOAM®*, Chalmers University of Technology.
- ANDERSON JR, J. 1992. Governing equations of fluid dynamics. *Computational fluid dynamics*. Springer.
- ANSYS. 2009. *Variable Time Step Settings Dialog Box* [Online]. Available: <http://www.afs.enea.it/project/neptunius/docs/fluent/html/ug/node1184.htm> [Accessed].
- ANSYS. 2015. *The Detached Eddy Simulation Model (DES)* [Online]. Available: [https://www.sharcnet.ca/Software/Ansys/16.2.3/en-us/help/cfx\\_mod/i1303200.html](https://www.sharcnet.ca/Software/Ansys/16.2.3/en-us/help/cfx_mod/i1303200.html) [Accessed 08/08/2017].
- ANSYS. 2016. *Choosing Volume Fraction Formulation* [Online]. Available: [https://www.sharcnet.ca/Software/Ansys/16.2.3/en-us/help/flu\\_ug/flu\\_ug\\_vof\\_formulation.html](https://www.sharcnet.ca/Software/Ansys/16.2.3/en-us/help/flu_ug/flu_ug_vof_formulation.html) [Accessed].
- BAE, B., AHN, T., JEONG, J., KIM, K. & YUN, B. 2017. Characteristics of an interfacial wave in a horizontal air-water stratified flow. *International Journal of Multiphase Flow*, 97, 197-205.
- BAILLIE, C. 2008. Assessment of evaporation losses and evaporation mitigation technologies for on farm water storages across Australia. *Cooperative Research Centre for Irrigation Futures, Irrigation Matters Series*, 5.
- BARNES, G. T. 2008. The potential for monolayers to reduce the evaporation of water from large water storages. *agricultural water management*, 95, 339-353.
- BARNETT, T. & KENYON, K. 1975. Recent advances in the study of wind waves. *Reports on Progress in Physics*, 38, 667.
- BOM. 2006. *Average annual, monthly and seasonal evaporation* [Online]. Available: [http://www.bom.gov.au/jsp/ncc/climate\\_averages/evaporation/index.jsp?period=an#maps](http://www.bom.gov.au/jsp/ncc/climate_averages/evaporation/index.jsp?period=an#maps) [Accessed].

- BOM. 2017. *Drought* [Online]. Available: <http://www.bom.gov.au/climate/drought/drought.shtml> [Accessed].
- BPMO. 2006. *EVAPORATION CONTROL IN RESERVOIRS* [Online]. Available: <http://cwc.gov.in/main/downloads/Evaporation%20Control%20in%20reservoirs.pdf> [Accessed].
- BRANDLE, J. R., HODGES, L. & ZHOU, X. H. 2004. Windbreaks in North American agricultural systems. *New vistas in agroforestry*. Springer.
- BÜHLER, O., SHATAH, J., WALSH, S. & ZENG, C. 2016. On the wind generation of water waves. *Archive for Rational Mechanics and Analysis*, 222, 827-878.
- CAEAI. 2013. *CFD Meshing with*
- *ANSYS Workbench* [Online]. Available: [https://caeai.com/sites/default/files/CFD\\_Meshing\\_CAEA.pdf](https://caeai.com/sites/default/files/CFD_Meshing_CAEA.pdf) [Accessed 02/05/2017].
- CHALIKOV, D. V. 1978. The numerical simulation of wind-wave interaction. *Journal of Fluid Mechanics*, 87, 561-582.
- CHAPMAN, D. R. 1979. Computational aerodynamics development and outlook. *AIAA J*, 17, 1293-1313.
- CHEN, L., ZANG, J., HILLIS, A., MORGAN, G. & PLUMMER, A. 2014. Numerical investigation of wave–structure interaction using OpenFOAM. *Ocean Engineering*, 88, 91-109.
- CITYOFSYDNEY 2015. Trees and their effects on drains and pipes.
- CONSIDINE, M.-L. 2007. Putting a thin lid on evaporation losses. *ECOS, CSIRO Publishing*.
- CRAIG, I., ARAVINTHAN, V., BAILLIE, C. P., BESWICK, A., BARNES, G., BRADBURY, R., CONNELL, L., COOPER, P., FELLOWS, C. & FITZMAURICE, L. 2007. Evaporation, seepage and water quality management in storage dams: a review of research methods. *Environmental Health*, 7, 84-97.



- CRAIG, I., GREEN, A., SCOBIE, M. & SCHMIDT, E. 2005. Controlling evaporation loss from water storages.
- CROW, F. R. 1963. *The effect of wind on evaporation suppressing films and methods of modification*, Oklahoma State University.
- DEAN, R. G. & DALRYMPLE, R. A. 1991. *Water wave mechanics for engineers and scientists*, world scientific publishing Co Inc.
- DECK, S. & THORIGNY, P. 2007. Unsteadiness of an axisymmetric separating-reattaching flow: Numerical investigation. *Physics of fluids*, 19, 065103.
- DEO, M. C. 2013. WAVES AND STRUCTURES.
- DPIRD. 2017. *Drought and dry seasons* [Online]. Available: <https://www.agric.wa.gov.au/climate-land-water/climate-weather/drought-and-dry-seasons> [Accessed].
- FINN, N. & BARNES, S. 2007. The benefits of shade-cloth covers for potable water storages. *CSIRO Textile & Fibre Technology, CSIRO Gale Pacific*.
- FITZGERALD, L. & VINES, R. 1963. Retardation of evaporation by monolayers: practical aspects of the treatment of large water storages. *Australian Journal of Applied Science*, 14, 340-346.
- FRÖHLICH, J. & VON TERZI, D. 2008. Hybrid LES/RANS methods for the simulation of turbulent flows. *Progress in Aerospace Sciences*, 44, 349-377.
- GREIG, E. S. 2013. Numerical simulation of water waves in reservoirs affecting evaporation.
- GROUPSSC. 2014. *Mesh Quality Metrics Skewness* [Online]. Available: [http://www.grupossc.com/ponencias/ponencia\\_39114164442.pdf](http://www.grupossc.com/ponencias/ponencia_39114164442.pdf) [Accessed].
- GUGLIOTTI, M., BAPTISTA, M. S. & POLITI, M. J. 2005. Reduction of evaporation of natural water samples by monomolecular films. *Journal of the Brazilian Chemical Society*, 16, 1186-1190.
- HARDY, W. 1912. The tension of composite fluid surfaces and the mechanical stability of films of fluid. *Proceedings of the Royal*

*Society of London. Series A, Containing Papers of a Mathematical and Physical Character*, 86, 610-635.

- HELFER, F., LEMCKERT, C. & ZHANG, H. 2012. Impacts of climate change on temperature and evaporation from a large reservoir in Australia. *Journal of hydrology*, 475, 365-378.
- HELFER, F., ZHANG, H. & LEMCKERT, C. 2009. *Evaporation reduction by windbreaks: Overview, modelling and efficiency*, Urban Water Security Research Alliance.
- HELMHOLTZ, P. 1868. XLIII. On discontinuous movements of fluids. *The London, Edinburgh, and Dublin Philosophical Magazine and Journal of Science*, 36, 337-346.
- HIPSEY, M., SIVAPALAN, M. & CLEMENT, T. 2004. A numerical and field investigation of surface heat fluxes from small wind-sheltered waterbodies in semi-arid Western Australia. *Environmental Fluid Mechanics*, 4, 79-106.
- HORKO, M. 2008. *CFD Optimisation of an Oscillating Water Column Wave Energy Converter*, University of Western Australia.
- HUANG, Y., ZHANG, H., LEMCKERT, C. & SCHOUTEN, P. Numerical Study of the Seasonal Wave Action Developed at an Agricultural Water Reserve. Proceedings of the 34th World Congress of the International Association for Hydro-Environment Research and Engineering: 33rd Hydrology and Water Resources Symposium and 10th Conference on Hydraulics in Water Engineering, 2011. Engineers Australia, 559.
- IIHR. 2012. *Large Eddy Simulation IV* [Online]. Available: [http://www.iihr.uiowa.edu/gconstantinescu/files/2012/10/LES\\_models\\_4.pdf](http://www.iihr.uiowa.edu/gconstantinescu/files/2012/10/LES_models_4.pdf) [Accessed 08/08/2017].
- JANSSEN, P. 2004. *The interaction of ocean waves and wind*, Cambridge University Press.
- JEFFREYS, H. 1925. On the formation of water waves by wind. *Proceedings of the Royal Society of London. Series A, Containing Papers of a Mathematical and Physical Character*, 107, 189-206.

- JENNISON, I. 2003. Methods for reducing evaporation from storages used for urban water supplies. *GHD Department of Natural Resources and Mines Queensland Technical Report*.
- KAPADIA, S., ROY, S., VALLERO, M., WURTZLER, K. & FORSYTHE, J. 2004. Detached-eddy simulation over a reference Ahmed car model. *Direct and large-eddy simulation V*. Springer.
- KARIMPOUR, A. & CHEN, Q. 2017. Wind Wave Analysis in Depth Limited Water Using OCEANLYZ, a MATLAB toolbox. *Computers & Geosciences*.
- KNIGHTS, S. 2005. Reducing evaporation with chemical monolayer technology. *Aust. Cottongrower*, 26, 32-33.
- KUNISHI, H. 1963. An experimental study on the generation and growth of wind waves.
- LAUNDER, B. & SHARMA, B. 1974. Application of the energy-dissipation model of turbulence to the calculation of flow near a spinning disc. *Letters in heat and mass transfer*, 1, 131-137.
- LIN, M.-Y., MOENG, C.-H., TSAI, W.-T., SULLIVAN, P. P. & BELCHER, S. E. 2008. Direct numerical simulation of wind-wave generation processes. *Journal of Fluid Mechanics*, 616, 1-30.
- LONGO, S., LIANG, D., CHIAPPONI, L. & JIMÉNEZ, L. A. 2012. Turbulent flow structure in experimental laboratory wind-generated gravity waves. *Coastal Engineering*, 64, 1-15.
- MANTILLA, I. 2008. *Mechanistic modeling of liquid entrainment in gas in horizontal pipes*.
- MCJANNET, D., COOK, F., KNIGHT, J. & BURN, S. 2008. Evaporation reduction by monolayers: overview, modelling and effectiveness. *Urban Water Security Research Alliance Technical Report*, 6, 1-32.
- MERCIER, R. S. & NIEDZWECKI, J. M. 1994. Experimental measurement of second-order diffraction by a truncated vertical cylinder in monochromatic waves.
- MILES, J. W. 1957. On the generation of surface waves by shear flows. *Journal of Fluid Mechanics*, 3, 185-204.

- MORGAN, G. C. J., ZANG, J., GREAVES, D., HEATH, A., WHITLOW, C. & YOUNG, J. 2011. Using the rasInterFoam CFD model for wave transformation and coastal modelling. *Coastal Engineering Proceedings*, 1, 23.
- NISHINO, T., ROBERTS, G. T. & ZHANG, X. 2008. Unsteady RANS and detached-eddy simulations of flow around a circular cylinder in ground effect. *Journal of Fluids and Structures*, 24, 18-33.
- OLSEN, M. 2011. *Waves Fact Sheet* [Online]. Available: [http://secoora.org/wp-content/uploads/2017/01/wave\\_fact\\_sheet.pdf](http://secoora.org/wp-content/uploads/2017/01/wave_fact_sheet.pdf) [Accessed].
- OTTENS, M., KLINKSPOOR, K., HOEFSLOOT, H. C. & HAMERSMA, P. J. 1999. Wave characteristics during cocurrent gas-liquid pipe flow. *Experimental thermal and fluid science*, 19, 140-150.
- PALADA, C., SCHOUTEN, P. & LEMCKERT, C. 2012. Testing the effectiveness of monolayers under wind and wave conditions. *Water Science and Technology*, 65, 1137-1141.
- PANJABI, K., RUDRA, R. & GOEL, P. 2016. Evaporation Retardation by Monomolecular Layers: An Experimental Study at the Aji Reservoir (India). *Open Journal of Civil Engineering*, 6, 346.
- PAQUIER, A., MOISY, F. & RABAUD, M. 2015. Surface deformations and wave generation by wind blowing over a viscous liquid. *Physics of Fluids*, 27, 122103.
- PARK, J.-C., KIM, M.-H. & MIYATA, H. 2001. Three-dimensional numerical wave tank simulations on fully nonlinear wave-current-body interactions. *Journal of Marine Science and Technology*, 6, 70-82.
- PHILLIPS, O. M. 1957. On the generation of waves by turbulent wind. *Journal of fluid mechanics*, 2, 417-445.
- PICHÉ, R. *Constant time step vs. variable time step* [Online]. Available: <http://virtual.cvut.cz/odl/partners/tut/unit2/node5.html#SECTIO N00021000000000000000> [Accessed].

- PRASHAR, D. 2012. Self assembled monolayers-a review. *Int. J. ChemTech Res*, 4, 258-265.
- PRIME, E. L., TRAN, D. N., PLAZZER, M., SUNARTIO, D., LEUNG, A. H., YIAPANIS, G., BAOUKINA, S., YAROVSKY, I., QIAO, G. G. & SOLOMON, D. H. 2012. Rational design of monolayers for improved water evaporation mitigation. *Colloids and Surfaces A: Physicochemical and Engineering Aspects*, 415, 47-58.
- SAWAN, A. 2003. wind generated waves.
- SCHOUTEN, P., PALADA, C., LEMCKERT, C., SUNARTIO, D. & SOLOMON, D. Analysis of chemical film monolayers under wind and wave conditions. Proceedings of the 34th World Congress of the International Association for Hydro-Environment Research and Engineering: 33rd Hydrology and Water Resources Symposium and 10th Conference on Hydraulics in Water Engineering, 2011. Engineers Australia, 2161.
- SCHREIBER, F. 2000. Structure and growth of self-assembling monolayers. *Progress in surface science*, 65, 151-257.
- SHANAS, P., ABOOBACKER, V., ALAA, M. A. & KHALID, M. Z. 2017. Superimposed wind-waves in the Red Sea. *Ocean Engineering*, 138, 9-22.
- SHERMAN, B., LEMCKERT, C. & ZHANG, H. 2010. *The impact of artificial destratification on reservoir evaporation*, Urban Water Security Research Alliance.
- SILVA, M., VITOLA, M., ESPERANÇA, P., SPHAIER, S. & LEVI, C. 2015. Numerical simulations of regular waves in an ocean basin. *Marine Systems & Ocean Technology*, 10, 131-144.
- SPALART, P., JOU, W., STRELETS, M. & ALLMARAS, S. 1997. Comments on the feasibility of LES for wings, and on a hybrid RANS/LES approach. *Advances in DNS/LES*, 1, 4-8.
- SPALART, P. R. 2009. Detached-eddy simulation. *Annual review of fluid mechanics*, 41, 181-202.
- SQUIRES, K. D. 2004. Detached-eddy simulation: current status and perspectives. *Direct and large-eddy simulation V*. Springer.

- SREENIVAS, K., PANKAJAKSHAN, R., NICHOLS, D. S., MITCHELL, B., TAYLOR, L. K. & WHITFIELD, D. L. 2006. Aerodynamic simulation of heavy trucks with rotating wheels. *AIAA Paper*, 1394.
- STEFFEN, W. 2015. Thirsty country: climate change and drought in Australia.
- SULLIVAN, P. P. & MCWILLIAMS, J. C. 2010. Dynamics of winds and currents coupled to surface waves. *Annual Review of Fluid Mechanics*, 42.
- SULLIVAN, P. P., MCWILLIAMS, J. C. & MOENG, C.-H. 2000. Simulation of turbulent flow over idealized water waves. *Journal of Fluid Mechanics*, 404, 47-85.
- THOMSON 1887. On the waves produced by a single impulse in water of any depth, or in a dispersive medium. *Proceedings of the Royal Society of London*, 42, 80-83.
- THOMSON 1981a. *Oceanography of the British Columbia coast*, Gordon Soules Book Pub.
- THOMSON, R. E. 1981b. *Oceanography of the British Columbia coast*, Gordon Soules Book Pub.
- TOREKI, R. 2015. *The General Chemistry Demo Lab* [Online]. Available: <http://www.ilpi.com/genchem/demo/tension/> [Accessed 20/05/2017].
- TRAPIER, S., DECK, S. & DUVEAU, P. 2008. Delayed detached-eddy simulation and analysis of supersonic inlet buzz. *AIAA journal*, 46, 118.
- VAN DIJK, M. & VAN VUUREN, S. 2009. Destratification induced by bubble plumes as a means to reduce evaporation from open impoundments. *Water SA*, 35, 158-167.
- VERLEE, D. & ZETLAND, D. 2014. Extending water supply by reducing reservoir evaporation: a case study from Wichita Falls, Texas.
- VINES, R. 1962. Evaporation control: A method of treating large water storages.

- WANDEL, A. P., BRINK, G. N., HANCOCK, N. H. & PATHER, S. 2017. Spreading rate and dispersion behavior of evaporation-suppressant monolayer on open water surfaces: Part 2–Under wind stress. *Experimental Thermal and Fluid Science*, 87, 171-181.
- WANG, H., TAKLE, E. S. & SHEN, J. 2001. Shelterbelts and windbreaks: mathematical modeling and computer simulations of turbulent flows. *Annual Review of Fluid Mechanics*, 33, 549-586.
- WATTS, P. J. 2005. Reduction of evaporation from farm dams.
- WILLIAMS, W. J. 2014. Numerical simulations of water surfaces for improved evaporation prediction.
- XU, F., PERRIE, W., TOULANY, B. & SMITH, P. C. 2007. Wind-generated waves in Hurricane Juan. *Ocean Modelling*, 16, 188-205.
- YAO, X., ZHANG, H., LEMCKERT, C., BROOK, A. & SCHOUTEN, P. 2010. Evaporation reduction by suspended and floating covers: overview, modelling and efficiency. *Urban water security research alliance technical report*.
- ZUO, W. 2005. Introduction of Computational Fluid Dynamics. *FAU Erlange-Nürnberg, St. Petersburg*.

# **APPENDIX A: PROJECT SPECIFICATION**

University of Southern Queensland

Faculty of Health, Engineering and Sciences

**ENG 8411/8412/8414 MASTERS Engineering Research Project A/B/D**

## **PROJECT SPECIFICATION**

For: Prof. Karu Karunasena

Topic: Detailed simulations of sub-surface boundary layer in wind-generated waves

Supervisor: Andrew Wandel  
Khalid Saleh

ENROLMENT: S1 ENG8411  
S2 ENG8414

PROJECT AIM: The aim of this project is to use Computational Fluid Dynamics Software ANSYS fluent to study the sub-surface layer of water under the effects of wind. This information can be used in evaporation mitigation strategies.

SPONSORSHIP: University of Southern Queensland



PROGRAMME:

1. Research on the theory of wind and water wave.
2. Define the monolayer and the benefits of use it to prevent the evaporation.
3. Investigate different models of Computational Fluid Dynamics (CFD) such as Reynolds Averaged Navier-Stokes (RANS) and Large Eddy Simulation LES, and how they produce the Detached Eddy Simulations (DES) model.
4. Investigate different two-phase CFD models to determine the most appropriate for this case.
5. Develop CFD model of problem.
6. Using DES model with a two-phase model from air and water which will be simulated to study the conditions of water surface for a small tank.

As time permits:

Changing the boundary conditions and the area of research to bigger area than a small tank.

Agreed:

Student Name:

Hayder Al-lami

Date: 31 March 2017  
Supervisor Name: Dr. Andrew Wandel  
Date: 31 March 2017  
Supervisor Name: Dr. Khalid Saleh  
Date: 31 March 2017  
Examiner/Co-Examiner: Prof. Karu Karunasena  
Date: 31 March 2017

## APPENDIX B: FURTHER RESULTS AND PLOTS

In this appendix, more results will be shown under different wind speeds and as follow:

### B.1 At wind speed 0.9 m/s

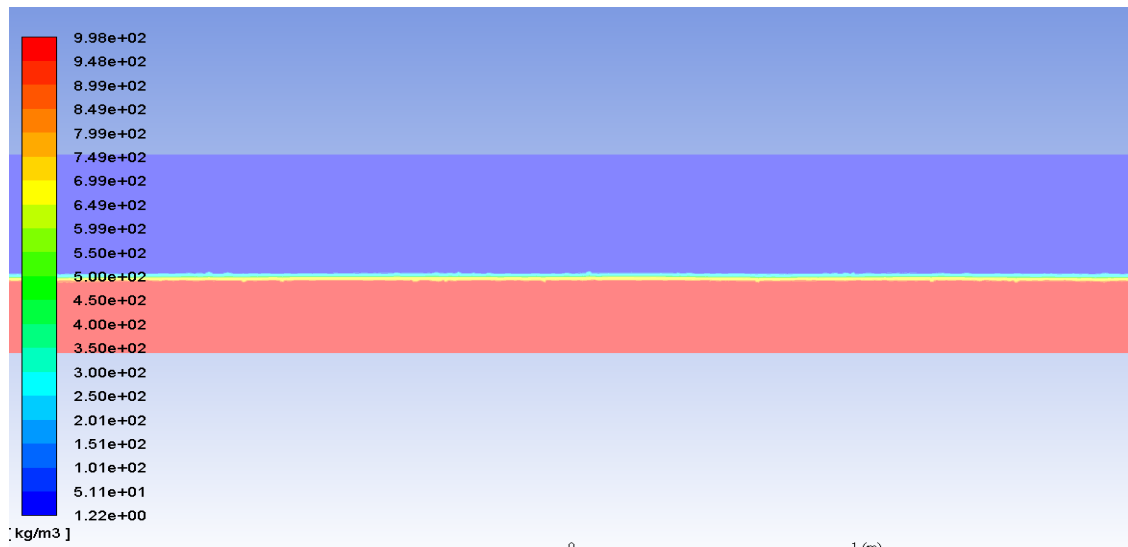


Figure 68: The density of the mixture at the middle of model at wind speed 0.9 m/s

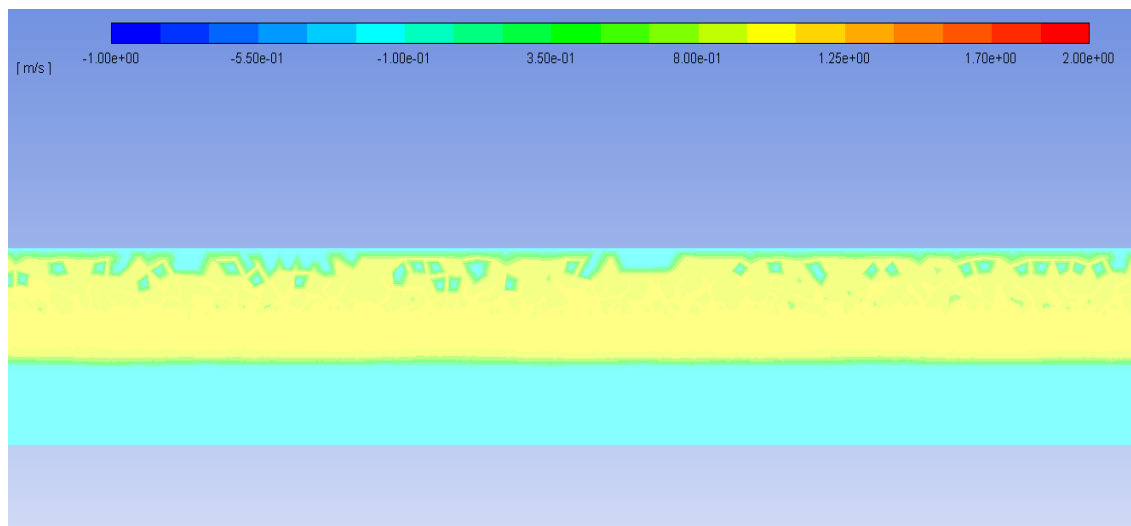
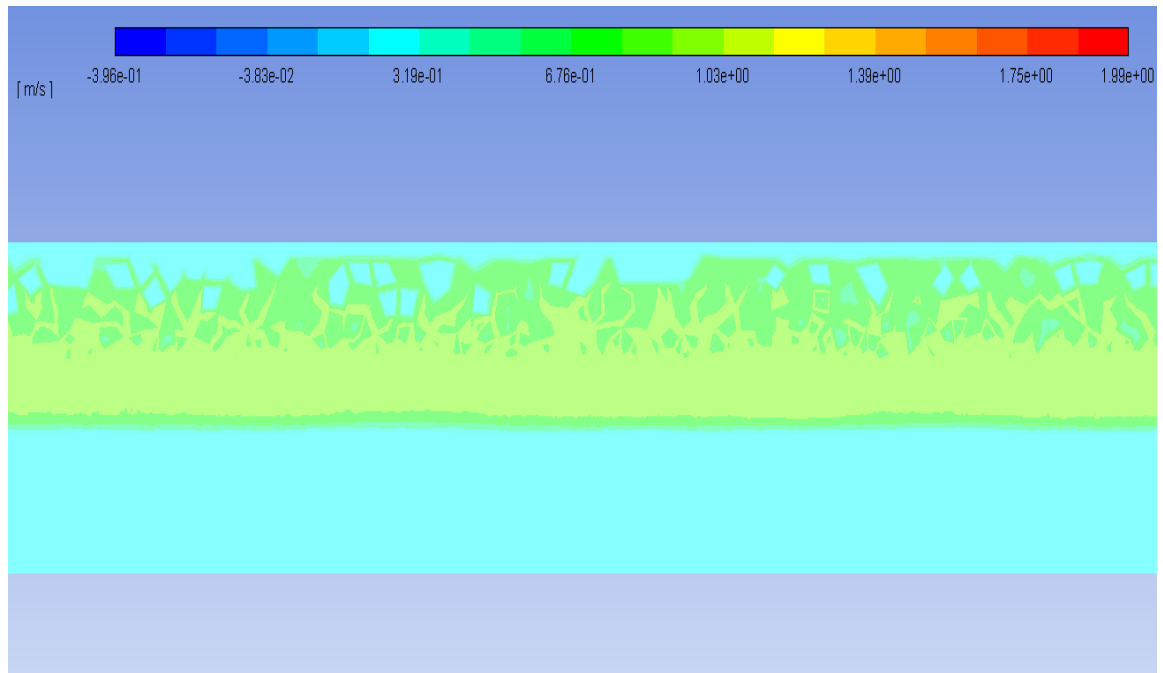
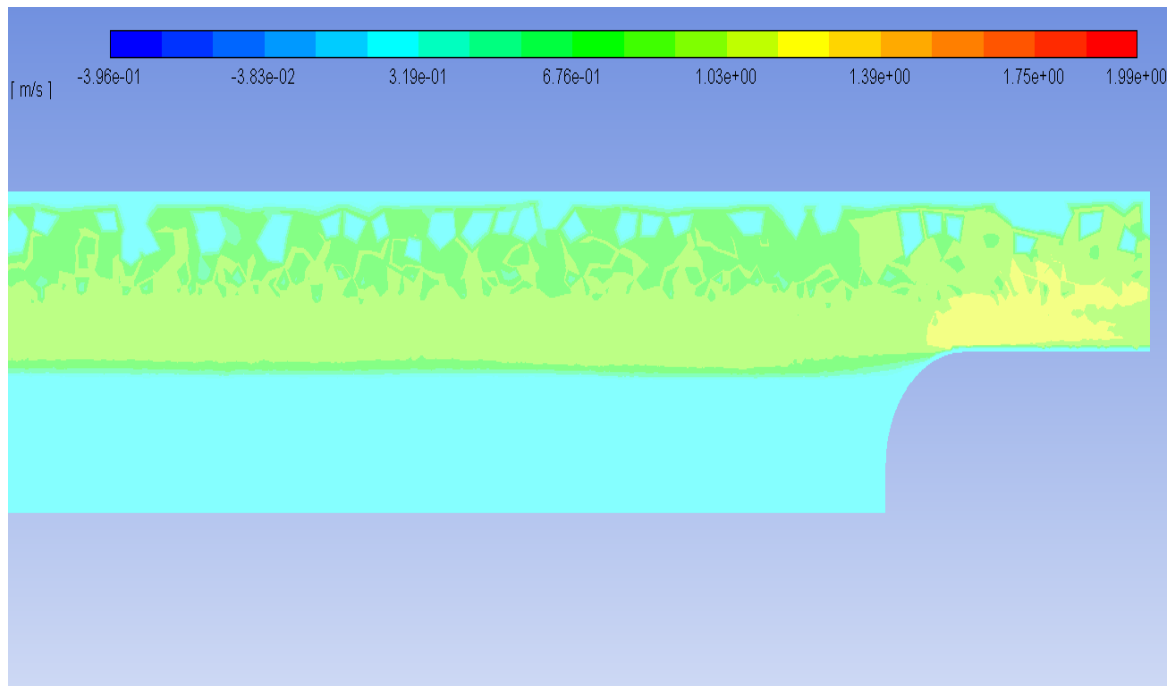


Figure 69: The velocity magnitude at the middle of the model at wind speed 0.9 m/s



**Figure 70: The velocity in z-direction in the middle of the model at wind speed 0.9 m/s**



**Figure 71: The velocity in z-direction at the inlet at wind speed 0.9 m/s**

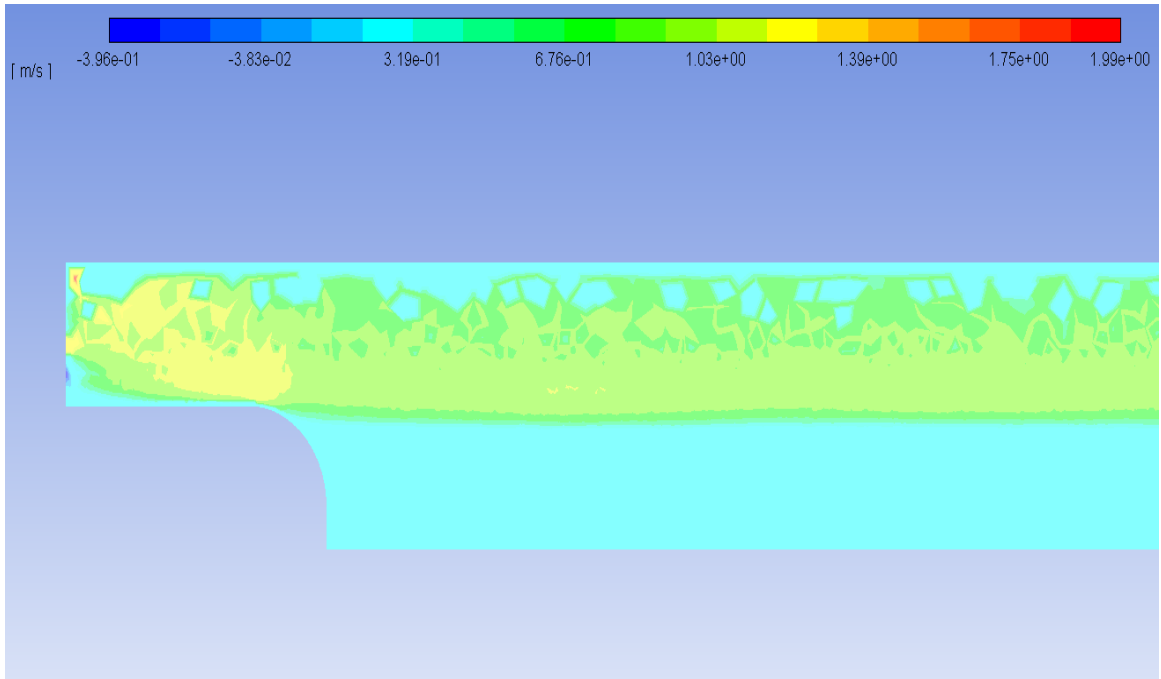


**Figure 72: The velocity in z-direction at the outlet at wind speed 0.9 m/s**

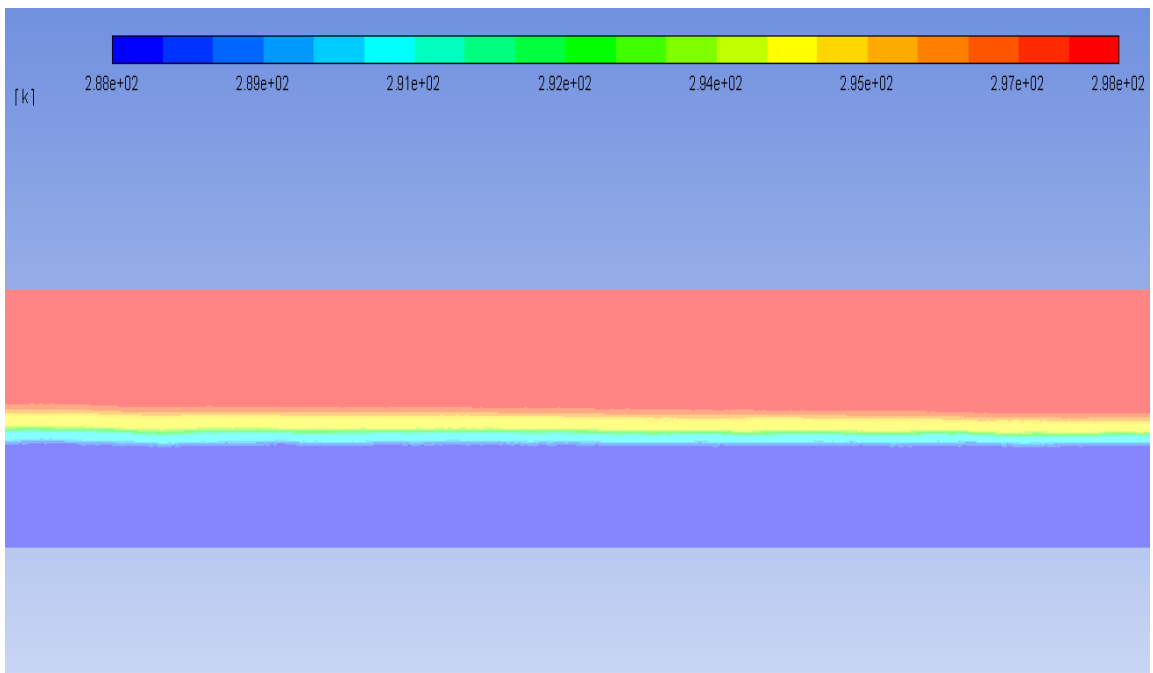


**Figure 73: The total temperature in the middle of the model at wind speed 0.9 m/s**

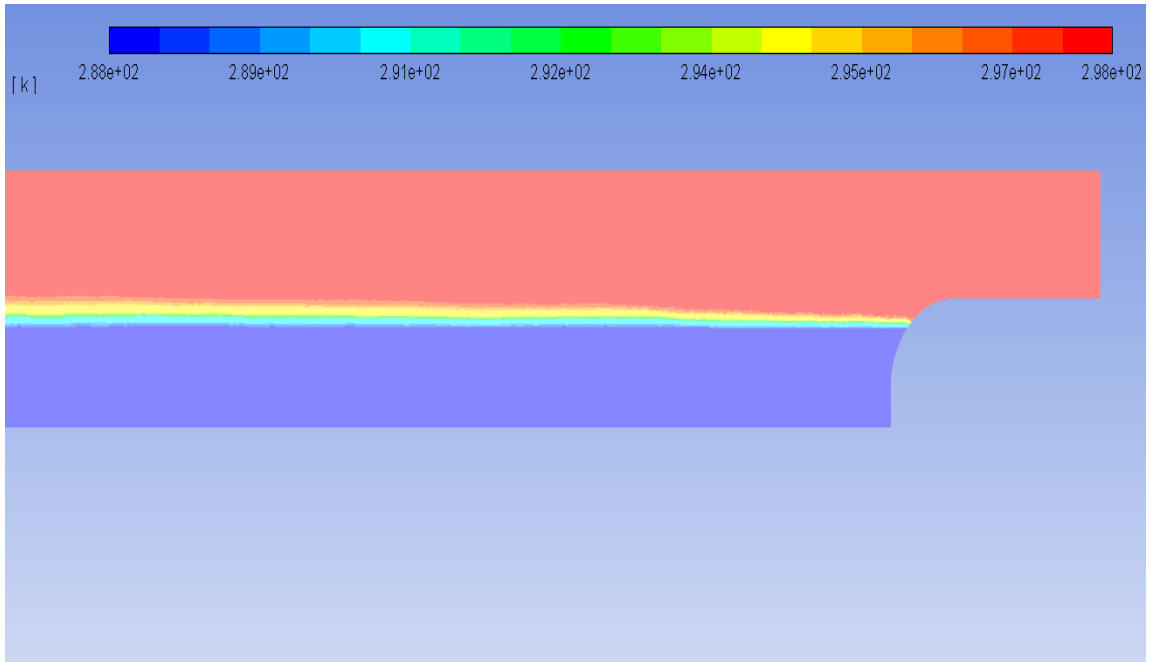


**Figure 74: The total temperature at the inlet at wind speed 0.9 m/s**

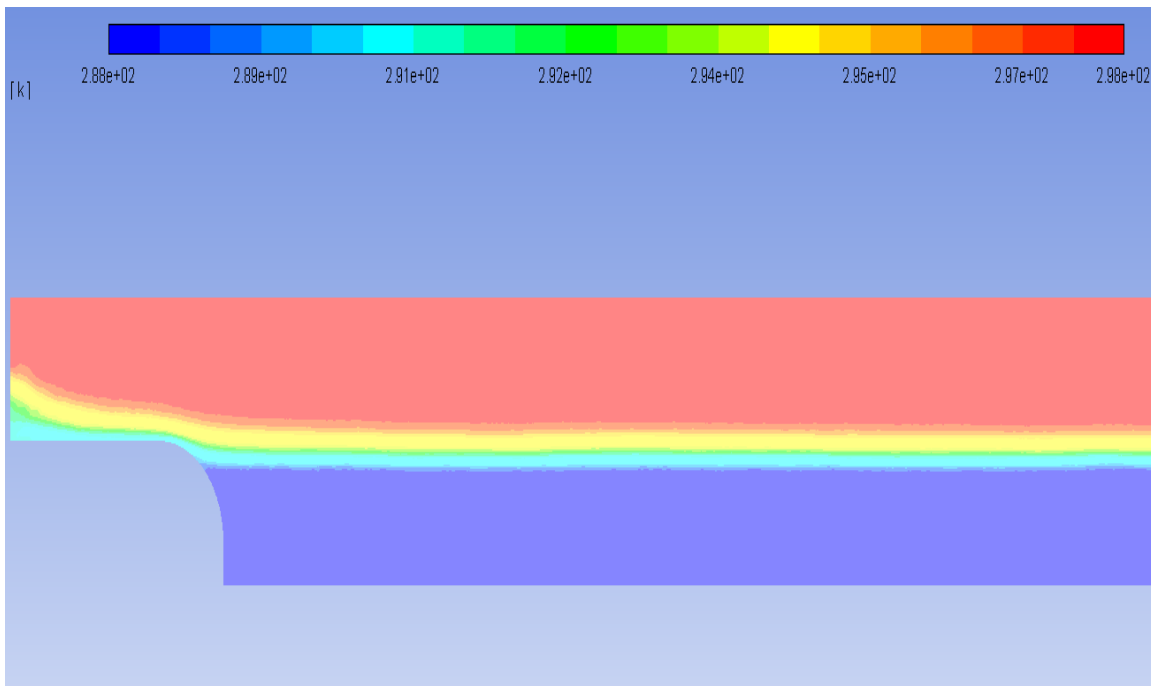


**Figure 75: The total temperature at the outlet at wind speed 0.9 m/s**

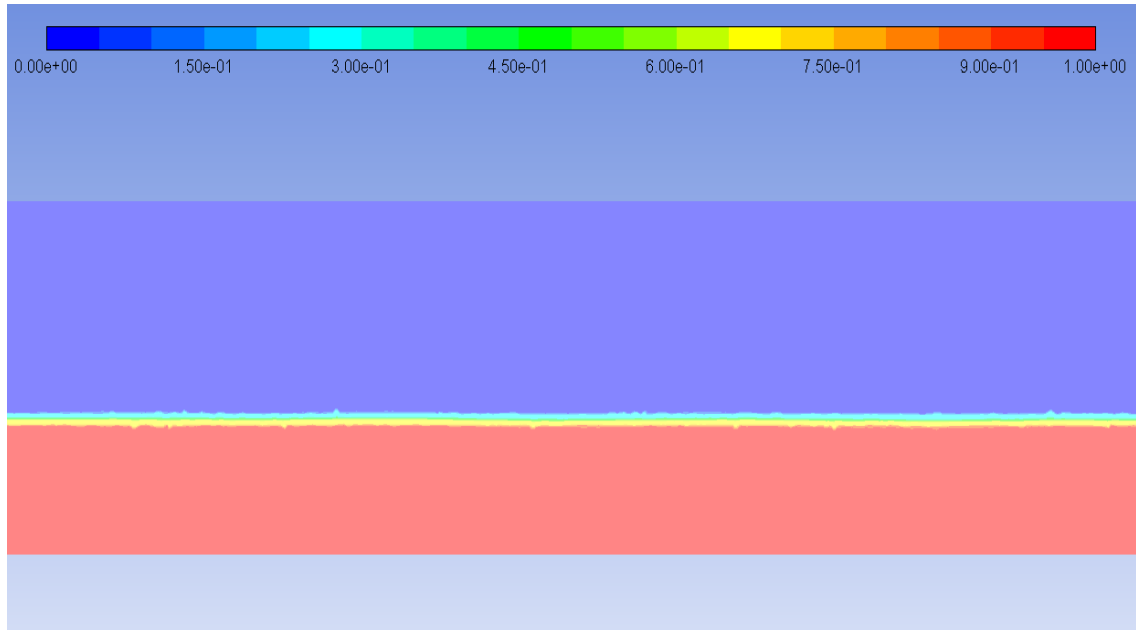


**Figure 76: The volume fraction of phase 2 (water) in the middle of the model at wind speed 0.9 m/s**

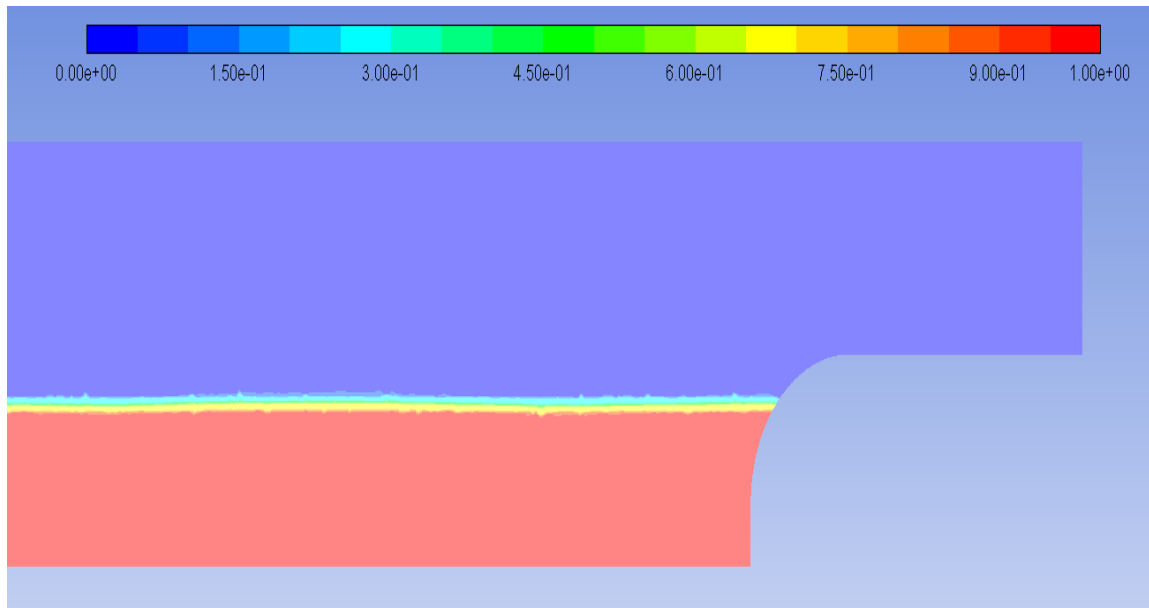


**Figure 77: The volume fraction of phase 2 (water) at the inlet at wind speed 0.9 m/s**

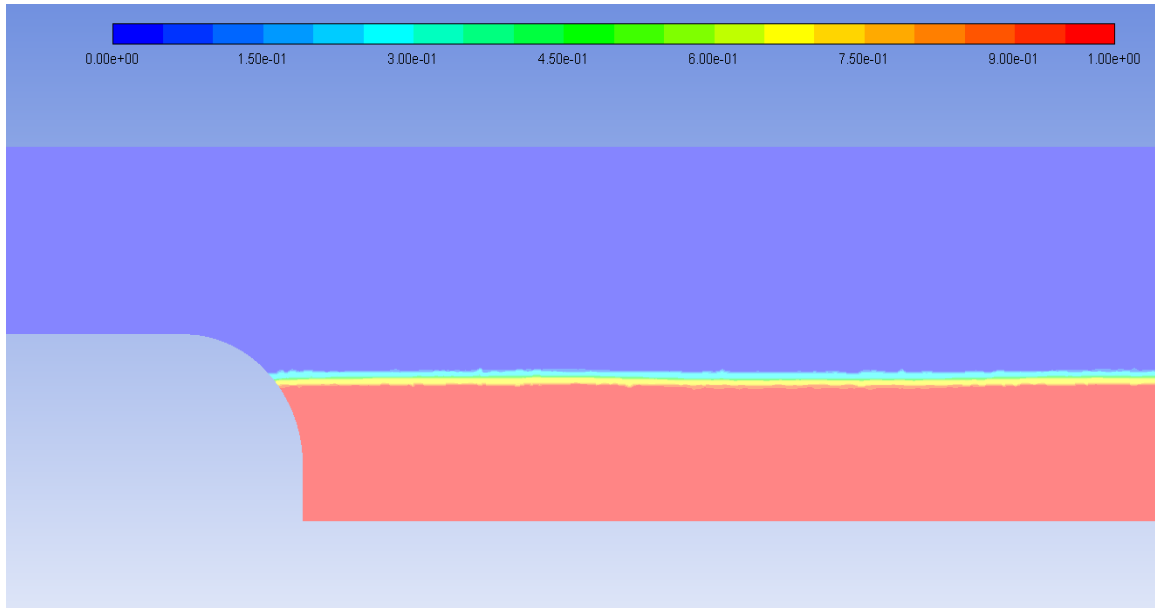


**Figure 78: The volume fraction of phase 2 (water) at the outlet at wind speed 0.9 m/s**

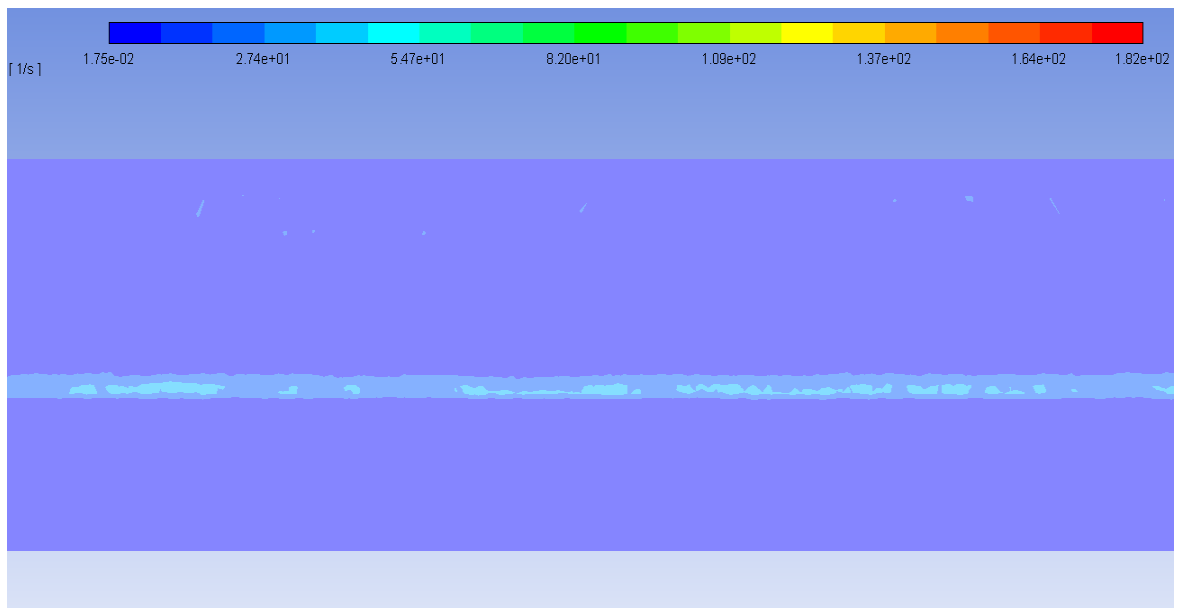


**Figure 79: The strain rate in the middle of model at wind speed 0.9 m/s**



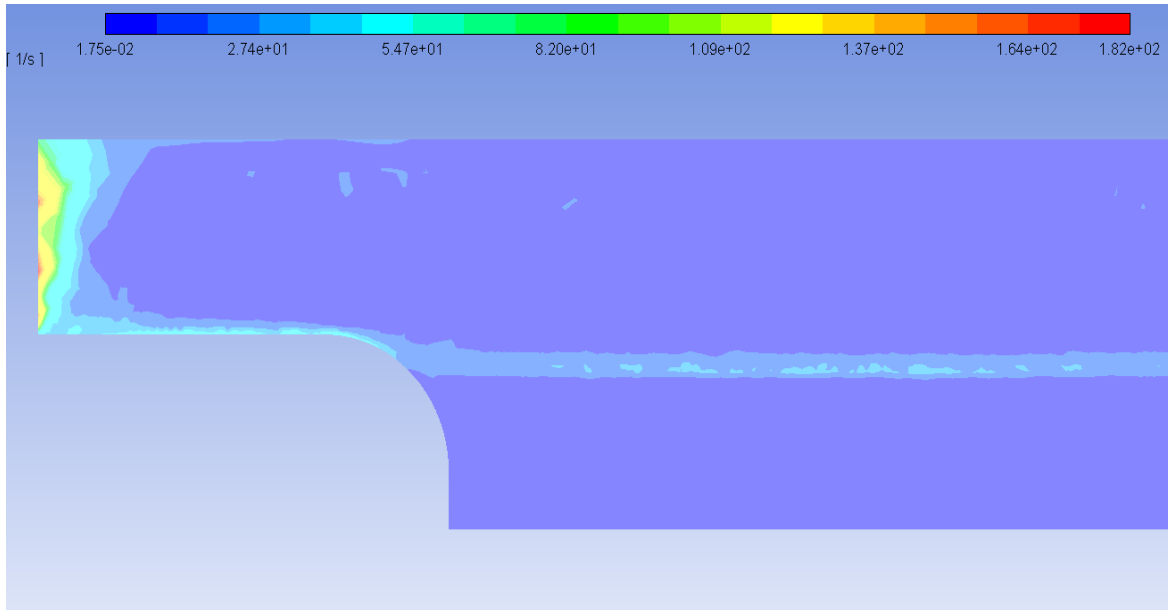


**Figure 80: The strain rate at the outlet at wind speed 0.9 m/s**

## B.2 At wind speed 1.3 m/s

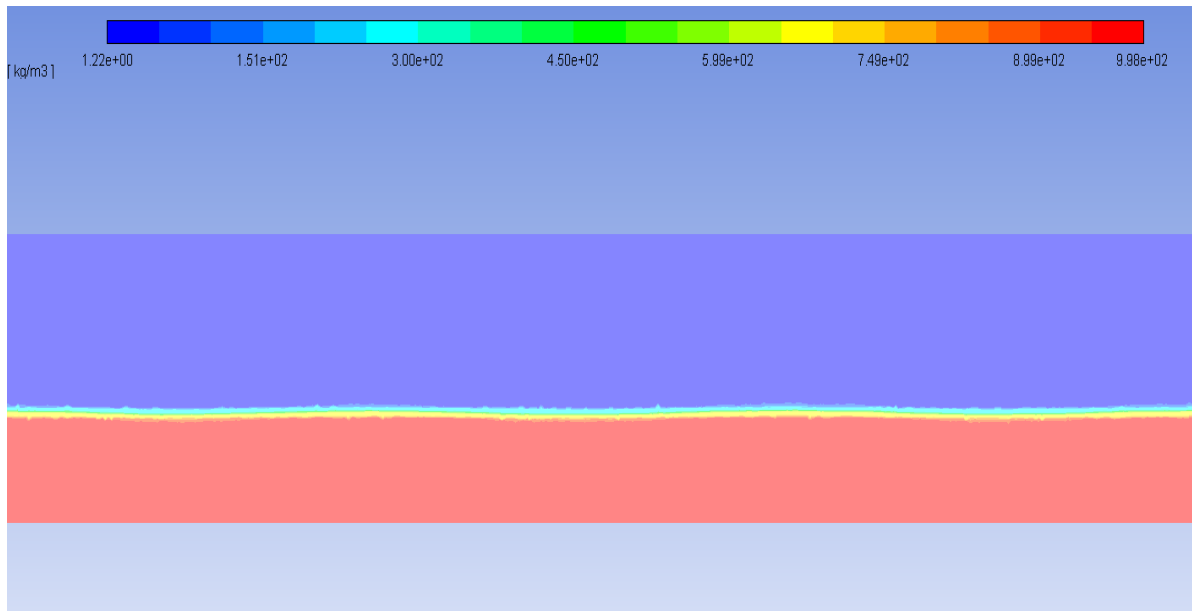


**Figure 81: The density of the mixture at the middle of model at wind speed 1.3 m/s**

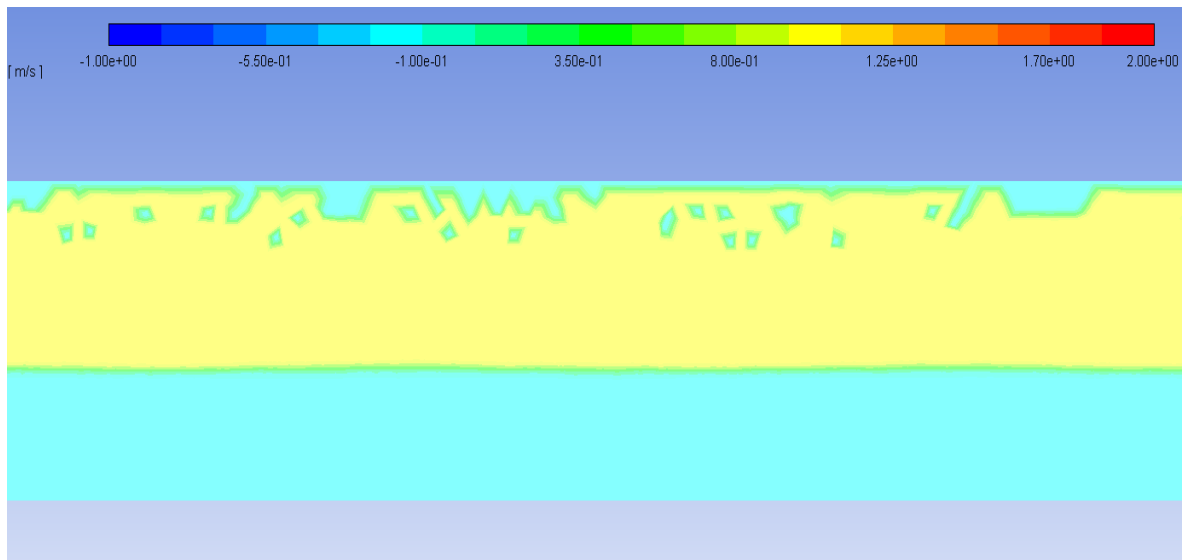


**Figure 82: The velocity magnitude at the middle of the model at wind speed 1.3 m/s**

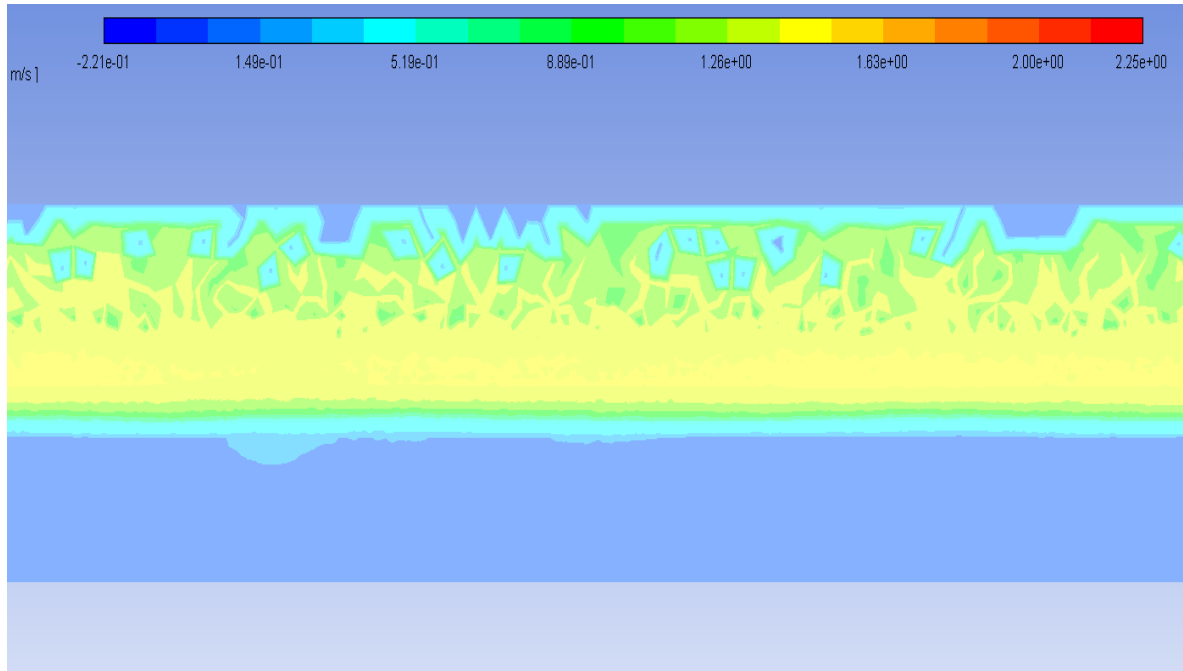


**Figure 83: The velocity in z-direction in the middle of the model at wind speed 1.3 m/s**

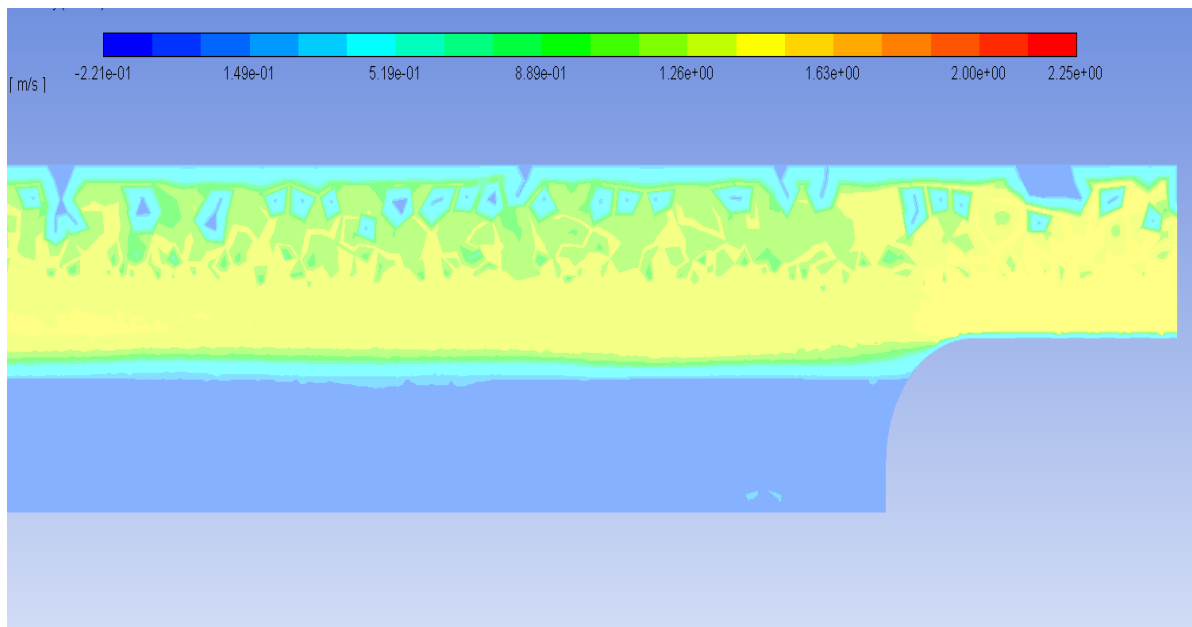


**Figure 84: The velocity in z-direction at the inlet at wind speed 1.3 m/s**

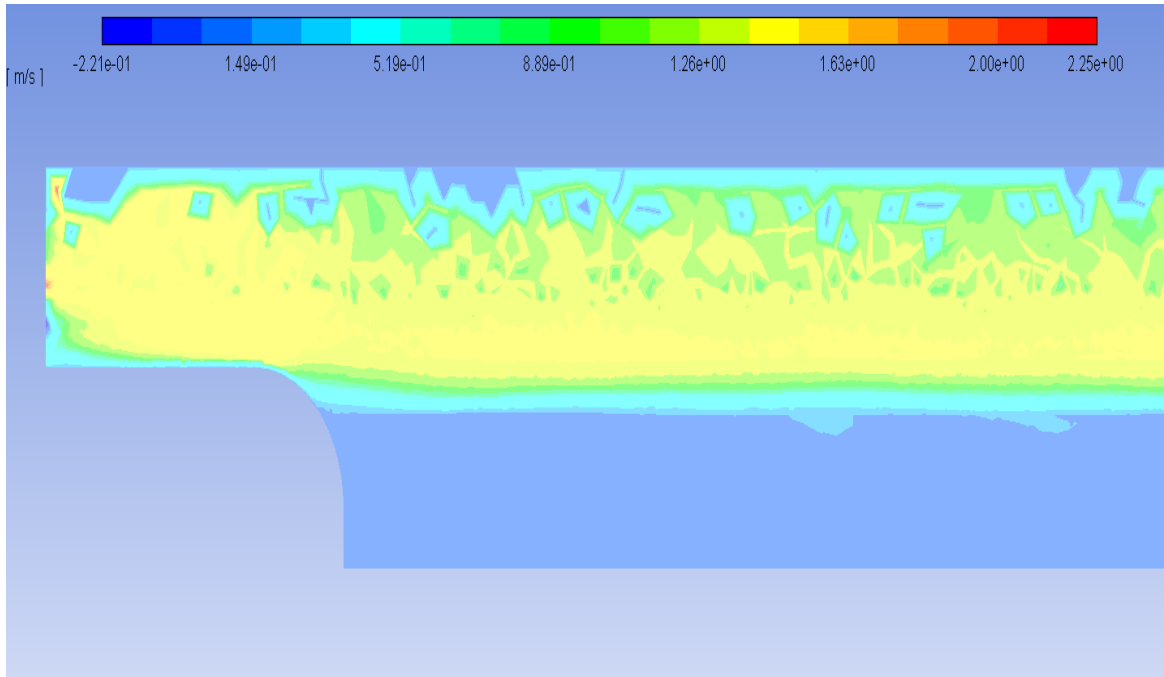


**Figure 85: The velocity in z-direction at the outlet at wind speed 1.3 m/s**

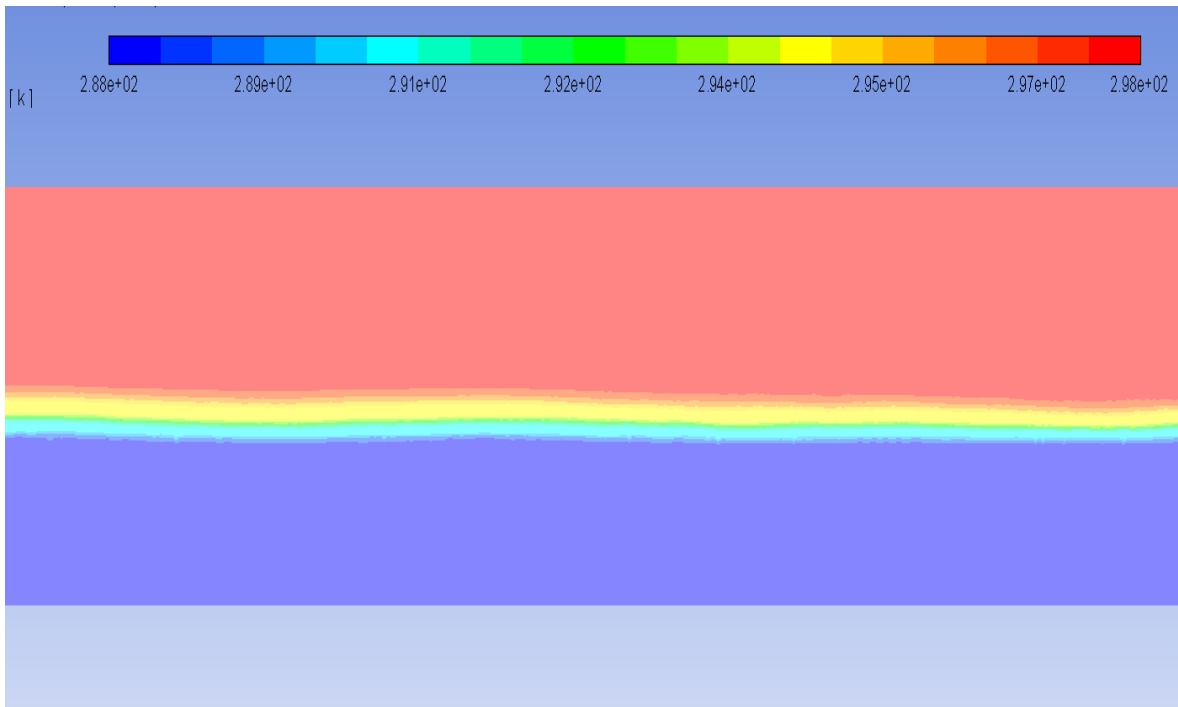


**Figure 86: The total temperature in the middle of the model at wind speed 1.3 m/s**

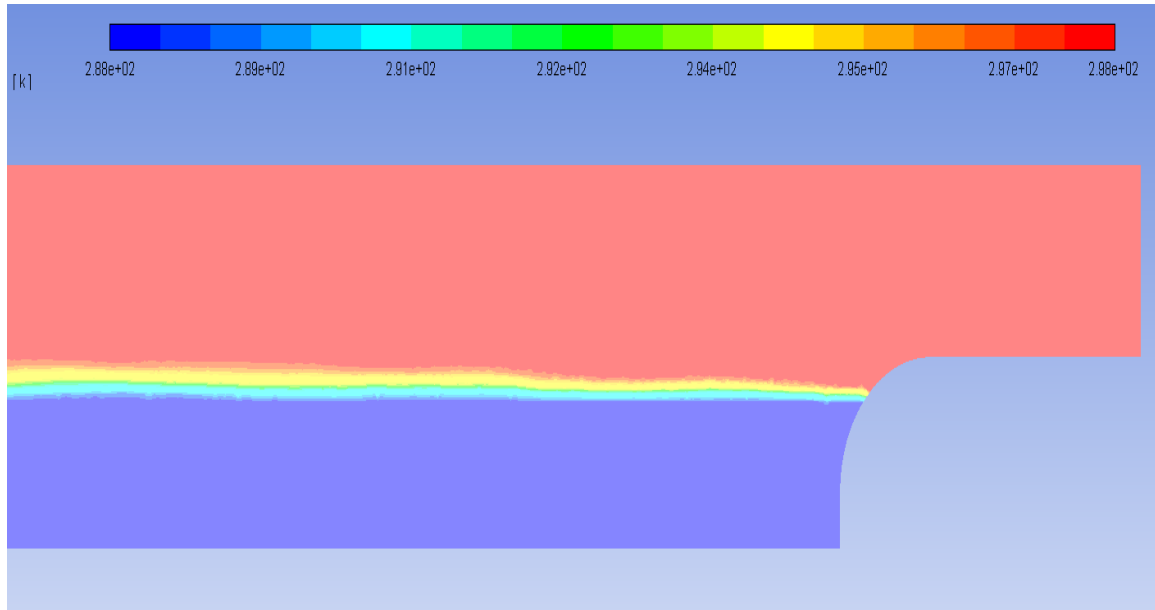


**Figure 87: The total temperature at the inlet at wind speed 1.3 m/s**

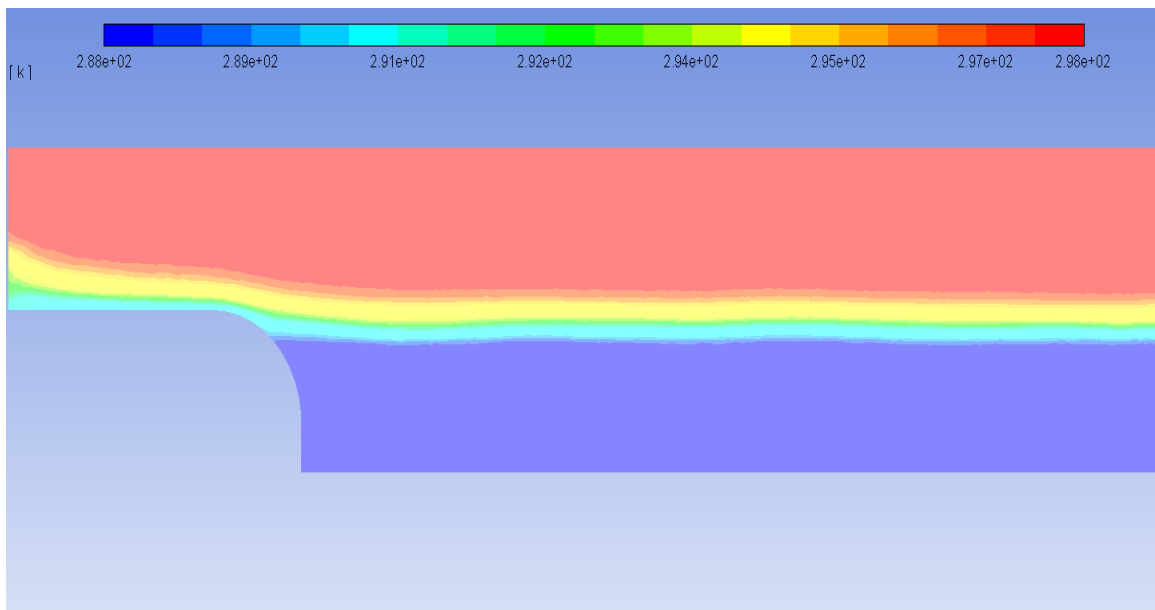


**Figure 88: The total temperature at the outlet at wind speed 1.3 m/s**

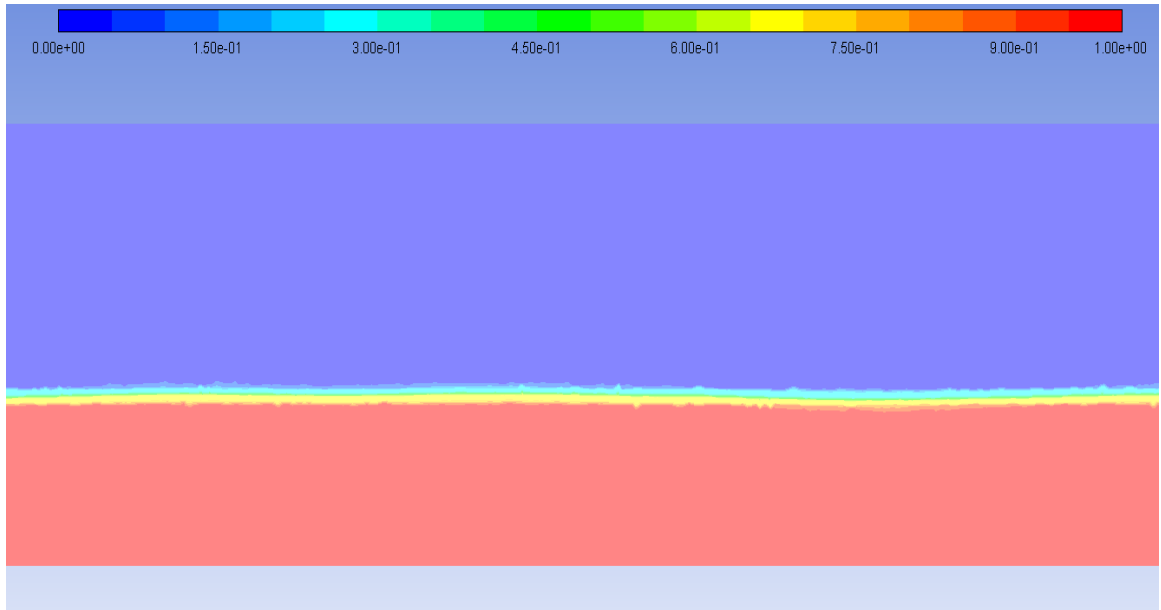


**Figure 89: The volume fraction of phase 2 (water) in the middle of the model at wind speed 1.3 m/s**

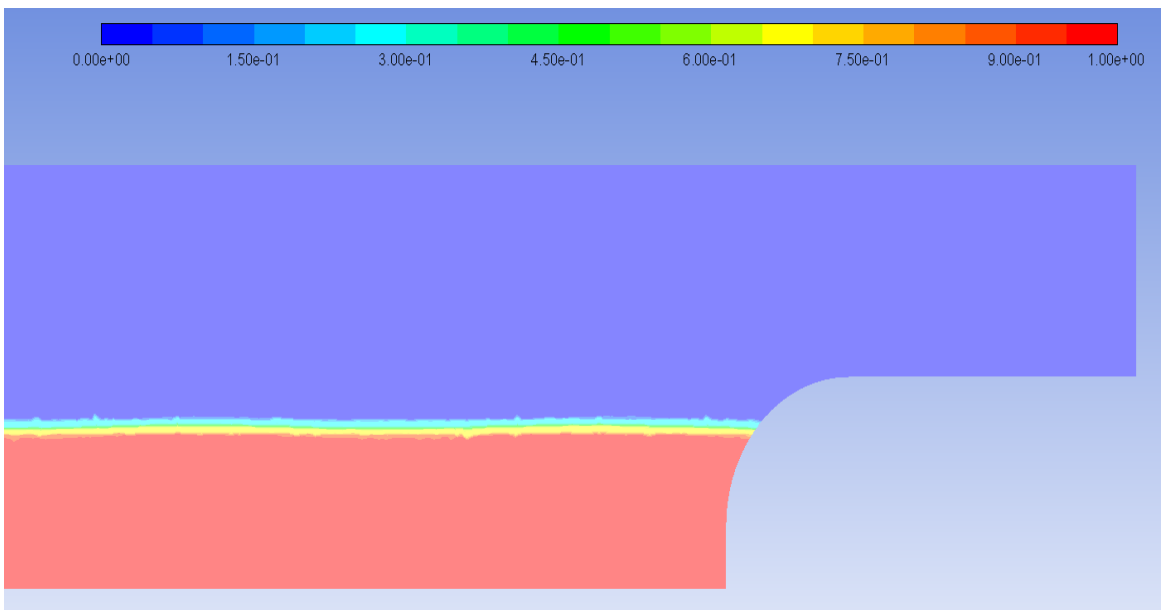


**Figure 90: The volume fraction of phase 2 (water) at the inlet at wind speed 1.3 m/s**

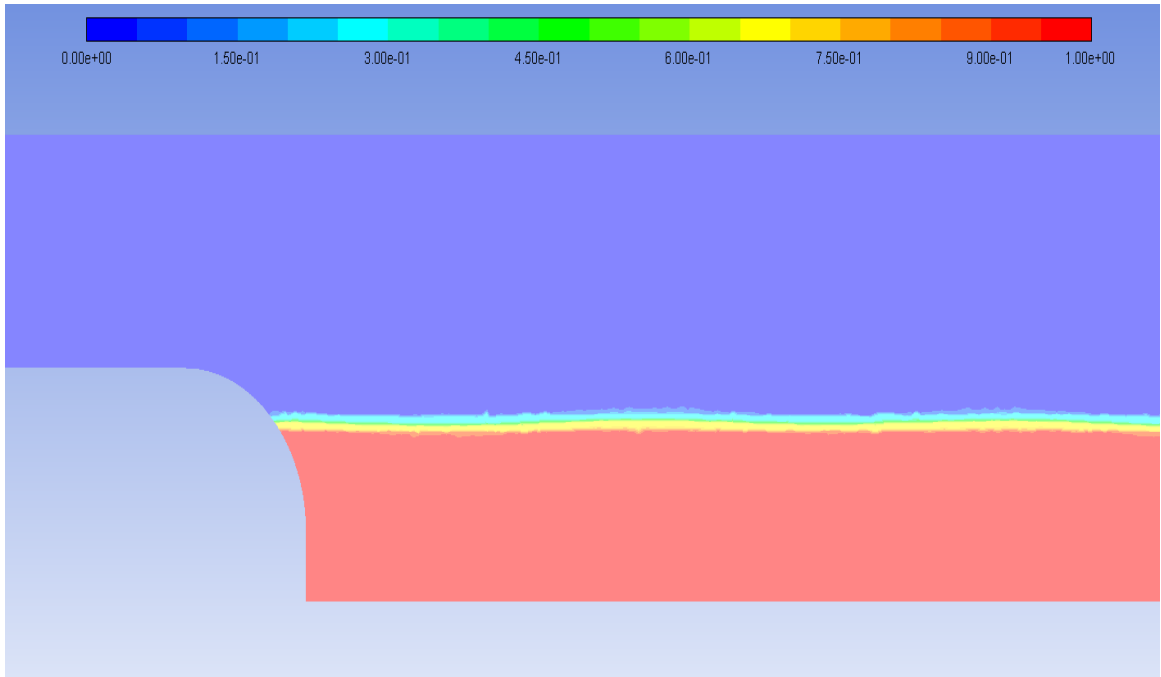


**Figure 91: The volume fraction of phase 2 (water) at the outlet at wind speed 1.3 m/s**

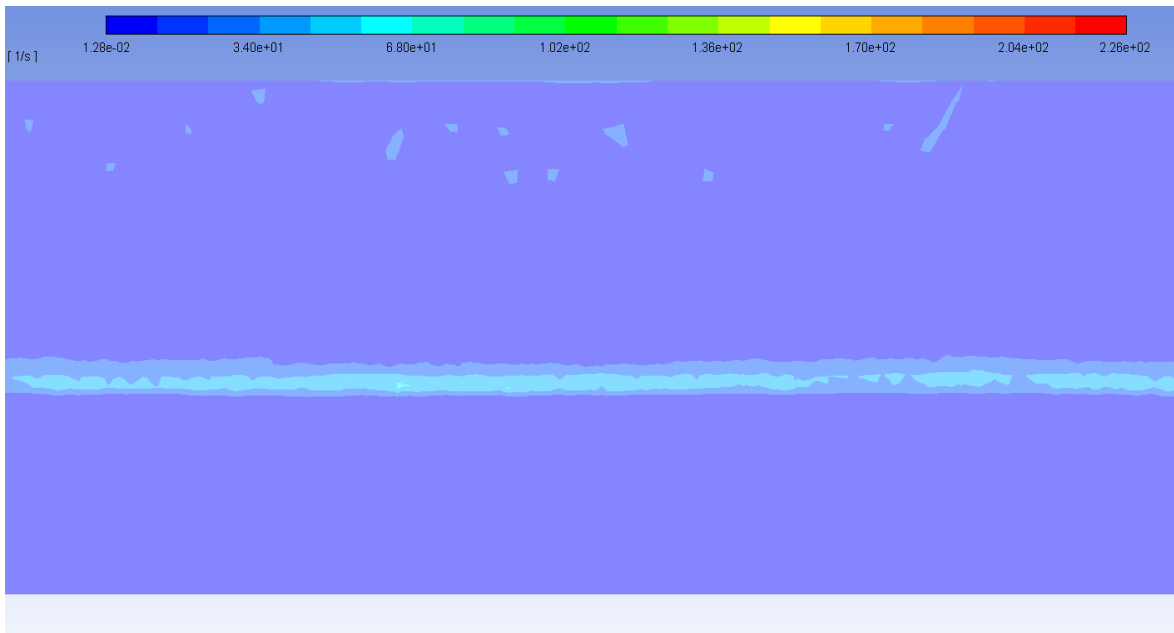


**Figure 92: The strain rate in the middle of model at wind speed 1.3 m/s**

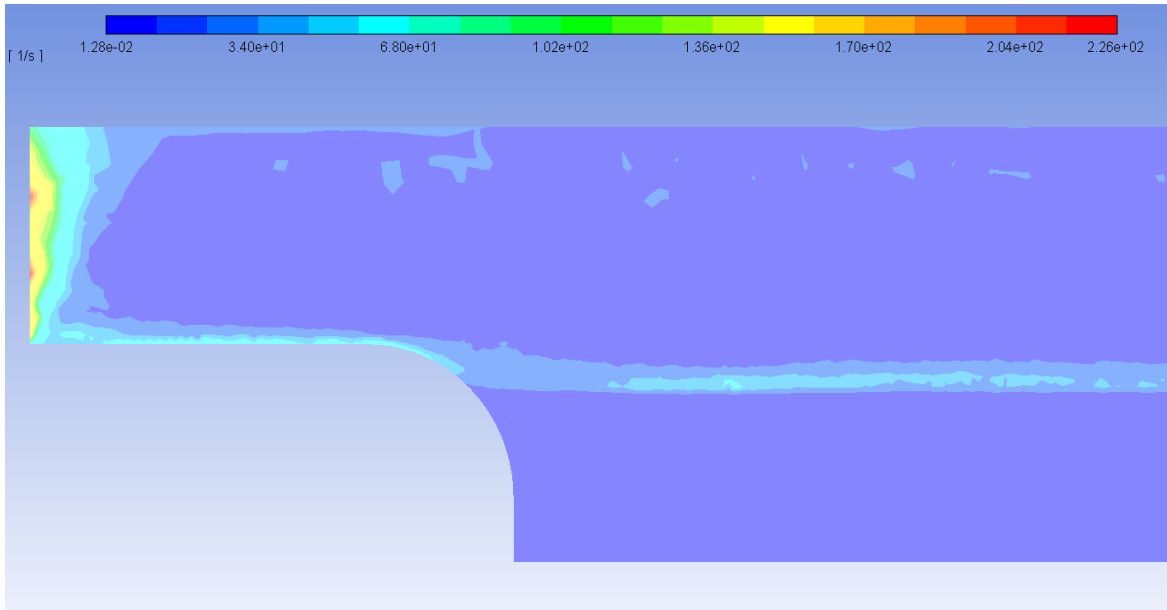


**Figure 93: The strain rate at the outlet at wind speed 1.3 m/s**

### **B.3 At wind speed 2 m/s**

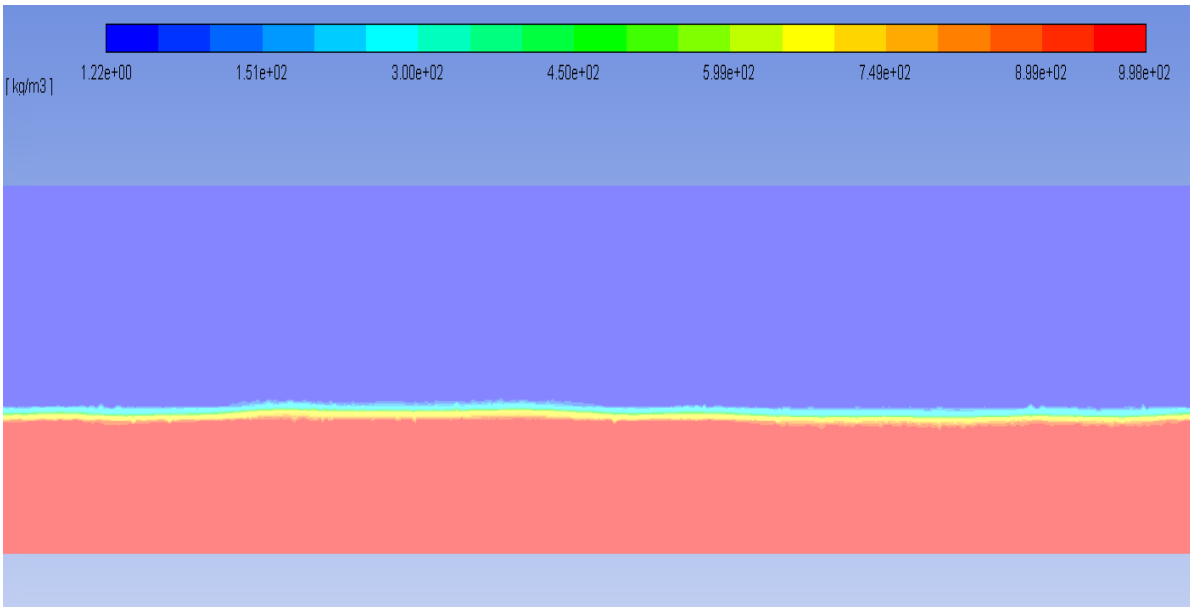


**Figure 94: The density of the mixture at the middle of model at wind speed 2 m/s**



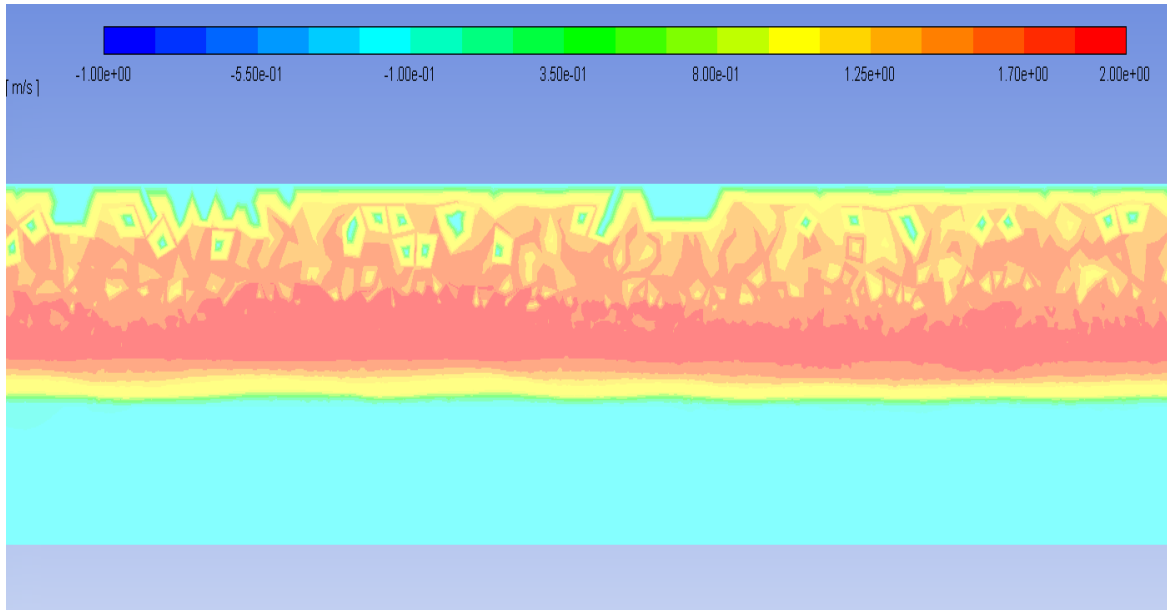


**Figure 95: The velocity magnitude at the middle of the model at wind speed 2 m/s**

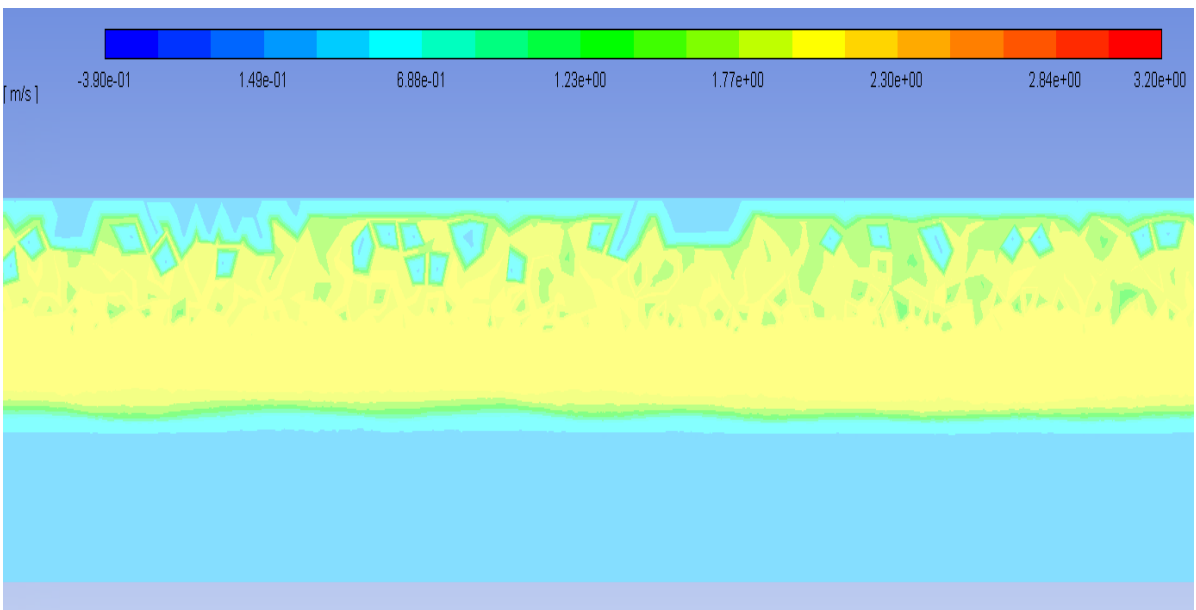


**Figure 96: The velocity in z-direction in the middle of the model at wind speed 2**

**m/s**

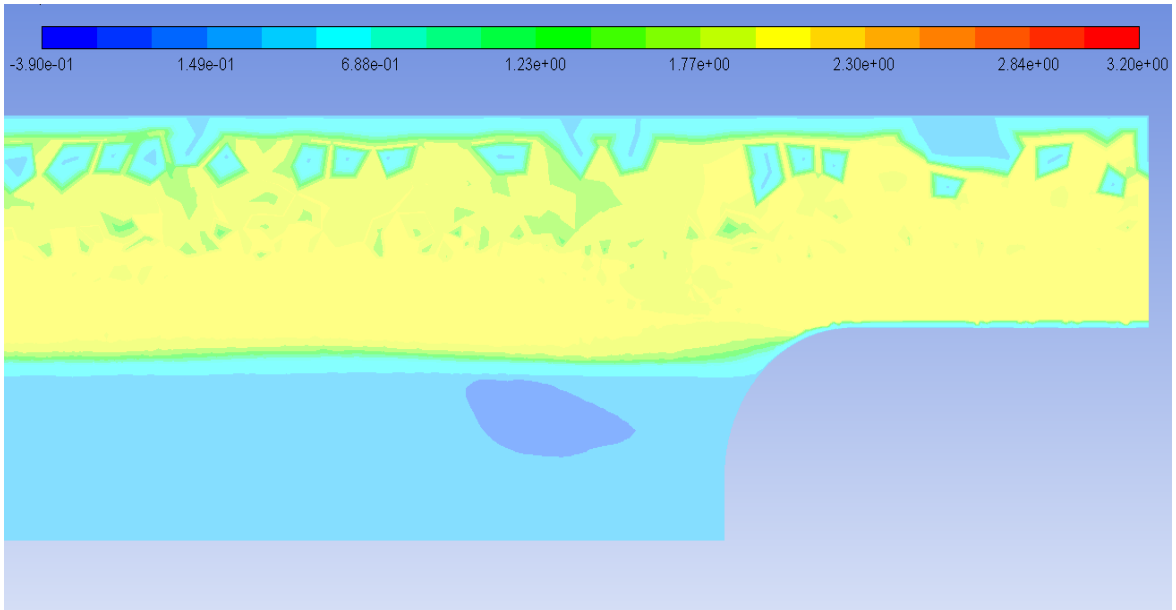


**Figure 97: The velocity in z-direction at the inlet at wind speed 2 m/s**

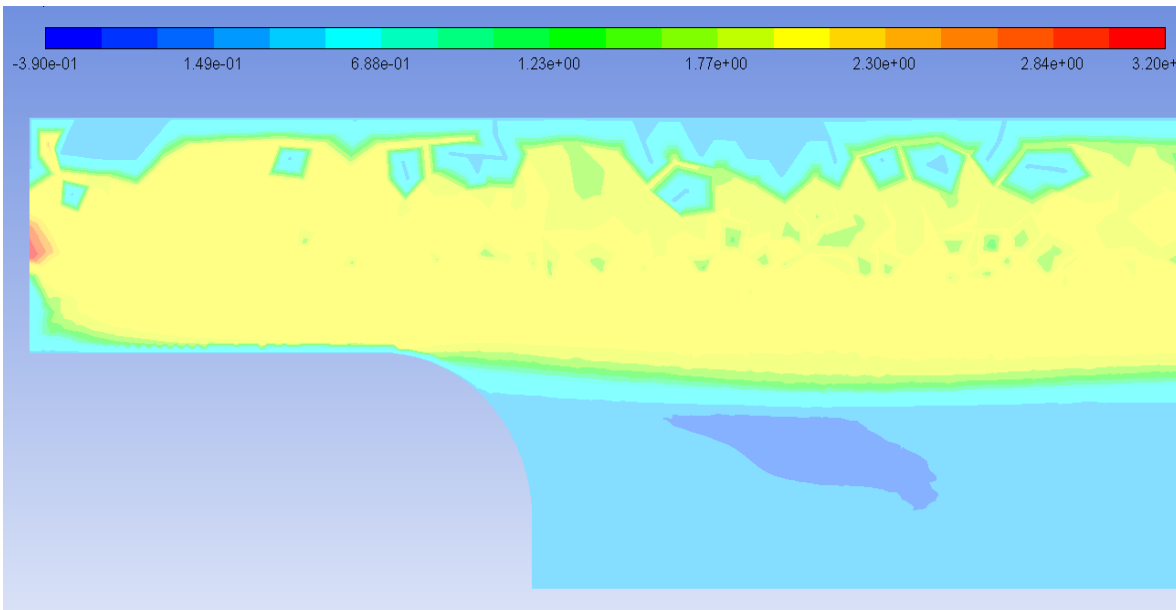


**Figure 98: The velocity in z-direction at the outlet at wind speed 2 m/s**

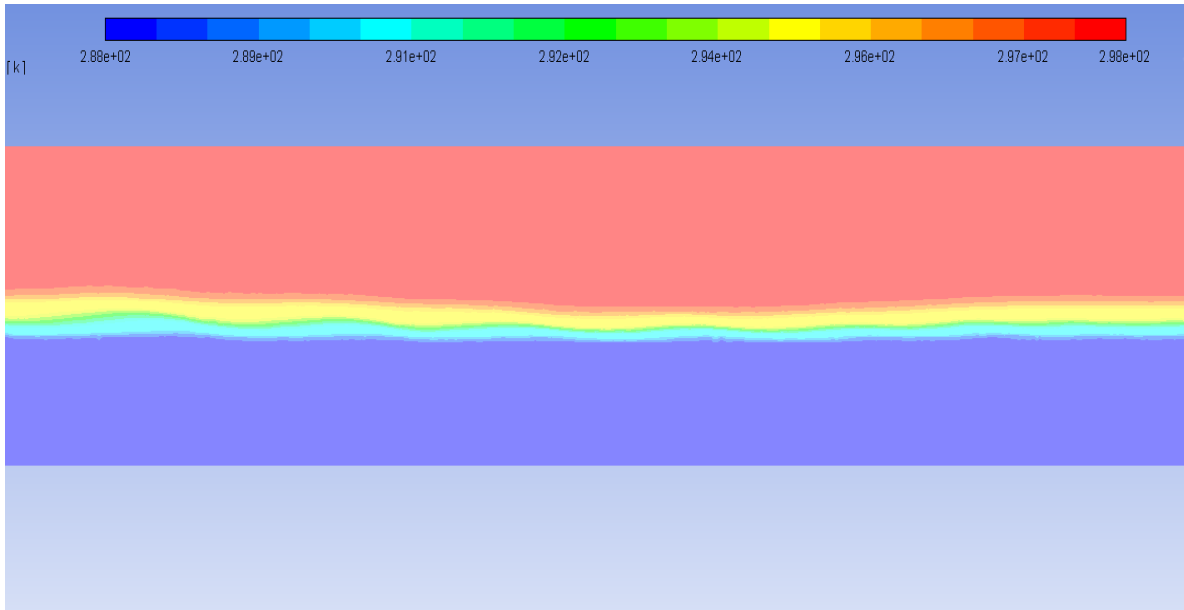


**Figure 99: The total temperature in the middle of the model, wind speed 2 m/s**

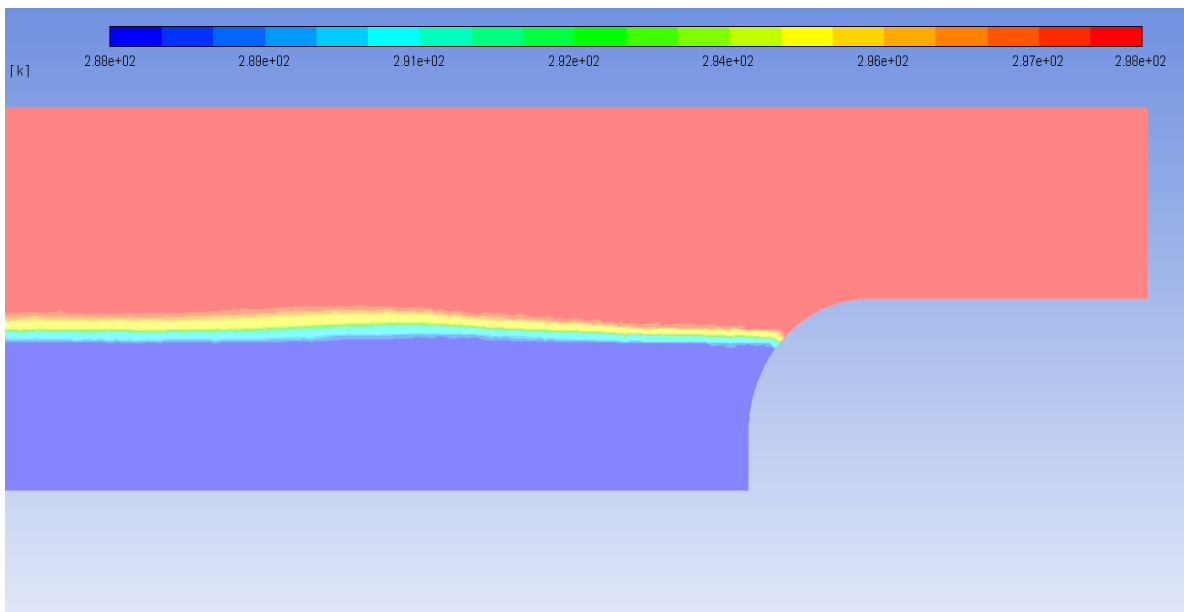


**Figure 100: The total temperature at the inlet, wind speed 2 m/s**

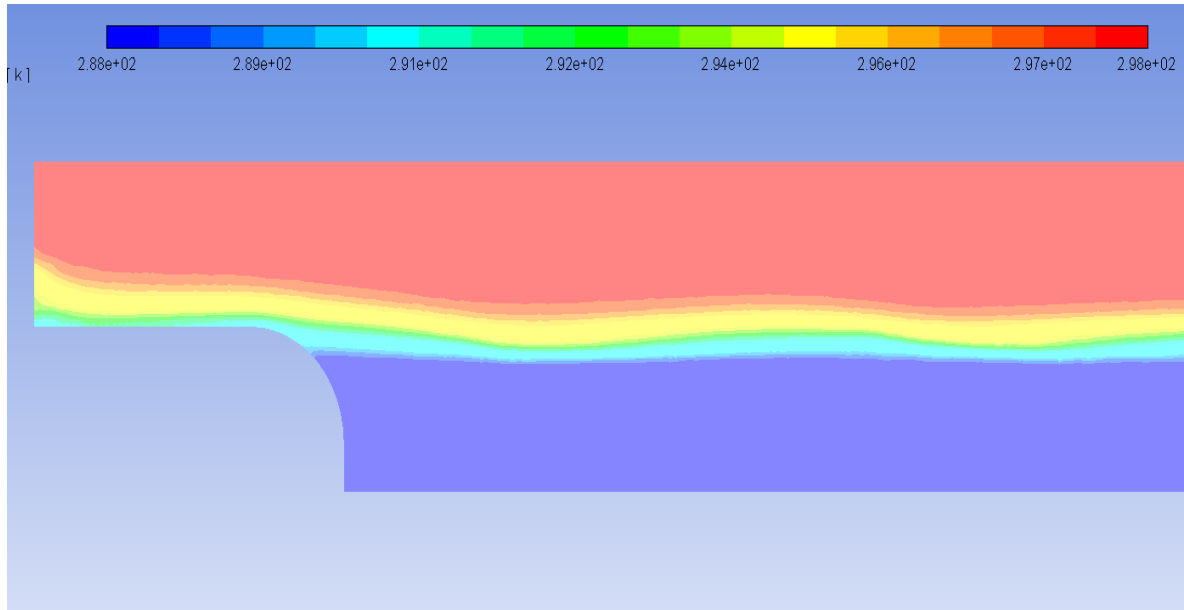


**Figure 101: The total temperature at the outlet, wind speed 2 m/s**

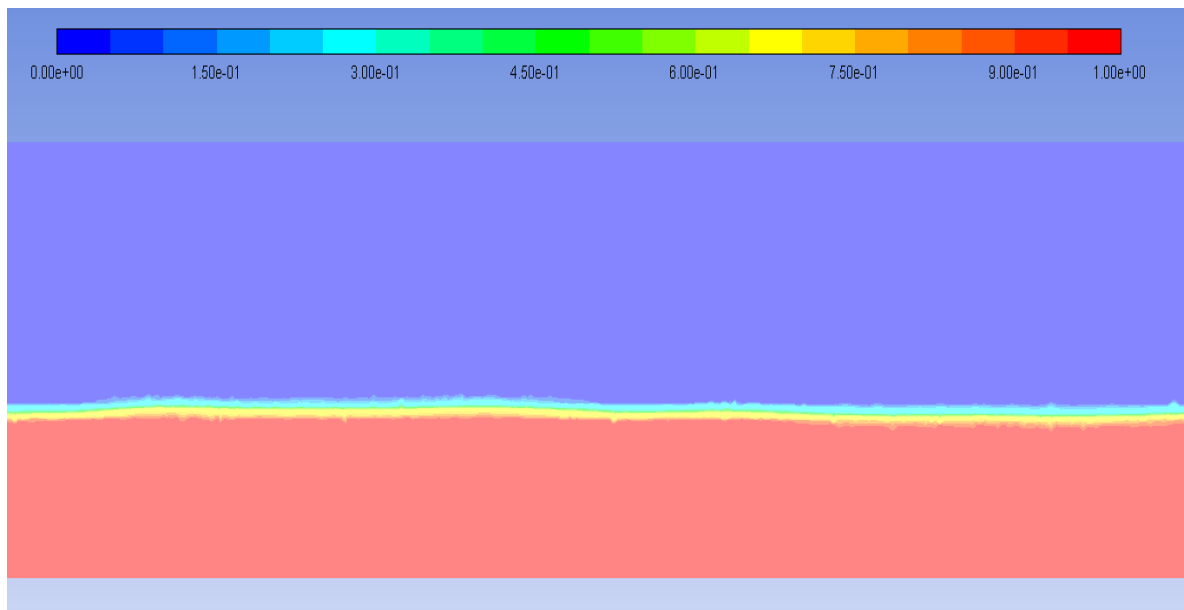


**Figure 102: The volume fraction of phase 2 (water) in the middle of the model,  
wind speed 2 m/s**

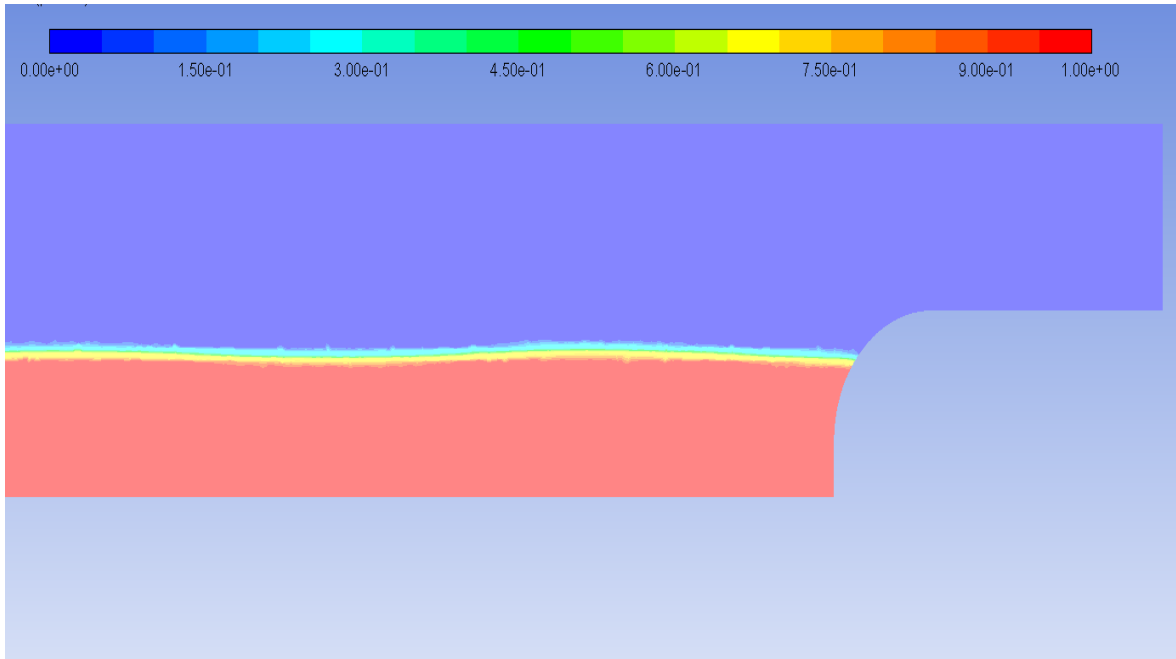


**Figure 103: The volume fraction of phase 2 (water) at the inlet, wind speed 2 m/s**

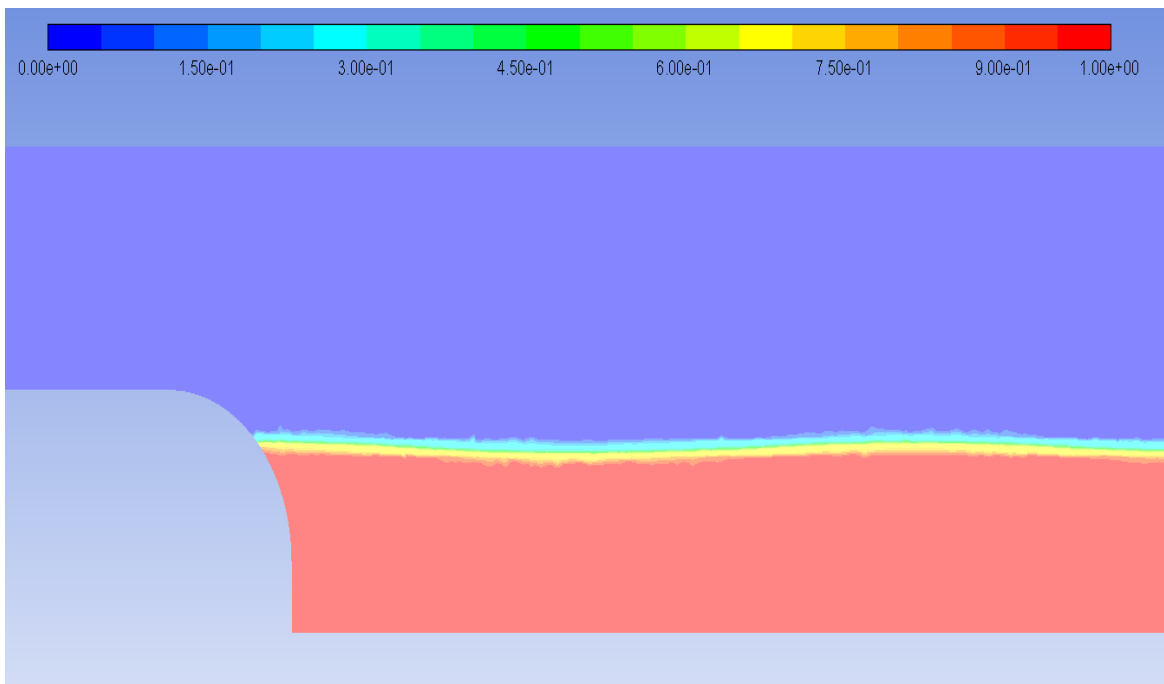


**Figure 104: The volume fraction of phase 2 (water) at the outlet, wind speed 2 m/s**

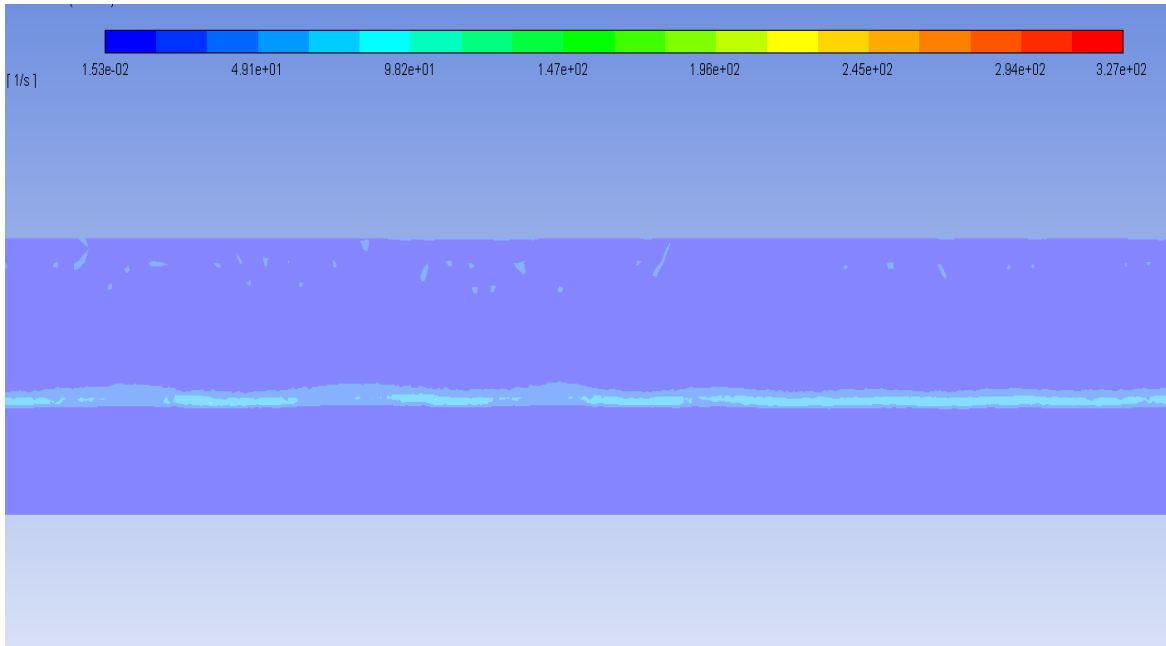


**Figure 105: The strain rate in the middle of model, wind speed 2 m/s**

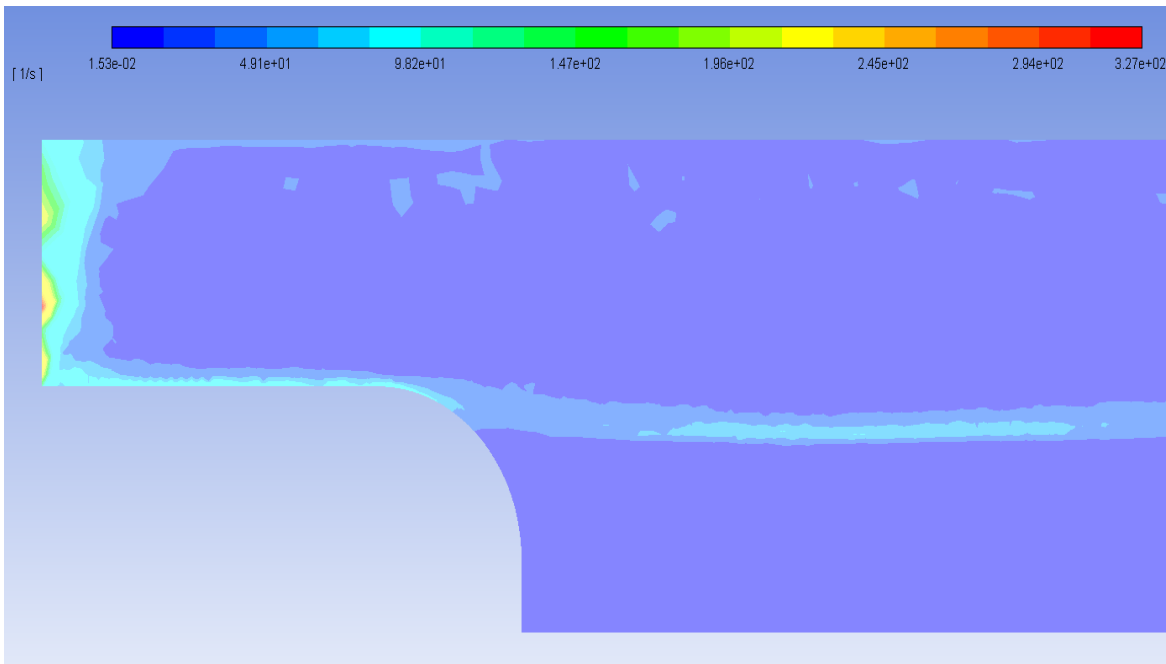


**Figure 106: The strain rate at the outlet, wind speed 2**

## B.4 At wind speed 3.2 m/s

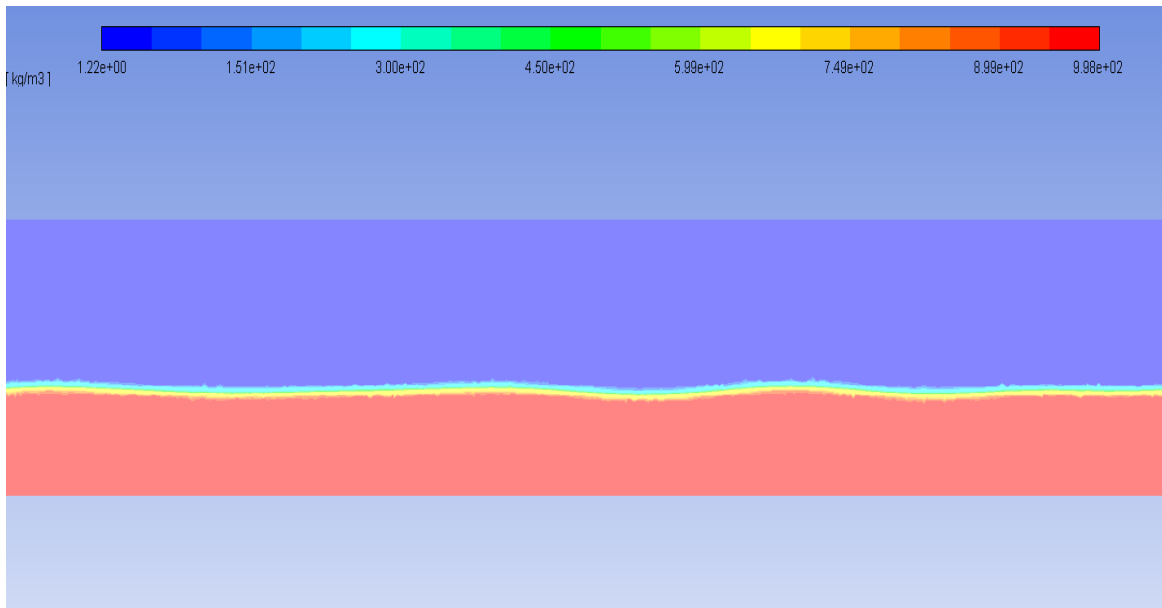


**Figure 107: The density of the mixture at the middle of model at wind speed 3.2 m/s**

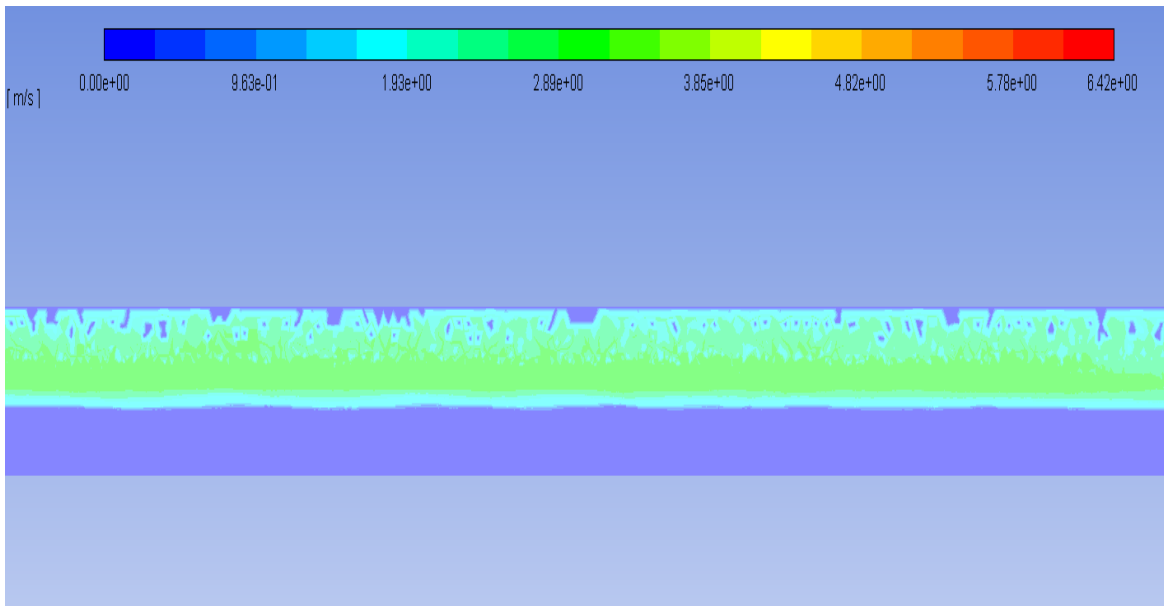


**Figure 108: The velocity magnitude at the middle of the model at wind speed 3.2 m/s**

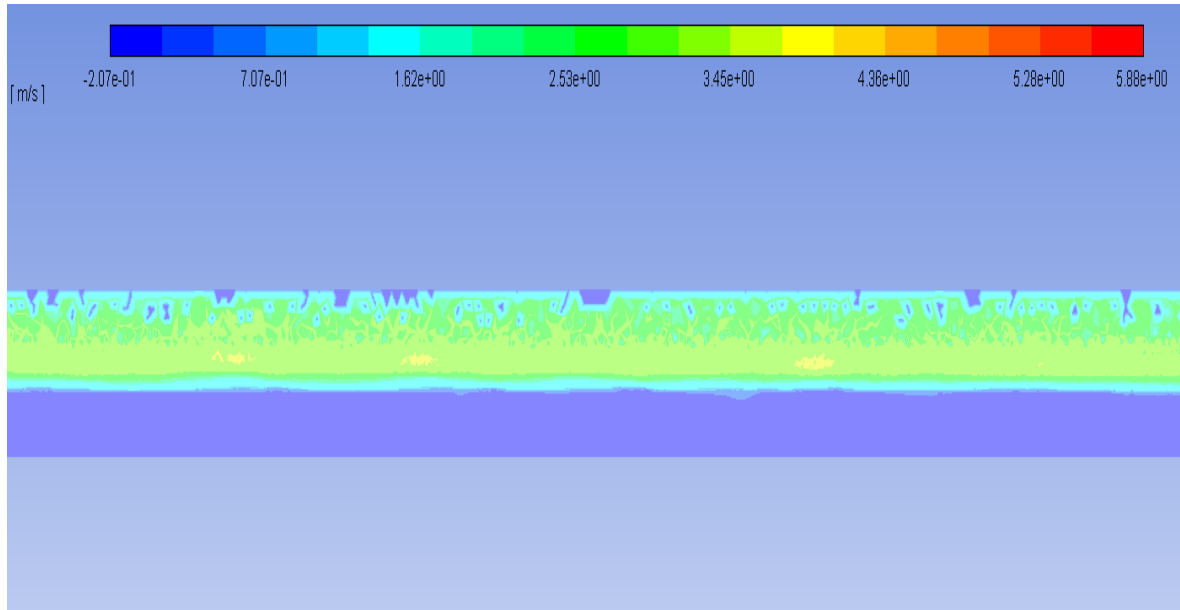


**Figure 109: The velocity in z-direction in the middle of the model at wind speed 3.2 m/s**

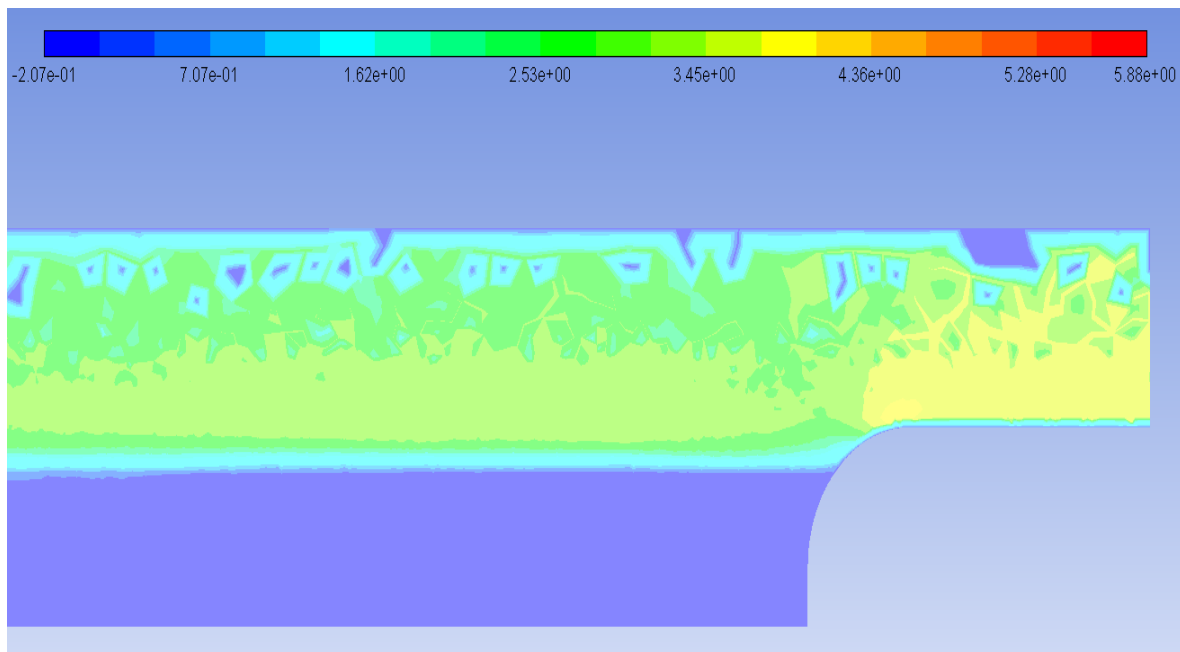


**Figure 110: The velocity in z-direction at the inlet at wind speed 3.2 m/s**



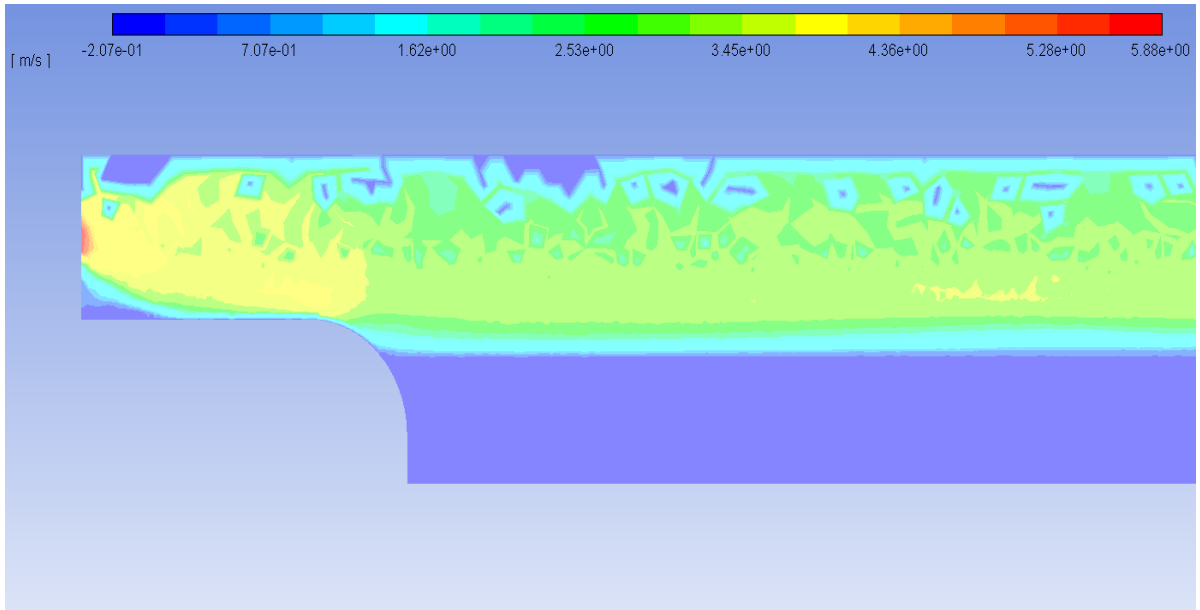


**Figure 111: The velocity in z-direction at the outlet at wind speed 3.2 m/s**

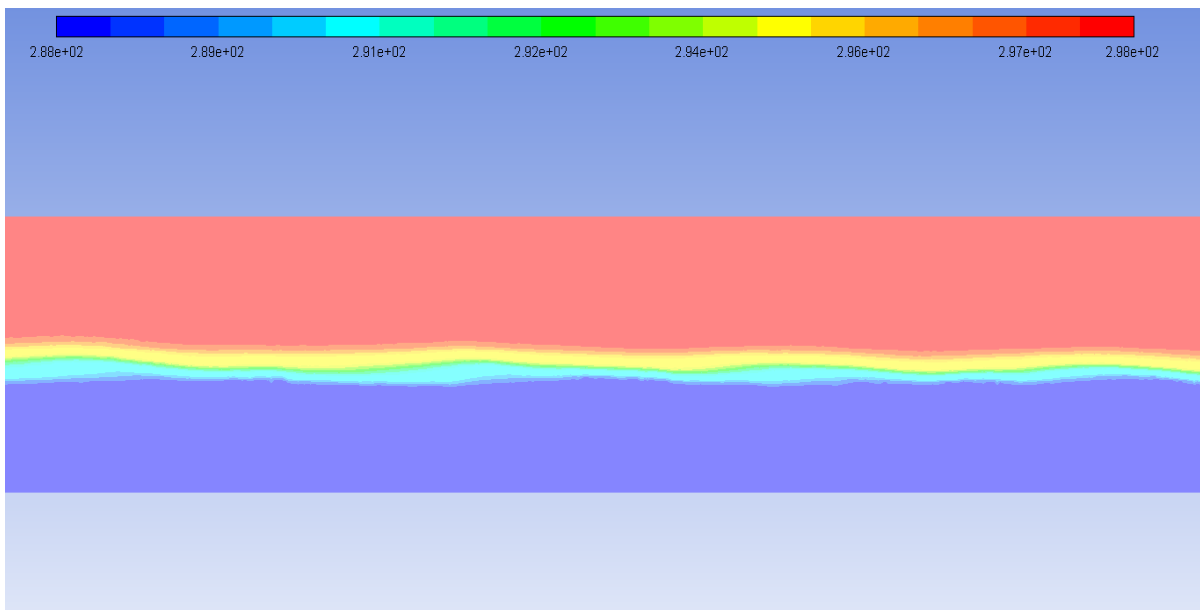


**Figure 112: The total temperature in the middle of the model at wind speed 3.2 m/s**

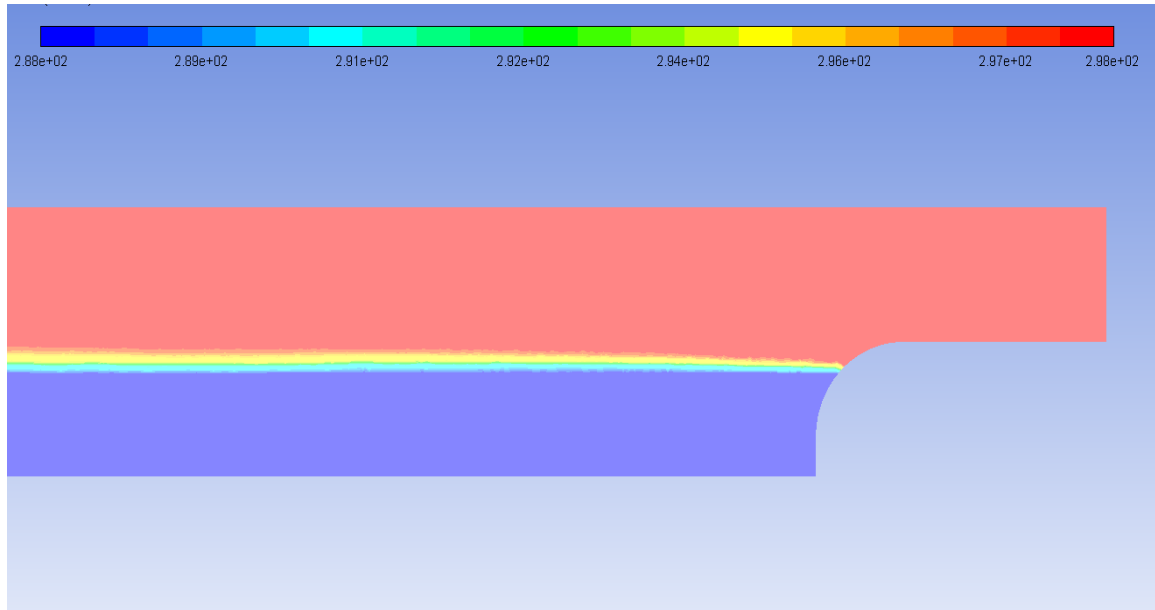


**Figure 113: The total temperature at the inlet at wind speed 3.2 m/s**

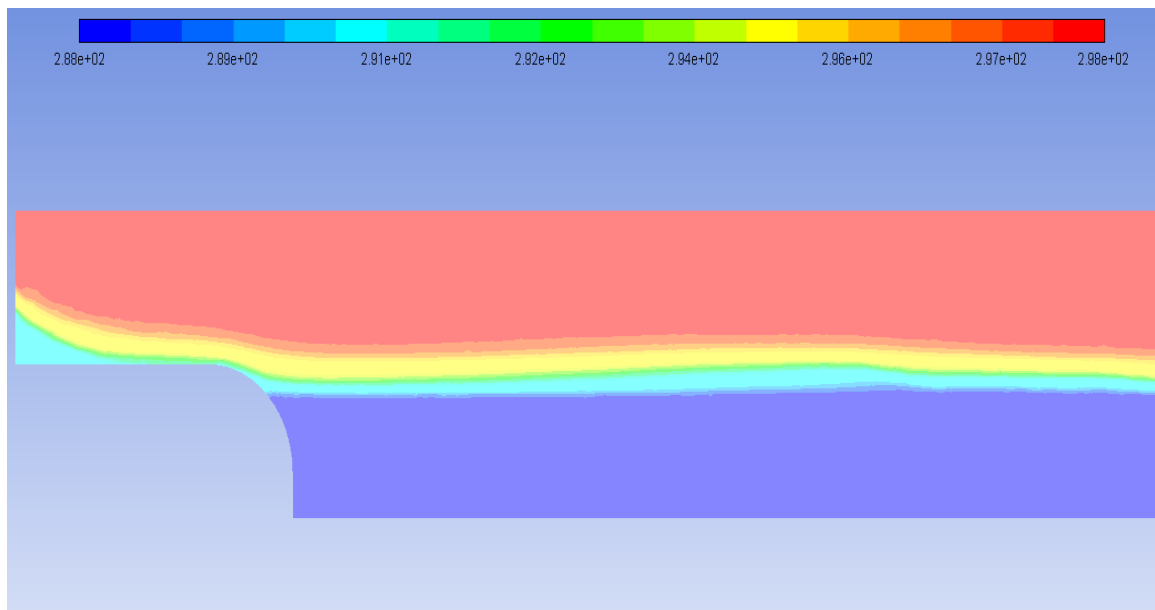


**Figure 114: The total temperature at the outlet at wind speed 3.2 m/s**

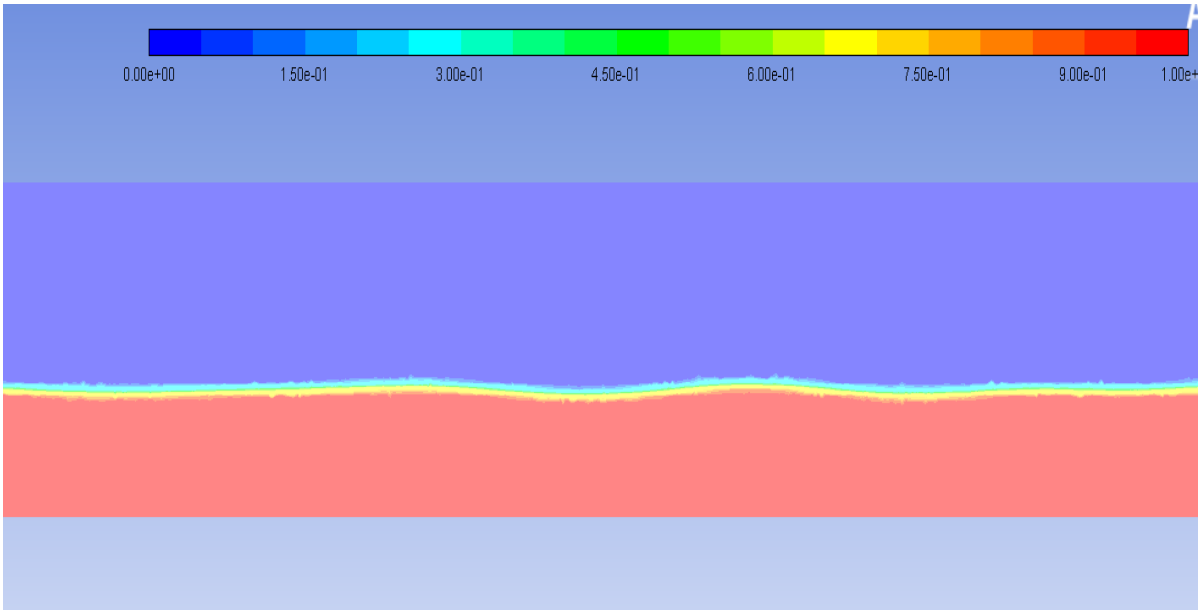


**Figure 115: The volume fraction of phase 2 (water) in the middle of the model at wind speed 3.2 m/s**

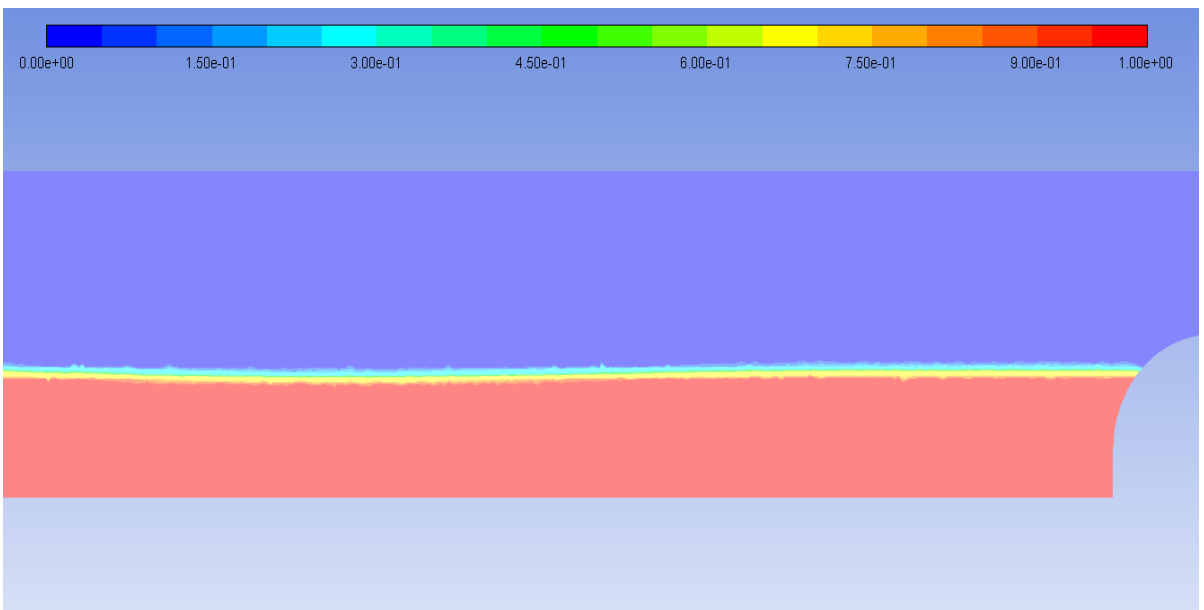


**Figure 116: The volume fraction of phase 2 (water) at the inlet at wind speed 3.2 m/s**

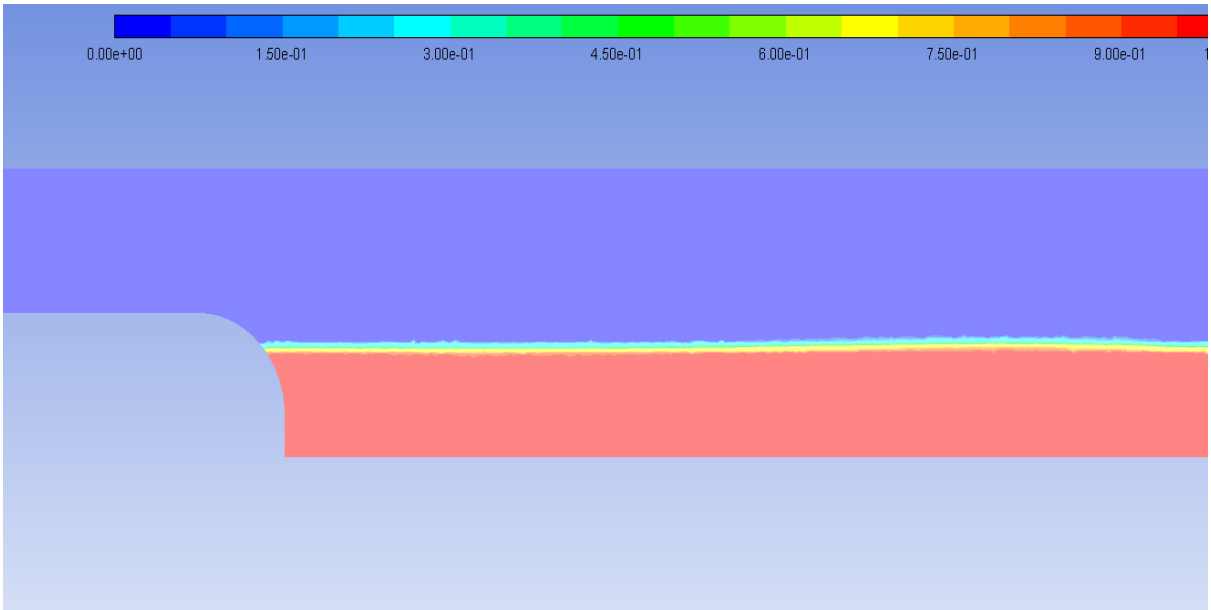


**Figure 117: The volume fraction of phase 2 (water) at the outlet at wind speed 3.2 m/s**

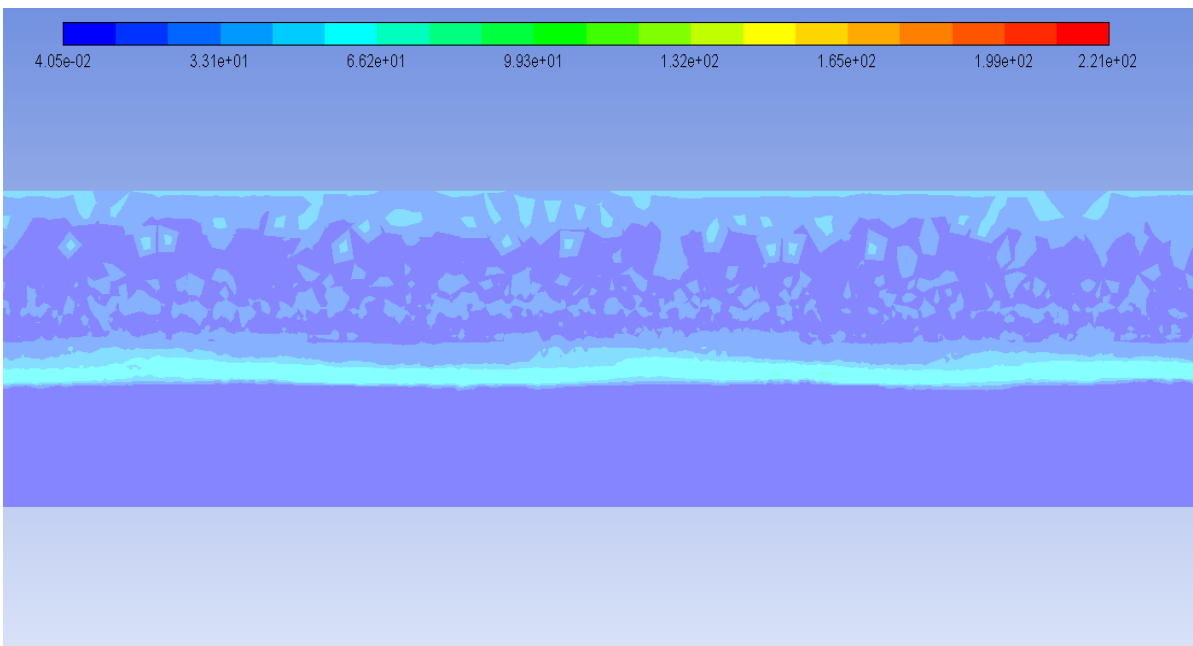


**Figure 118: The strain rate in the middle of model at wind speed 3.2 m/s**

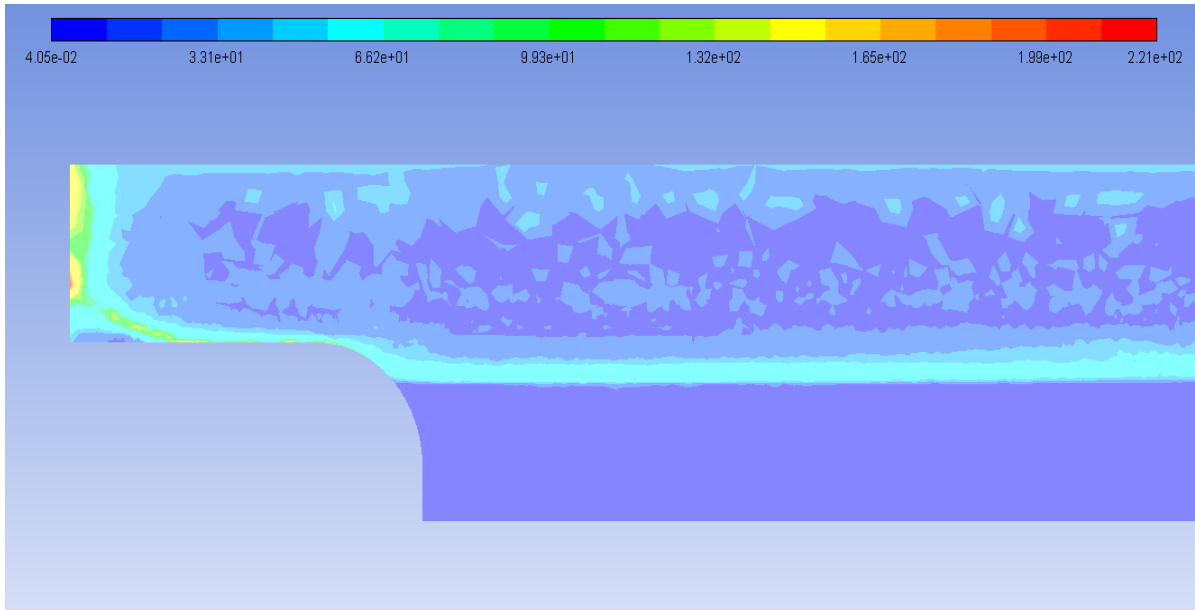


**Figure 119: The strain rate at the outlet at wind speed 3.2 m/s**

## APPENDIX C: MATLAB CODES

### C.1: Code for plotting the temperature for different mesh sizes

```
% File to average the data not equally space in Z directions.
% export and plotting data for different mesh sizes.
clc,clear,
close all
%%
% Temperature for mesh size 0.042
% load the file
load('matlab4.mat');
% Delta Z
dZ = 0.05;
binedeges = 0:dZ:17;
nbins = length(binedeges)-1;
binsum = zeros(1,nbins);
xave = zeros(1,nbins);
binsum_1 = zeros(1,nbins);
bincount = zeros(1,nbins);
%load the data from the file
z = temp1(:,1);
tem = temp1(:,2);
```

```

% creating loops
for j=1:nbins
    for i = 1:length(temp1(:,1))
        if z(i) >= binedeges(j) && z(i) < binedeges(j+1)
            binsum(j) = binsum(j) + z(i);
            binsum_1(j) = binsum_1(j) + tem(i);
            bincount(j) = bincount(j) + 1;
        end
    end
end

%find the average
xave(j) = binsum(j)./bincount(j);
temAve(j) = binsum_1(j)./bincount(j);
end

%%
% Temperature for mesh size 0.022
% Delta Z
dZ2 = 0.05;
binedeges2 = 0:dZ2:17;
nbins2 = length(binedeges2)-1;
binsum2 = zeros(1,nbins2);
xave2 = zeros(1,nbins2);
temAve2 = zeros(1,nbins2);
binsum_2 = zeros(1,nbins2);
bincount2 = zeros(1,nbins2);

```

```

%load the data from the file

z2 = temp2(:,1);
tem2 = temp2(:,2);

% creating loops
for j=1:nbins2
    for i = 1:length(temp2(:,1))
        if z2(i) >= binedeges2(i) && z2(i) < binedeges2(j+1)
            binsum2(j) = binsum2(j) + z2(i);
            binsum_2(j) = binsum_2(j) + tem2(i);
            bincount2(j) = bincount2(j) + 1;
        end
    end
end

%find the average
xave2(j) = binsum2(j)./bincount2(j);
temAve2(j) = binsum_2(j)./bincount2(j);
end

%%

% Temperature for mesh size 0.03
% Delta Z
dZ3 = 0.05;
binedeges3 = 0:dZ3:17;
nbins3 = length(binedeges3)-1;
binsum3 = zeros(1,nbins3);

```



```

xave3 = zeros(1,nbins3);
temAve3 = zeros(1,nbins3);
binsum_3 = zeros(1,nbins3);
bincount3 = zeros(1,nbins3);
%load the data from the file
z3 = temp4(:,1);
tem3 = temp4(:,2);
% creating loops
for j=1:nbins3
    for i = 1:length(temp4(:,1))
        if z3(i) >= binedeges3(j) && z3(i) < binedeges3(j+1)
            binsum3(i) = binsum3(j) + z3(i);
            binsum_3(j) = binsum_3(j) + tem3(i);
            bincount3(j) = bincount3(j) + 1;
        end
    end
    %find the average
    xave3(j) = binsum3(j)./bincount3(j);
    temAve3(j) = binsum_3(j)./bincount3(j);
end
%plotting the data
figure(1)
plot(xave2,temAve2,xave3,temAve3,xave,temAve)
grid on

```

```

title ( 'Graph of the Temperatures for different size mesh')
xlabel('z (m)')
ylabel('Total Temperature (k)')
legend('for mesh size 0.022','for mesh size 0.03','for mesh size
0.042','Location','southwest')

```

## **C.2: Code for plotting the velocity magnitude for different mesh sizes.**

```

% File to average the data not equally space in Z directions.
% export and plotting data for different mesh sizes.
clc,clear,
close all
%%
% load the file
load('matlab5.mat');
%%
% velocity magnitude for mesh size 0.042
% Delta Z
dZ = 0.09;
binedeges4 = 0:dZ:17;
nbins4 = length(binedeges4)-1;
binsum4 = zeros(1,nbins4);
xave4 = zeros(1,nbins4);
temAve4 = zeros(1,nbins4);

```

```

binsum_4 = zeros(1,nbins4);
bincount4 = zeros(1,nbins4);
%load the data from the file
z4 = v1(:,1);
vel4 = v1(:,2);
% creating loops
for j=1:nbins4
    for i = 1:length(v1(:,1))
        if z4(i) >= binedeges4(j) && z4(i) < binedeges4(j+1)
            binsum4(j) = binsum4(j) + z4(i);
            binsum_4(j) = binsum_4(j) + vel4(i);
            bincount4(j) = bincount4(j) + 1;
        end
    end
    %find the average
    xave4(j) = binsum4(j)./bincount4(j);
    temAve4(j) = binsum_4(j)./bincount4(j);
end
%%
% velocity magnitude for mesh size 0.022
% Delta Z
dZ6 = 0.09;
binedeges5 = 0:dZ6:17;
nbins5 = length(binedeges5)-1;

```

```

binsum5 = zeros(1,nbins5);
xave5 = zeros(1,nbins5);
temAve5 = zeros(1,nbins5);
binsum_5 = zeros(1,nbins5);
bincount5 = zeros(1,nbins5);

%load the data from the file
z5 = v2(:,1);
vel5 = v2(:,2);

% creating loops
for j=1:nbins5
    for i = 1:length(v2(:,1))
        if z5(i) >= binedeges5(j) && z5(i) < binedeges5(j+1)
            binsum5(j) = binsum5(j) + z5(i);
            binsum_5(j) = binsum_5(j) + vel5(i);
            bincount5(j) = bincount5(j) + 1;
        end
    end

    %find the average
    xave5(j) = binsum5(j)./bincount5(j);
    temAve5(j) = binsum_5(j)./bincount5(j);
end

%%
% velocity magnitude for mesh size 0.03
% Delta Z

```

```

dZ6 = 0.09;
binedeges6 = 0:dZ6:17;
nbins6 = length(binedeges6)-1;
binsum6 = zeros(1,nbins6);
xave6 = zeros(1,nbins6);
temAve6 = zeros(1,nbins6);
binsum_6 = zeros(1,nbins6);
bincount6 = zeros(1,nbins6);
%load the data from the file
z6 = v3(:,1);
vel6 = v3(:,2);
% creating loops
for j=1:nbins6
    for i = 1:length(v3(:,2))
        if z6(i) >= binedeges6(j) && z6(i) < binedeges6(j+1)
            binsum6(j) = binsum6(j) + z6(i);
            binsum_6(j) = binsum_6(j) + vel6(i);
            bincount6(j) = bincount6(j) + 1;
        end
    end
    %find the average
    xave6(j) = binsum6(j)./bincount6(j);
    temAve6(j) = binsum_6(j)./bincount6(j);
end

```

```

%%
%plotting the data
Figure (1)
plot(xave4,temAve4,xave6,temAve6,xave5,temAve5)
grid on
title ('Graph for velocity magnitude for different mesh sizes')
xlabel('z (m)')
ylabel('Velocity magnitude(m/s)')
legend('for mesh size 0.042','for mesh size 0.03','for mesh size
0.022','Location','south')

```

### **C.3: Code for plotting the velocity magnitude for different residence time.**

```

% Simulation for different residence time
% File to average the data not equally space in Z directions.
clc,clear,
close all
%%
% load the file
load('temp&velocity_diff_res_time.mat');
%%
% Velocity magnitude after 1 Residence time
% Delta Z
dZ = 0.05;

```

```

binedeges4 = 0:dZ:17;
nbins4 = length(binedeges4)-1;
binsum4 = zeros(1,nbins4);
xave4 = zeros(1,nbins4);
temAve4 = zeros(1,nbins4);
binsum_4 = zeros(1,nbins4);
bincount4 = zeros(1,nbins4);
%load the data from the file
z4 = v1(:,1);
vel4 = v1(:,2);
% creating loops
for j=1:nbins4
    for i = 1:length(v1(:,1))
        if z4(i) >= binedeges4(j) && z4(i) < binedeges4(j+1)
            binsum4(j) = binsum4(j) + z4(i);
            binsum_4(j) = binsum_4(j) + vel4(i);
            bincount4(j) = bincount4(j) + 1;
        end
    end
    %find the average
    xave4(j) = binsum4(j)./bincount4(j);
    temAve4(j) = binsum_4(j)./bincount4(j);
end
%%

```

```

% Velocity magnitude after 2 Residence time

% Delta Z

dZ6 = 0.05;

binedeges5 = 0:dZ6:17;

nbins5 = length(binedeges5)-1;

binsum5 = zeros(1,nbins5);

xave5 = zeros(1,nbins5);

temAve5 = zeros(1,nbins5);

binsum_5 = zeros(1,nbins5);

bincount5 = zeros(1,nbins5);

%load the data from the file

z5 = v6(:,1);

vel5 = v2(:,1);

% creating loops

for j=1:nbins5

    for i = 1:length(v2(:,1))

        if z5(i) >= binedeges5(j) && z5(i) < binedeges5(j+1)

            binsum5(j) = binsum5(j) + z5(i);

            binsum_5(i) = binsum_5(j) + vel5(i);

            bincount5(j) = bincount5(j) + 1;

        end

    end

%find the average

xave5(j) = binsum5(j)./bincount5(j);

```



```

    temAve5(j) = binsum_5(j)./bincount5(j);
end
%%
% Velocity magnitude after 3 Residence time
% Delta Z
dZ6 = 0.05;
binedeges6 = 0:dZ6:17;
nbins6 = length(binedeges6)-1;
binsum6 = zeros(1,nbins6);
xave6 = zeros(1,nbins6);
temAve6 = zeros(1,nbins6);
binsum_6 = zeros(1,nbins6);
bincount6 = zeros(1,nbins6);
%load the data from the file
z6 = v1(:,1);
vel6 = v3(:,1);
% creating loops
for j=1:nbins6
    for i = 1:length(v3(:,1))
        if z6(i) >= binedeges6(j) && z6(i) < binedeges6(j+1)
            binsum6(j) = binsum6(j) + z6(i);
            binsum_6(j) = binsum_6(j) + v3(i);
            bincount6(j) = bincount6(j) + 1;
        end
    end
end

```

```

end

% find the average
xave6(j) = binsum6(j)./bincount6(j);
temAve6(j) = binsum_6(j)./bincount6(j);

end

%%

% Velocity magnitude after 4 Residence time
% Delta Z
dZ7 = 0.05;
binedeges7 = 0:dZ7:17;
nbins7 = length(binedeges7)-1;
binsum7 = zeros(1,nbins7);
xave7 = zeros(1,nbins7);
temAve7 = zeros(1,nbins7);
binsum_7 = zeros(1,nbins7);
bincount7 = zeros(1,nbins7);

% load the data from the file
z7 = v1(:,1);
vel7 = v4(:,1);

% creating loops
for j=1:nbins7
    for i = 1:length(v4(:,1))
        if z7(i) >= binedeges7(j) && z7(i) < binedeges7(j+1)
            binsum7(j) = binsum7(j) + z7(i);
        end
    end
end

```

```

        binsum_7(j) = binsum_7(j) + v4(i);
        bincount7(j) = bincount7(j) + 1;
    end

end

%find the average
xave7(j) = binsum7(j)./bincount7(j);
temAve7(j) = binsum_7(j)./bincount7(j);
end

%% finding the average
%calculating the average of the data
V1=temAve4(1,:);
V2=temAve5(1,:);
V3=temAve6(1,:);
V4=temAve7(1,:);
V=[V1',V2',V3',V4'];
[m n]=size(V);
for i=1:m
    AVT2(i)=mean(V(i,:));
end;
avevel=AVT2';
%plotting the data
figure(1)
plot(xave4,temAve4,xave5,temAve5,xave6,temAve6,xave7,temAve7,xave4,avevel,'k'
)
grid on

```

```

title ('Velocity magnitude for different residence time')
xlabel('z (m)')
ylabel('Velocity magnitude(m/s)')

legend('for 1 residence time','for 2 residence time','for 3 residence time','for 2
residence time','Average','Location','south')

```

#### **C.4: Code for plotting the total temperature for different residence time.**

```

% Simulation for different residence time

% File to average the data not equally space in Z directions.

clc,clear,

close all

%%

% load the file

load('temp&velocity_diff_res_time.mat');

%%

% Total temperature after 1 Residence time

% Delta Z

dZ = 0.05;

binedeges = 0:dZ:17;

nbins = length(binedeges)-1;

binsum = zeros(1,nbins);

xave = zeros(1,nbins);

temAve = zeros(1,nbins);

```

```

binsum_1 = zeros(1,nbins);
bincount = zeros(1,nbins);
%load the data from the file
z = temp1(:,1);
tem = temp1(:,2);
% creating loops
for j=1:nbins
    for i = 1:length(temp1(:,1))
        if z(i) >= binedeges(j) && z(i) < binedeges(j+1)
            binsum(j) = binsum(j) + z(i);
            binsum_1(j) = binsum_1(j) + tem(i);
            bincount(j) = bincount(j) + 1;
        end
    end
    %find the average
    xave(j) = binsum(j)./bincount(j);
    temAve(j) = binsum_1(j)./bincount(j);
end
%%
% Total temperature after 2 Residence time

% Delta Z
dZ2 = 0.05;
binedeges2 = 0:dZ2:17;

```

```

nbins2 = length(binedeges2)-1;
binsum2 = zeros(1,nbins2);
xave2 = zeros(1,nbins2);
temAve2 = zeros(1,nbins2);
binsum_2 = zeros(1,nbins2);
bincount2 = zeros(1,nbins2);
%load the data from the file
z2 = temp1(:,1);
tem2 = temp2(:,1);
% creating loops
for j=1:nbins2
    for i = 1:length(temp2(:,1))
        if z2(i) >= binedeges2(j) && z2(i) < binedeges2(j+1)
            binsum2(j) = binsum2(j) + z2(i);
            binsum_2(j) = binsum_2(j) + tem2(i);
            bincount2(j) = bincount2(j) + 1;
        end
    end
    %find the average
    xave2(j) = binsum2(j)./bincount2(j);
    temAve2(j) = binsum_2(j)./bincount2(j);
end
%%
% Total temperature after 3 Residence time

```

```

% Delta Z
dZ3 = 0.05;
binedeges3 = 0:dZ3:17;
nbins3 = length(binedeges3)-1;
binsum3 = zeros(1,nbins3);
xave3 = zeros(1,nbins3);
temAve3 = zeros(1,nbins3);
binsum_3 = zeros(1,nbins3);
bincount3 = zeros(1,nbins3);
%load the data from the file
z3 = temp1(:,1);
tem3 = temp3(:,1);
% creating loops
for j=1:nbins3
    for i = 1:length(temp3(:,1))
        if z3(i) >= binedeges3(j) && z3(i) < binedeges3(j+1)
            binsum3(j) = binsum3(j) + z3(i);
            binsum_3(j) = binsum_3(j) + tem3(i);
            bincount3(j) = bincount3(j) + 1;
        end
    end
%find the average
xave3(j) = binsum3(j)./bincount3(j);
temAve3(j) = binsum_3(j)./bincount3(j);

```

```

end

%%

% Total temperature after 4 Residence time

% Delta Z

dZ4 = 0.05;

binedeges4 = 0:dZ4:17;

nbins4 = length(binedeges4)-1;

binsum4 = zeros(1,nbins4);

xave4 = zeros(1,nbins4);

temAve4 = zeros(1,nbins4);

binsum_4 = zeros(1,nbins4);

bincount4 = zeros(1,nbins4);

% load the data from the file

z4 = temp1(:,1);

tem4 = temp4(:,1);

% creating loops

for j=1:nbins4

    for i = 1:length(temp4(:,1))

        if z4(i) >= binedeges4(j) && z4(i) < binedeges4(j+1)

            binsum4(j) = binsum4(j) + z4(i);

            binsum_4(j) = binsum_4(j) + tem4(i);

            bincount4(j) = bincount4(j) + 1;

        end

    end

end

```



```

    %find the average

    xave4(j) = binsum4(j)./bincount4(j);

    temAve4(j) = binsum_4(j)./bincount4(j);

end

%% finding the average

%calculating the average of the data

t1=temAve(1,:);

t2=temAve2(1,:);

t3=temAve3(1,:);

t4=temAve4(1,:);

T=[t1',t2',t3',t4'];

[m n]=size(T);

for i=1:m

    AVT(i)=mean(T(i,:));

end;

avetemp=AVT';

%plotting the data

figure(1)

plot(xave,temAve,xave2,temAve2,xave3,temAve3,xave4,temAve4,xave,avetemp,'k')

grid on

title ('Graph of the temperatures for different residence time')

xlabel('z (m)')

ylabel('Total Temperature (k)')

legend('for 1 residence time','for 2 residence time','for 3 residence time','for 4
residence time','Average','Location','southwest')

```

## C.5: Code for plotting the temperature for different mesh sizes (final model)

```
% find the mesh independency for different mesh size for the final model
% File to average the data not equally space in Z directions.
% export and plotting data for different mesh sizes.

clc,clear,

close all

%%

% Temperature for mesh size 0.042

% load the file

load('temp&velocity_diff_meshsize_newmodel.mat');

% Delta Z

dZ = 0.05;

binedeges = 0:dZ:17;

nbins = length(binedeges)-1;

binsum = zeros(1,nbins);

xave = zeros(1,nbins);

temAve = zeros(1,nbins);

binsum_1 = zeros(1,nbins);

bincount = zeros(1,nbins);

%load the data from the file

z = temp1(:,1);

tem = temp1(:,2);
```

```

% creating loops
for j=1:nbins
    for i = 1:length(temp1(:,1))
        if z(i) >= binedeges(j) && z(i) < binedeges(j+1)
            binsum(j) = binsum(j) + z(i);
            binsum_1(j) = binsum_1(j) + tem(i);
            bincount(j) = bincount(j) + 1;
        end
    end
end

%find the average
xave(j) = binsum(j)./bincount(j);
temAve(j) = binsum_1(j)./bincount(j);
end

%%
% Temperature for mesh size 0.022
% Delta Z
dZ2 = 0.05;
binedeges2 = 0:dZ2:17;
nbins2 = length(binedeges2)-1;
binsum2 = zeros(1,nbins2);
xave2 = zeros(1,nbins2);
temAve2 = zeros(1,nbins2);
binsum_2 = zeros(1,nbins2);
bincount2 = zeros(1,nbins2);

```

```

%load the data from the file

z2 = temp2(:,1);
tem2 = temp2(:,2);

% creating loops
for j=1:nbins2
    for i = 1:length(temp2(:,1))
        if z2(i) >= binedeges2(j) && z2(i) < binedeges2(j+1)
            binsum2(j) = binsum2(j) + z2(i);
            binsum_2(j) = binsum_2(j) + tem2(i);
            bincount2(j) = bincount2(j) + 1;
        end
    end

    %find the average
    xave2(j) = binsum2(j)./bincount2(j);
    temAve2(j) = binsum_2(j)./bincount2(j);
end

%%
%Temperature for mesh size 0.03
% Delta Z
dZ3 = 0.05;
binedeges3 = 0:dZ3:17;
nbins3 = length(binedeges3)-1;
binsum3 = zeros(1,nbins3);
xave3 = zeros(1,nbins3);

```

```

temAve3 = zeros(1,nbins3);
binsum_3 = zeros(1,nbins3);
bincount3 = zeros(1,nbins3);
%load the data from the file
z3 = temp4(:,1);
tem3 = temp4(:,2);
% creating loops
for j=1:nbins3
    for i = 1:length(temp4(:,1))
        if z3(i) >= binedeges3(j) && z3(i) < binedeges3(j+1)
            binsum3(j) = binsum3(j) + z3(i);
            binsum_3(j) = binsum_3(j) + tem3(i);
            bincount3(j) = bincount3(j) + 1;
        end
    end
    %find the average
    xave3(j) = binsum3(j)./bincount3(j);
    temAve3(j) = binsum_3(j)./bincount3(j);
end
%plotting the data
figure(1)
plot(xave2,temAve2,xave3,temAve3,xave,temAve)
grid on
title ( 'Graph of the Temperatures for different size mesh')

```

```

xlabel('z (m)')
ylabel('Total Temperature (k)')
legend('for mesh size 0.022','for mesh size 0.032','for mesh size
0.042','Location','southwest')

```

## **C.6: Code for plotting the velocity magnitude for different mesh sizes/final model**

```

% find the mesh independency for different mesh size for the final model
% File to average the data not equally space in Z directions.
% export and plotting data for different mesh sizes.
clc,clear,
close all
%%
% load the file
load('temp&velocity_diff_meshsize_newmodel.mat');
%%
% velocity magnitude for mesh size 0.042
% Delta Z
dZ = 0.09;
binedeges4 = 0:dZ:17;
nbins4 = length(binedeges4)-1;
binsum4 = zeros(1,nbins4);
xave4 = zeros(1,nbins4);
temAve4 = zeros(1,nbins4);

```

```

binsum_4 = zeros(1,nbins4);
bincount4 = zeros(1,nbins4);
%load the data from the file
z4 = v1(:,1);
vel4 = v1(:,2);
% creating loops
for j=1:nbins4
    for i = 1:length(v1(:,1))
        if z4(i) >= binedeges4(j) && z4(i) < binedeges4(j+1)
            binsum4(j) = binsum4(j) + z4(i);
            binsum_4(j) = binsum_4(j) + vel4(i);
            bincount4(j) = bincount4(j) + 1;
        end
    end
    %find the average
    xave4(j) = binsum4(j)./bincount4(j);
    temAve4(j) = binsum_4(j)./bincount4(j);
end
%%
% velocity magnitude for mesh size 0.022
% Delta Z
dZ6 = 0.09;
binedeges5 = 0:dZ6:17;
nbins5 = length(binedeges5)-1;

```

```

binsum5 = zeros(1,nbins5);
xave5 = zeros(1,nbins5);
temAve5 = zeros(1,nbins5);
binsum_5 = zeros(1,nbins5);
bincount5 = zeros(1,nbins5);

%load the data from the file
z5 = v2(:,1);
vel5 = v2(:,2);

% creating loops
for j=1:nbins5
    for i = 1:length(v2(:,1))
        if z5(i) >= binedeges5(j) && z5(i) < binedeges5(j+1)
            binsum5(j) = binsum5(j) + z5(i);
            binsum_5(j) = binsum_5(j) + vel5(i);
            bincount5(j) = bincount5(j) + 1;
        end
    end

    %find the average
    xave5(j) = binsum5(j)./bincount5(j);
    temAve5(j) = binsum_5(j)./bincount5(j);
end

%%
% velocity magnitude for mesh size 0.032
% Delta Z

```



```

dZ6 = 0.09;
binedeges6 = 0:dZ6:17;
nbins6 = length(binedeges6)-1;
binsum6 = zeros(1,nbins6);
xave6 = zeros(1,nbins6);
temAve6 = zeros(1,nbins6);
binsum_6 = zeros(1,nbins6);
bincount6 = zeros(1,nbins6);
%load the data from the file
z6 = v3(:,1);
vel6 = v3(:,2);
% creating loops
for j=1:nbins6
    for i = 1:length(v3(:,2))
        if z6(i) >= binedeges6(j) && z6(i) < binedeges6(j+1)
            binsum6(j) = binsum6(j) + z6(i);
            binsum_6(j) = binsum_6(j) + vel6(i);
            bincount6(j) = bincount6(j) + 1;
        end
    end
    %find the average
    xave6(j) = binsum6(j)./bincount6(j);
    temAve6(j) = binsum_6(j)./bincount6(j);
end

```

```

%%
%plotting the data
figure(1)
plot(xave4,temAve4,xave6,temAve6,xave5,temAve5)
grid on
title ('Graph for velocity magnitude for different mesh sizes')
xlabel('z (m)')
ylabel('Velocity magnitude(m/s)')
legend('for mesh size 0.042','for mesh size 0.032','for mesh size
0.022','Location','south')

```

### **C.7: Code for plotting the volume fraction (final model)**

Similar codes were used with different wind speeds to plot the volume fraction

```

% Code to calculate the volume fraction of waves in the required nodes...

```

```

...and plotting them

```

```

% Author: HAYDER AL-LAMI

```

```

% Date: October 2017

```

```

% Clear Variables and Command Window

```

```

clc

```

```

close all

```

```

clear all

```

```

figcnt = 0;

```

```

% only load data if doesn't exist in workspace

```

```

if ~exist('data','var')

```

```

    %read the exported data from CFD

```

```

data = xlsread('0.022_2nd time residence.csv');

end

% Read Y and Z coordinates form the data
Y = data(:,3);
Z = data(:,4);

% Read velocity magnitude at Y and Z coordinates from the data
VF = data(:,26);

% Making a grid of the Y and Z coordinates
% Taking the data from 0.25m to 0.45m at y coordinate
% Taking the data from 5m to 10m at Z coordinate
[Yq,Zq] = meshgrid(0.25:(0.45-0.25)/99:0.45,5:5/333:10);

% interpolates scattered data FOR Vq
VFq = griddata(Y,Z,VF,Yq,Zq);

%% plotting tha data by contour function in 10 levels
colormap default
cmapp = colormap('jet');
cmapp = cmapp(end:-1:1,:);
colormap(cmapp)
figcnt = figcnt + 1; figure (figcnt); clf
contour (Zq,Yq,VFq,10)
h = colorbar;
set(h, 'YDir', 'reverse');

grid on
xlabel('Distance from the inlet (Z) (m)')

```

```

ylabel('Distance from the base (Y) (m)')
% plotting the data by contourf function
figcnt = figcnt + 1; figure (figcnt); clf
contourf (Zq,Yq,VFq)
h = colorbar;
set(h, 'YDir', 'reverse');
grid on
xlabel('Distance from the inlet (Z) (m)')
ylabel('Distance from the base (Y) (m)')
% using surf function to plot new and real data and then compare between...
... them
figcnt = figcnt + 1; figure (figcnt); clf
surf(Zq,Yq,VFq)
hold on
colorbar
grid on
title ('comparing between data from new grids and the real data')
xlabel('Z coordinate (m)')
ylabel('Y coordinate (m)')
zlabel('volume fraction')
Y1 = find(Y>0.25 & Y<0.45);
Z1 = find(Z>5 & Z<10);
Vof = VF(Z1);
plot3(Z(Z1),Y(Z1),Vof, '*')

```

```

hold off

%%
% plotting the velocity magnitude vs the volume fraction to check if the
% velocity plots can represent the waves and water surface

V = data(:,5);

% Interpolates scattered data FOR Vq
Vq = griddata(Y,Z,V,Yq,Zq);

figcnt = figcnt + 1; figure (figcnt); clf
plot(max(VFq),max(Vq),'!')

hold on

plot(min(VFq),min(Vq),'+')

plot(mean(VFq),mean(Vq))

title ( 'Velocity Magnitude vs Volume Fraction')

xlabel('Volume Fraction, VF')

ylabel( 'Velocity Magnitude m/s')

legend('maximum values of VFq & Vq','minmum values of VFq & Vq','mean values
of VFq & Vq1','Location','northeast')

hold off

```

### **C.8: Code for determining and plotting the amplitude of waves (final model)**

```

% Code to calculate frequency, amplitude and wavelength of waves

```

```

% Author: HAYDER AL-LAMI 2017

% Clear Variables and Command Window

clc

close all

clear all

figcnt = 0;

% Only load data if doesn't exist in workspace
if ~exist('data','var')

    %Read the data file

    data = xlsread('v2.csv');

end

%Read X, Y and Z coordinates form the data

Y= data(:,3);

Z= data(:,4);

% Read volume fraction at X, Y and Z coordinates form the data

VF = data(:,17);

% Taking the data from 0.25m to 0.45m at y coordinate

% taking the data from 5m to 10m at Z coordinate

YY = 0.25:(0.45-0.25)/99:0.45;

dZ = 7/333;

ZZ = 5:dZ:12;

% make a grid of the X, Y and Z coordinates

[Yq,Zq] = meshgrid(YY,ZZ);

% Interpolates scattered data for volume fraction

```

```

VFq = griddata(Y,Z,VF,Yq,Zq);

% Find water surface

VFsurf = 0.5;

Ysurf = nan(size(ZZ));

for i = 1:length(ZZ)

    % Filter out data that's purely water or purely air

    VFqs = VFq(i,:);

    dd = diff(VFqs);

    ddin = find(abs(dd) > 100*eps);

    VFqs = VFqs(ddin);

    Yqs = Yq(i,ddin);

    Ysurf(i) = interp1(VFqs,Yqs,VFsurf);

end

% using fft with the volume fraction data

freq=fft(Ysurf);

N = length(Ysurf);

Tot_time = diff(ZZ([1 end]));           % Total time in Second

Fs = N/Tot_time ;                       % Samples per second

No_bins = (0 : N-1);

Hz = No_bins*Fs/N;

% From the help for fft

freq2 = abs(freq/N);

freq3 = freq2(1:N/2+1);

freq3(2:end-1) = 2*freq3(2:end-1);

```

```

Hz = 1/dZ * (0:(N/2))/N;

% plotting the results

% wave surface

freq2 = freq3;

figcnt = figcnt + 1; figure (figcnt); clf

plot(ZZ,Ysurf)

xlabel('Z (m)')

ylabel('Y (m)')

title(['Water surface; Water Volume Fraction = ',num2str(VFsurf)])

% wave's amplitude vs wavelength

figcnt = figcnt + 1; figure (figcnt); clf

plot(1./Hz,freq2);

xlabel('Wavelength (m)')

ylabel('Amplitude (m)')

% wave's amplitude vs wave number

figcnt = figcnt + 1; figure (figcnt); clf

plot(Hz,freq2);

xlabel('Wavenumber (Period) (1/m)')

ylabel('Amplitude (m)')

```

### **C.9: Code for determining the shear stress on water surface/final model**

```

% Code to calculate the shear stress of waves on the water surface

% Author: HAYDER AL-LAMI

```



```

% Date: NOV 2017

% Clear Variables and Command Window

clc

close all

clear all

if ~exist('data','var')

    %Read the exported data from CFD

    data = xlsread('v2.csv');

end

%Read Y and Z coordinates from the data

Y= data(:,3);

Z= data(:,4);

% Read velocity gradient from the data

dz_dz = data(:,13);

dy_dy = data(:,9);

dz_dy = data(:,10);

dy_dz = data(:,12);

% Making a grid of the Y and Z coordinates

% Taking the data from 0.25m to 0.45m at y coordinate

% Taking the data from 5m to 10m at Z coordinate

yy= 0.25:(0.45-0.25)/99:0.45;

zz=5:5/333:10;

[Yq,Zq] = meshgrid(yy,zz);

% Interpolates scattered data for dv_dyq and dv_dzq

```

```

dz_dzq = griddata(Y,Z,dz_dz,Yq,Zq);
dy_dyq = griddata(Y,Z,dy_dy,Yq,Zq);
dz_dyq = griddata(Y,Z,dz_dy,Yq,Zq);
dy_dzq = griddata(Y,Z,dy_dz,Yq,Zq);
% Calculating the shear stress at the required nodes
% Dynimces viscosity of water at 15 C = 0.001139
sigma_zz=0.001139*dz_dzq;
sigma_yy=0.001139*dy_dyq;
tau_zy=0.001139*dz_dyq;
tau_yz=0.001139*dy_dzq;
% loading the data regarding the water surface
% calculating the values of theta
ss = [NaN,ss,NaN];
theta=atan(ss);
%using equation of Mohr's circle to find tau_xiyi
h=(sigma_yy-sigma_zz)/2;
hh = nan(size(ZZ));
for i = 1:length(ZZ)
    hh(i) = interp1(Yq(j,:),h(i,:),Ysurf(i),'spline');
    tt(i) = interp1(Yq(i,:),tau_yz(i,:),Ysurf(i),'spline');
end
s1=sin(2*theta);
c1=cos(2*theta);
tau_yizi=hh.*s1+tt.*c1;

```

```

% plotting the data of ZZ vs tau_yizi

figure(1)

plot(ZZ,tau_yizi)

xlabel('Z (m)')

ylabel('\tau (Pa)')

% plotting the data

figure (2)

[N,edges] = histcounts(tau_yizi(2:end-1),30);

N = N ./ sum(N.*diff(edges));

tt2 = 0.5*(edges(1:end-1)+edges(2:end));

bar(tt2,N)

hold on

[m,s]=normfit(tau_yizi(2:end-1));

ttmin = min(tau_yizi);

ttmax = max(tau_yizi);

tt1 = ttmin : (ttmax-ttmin)/1000 : ttmax;

plot(tt1,normpdf(tt1,m,s),'r')

hold off

xlabel('\tau (Pa)')

ylabel('Probability Density Function')

```

